AD NUMBER

AD839416

NEW LIMITATION CHANGE

TO

Approved for public release, distribution unlimited

FROM

Distribution authorized to U.S. Gov't. agencies and their contractors; Administrative/Operational Use; Jun 1968. Other requests shall be referred to Air Force Flight Dynamics Lab, Attn: FDCL, Wright-Patterson AFB, OH 45433.

AUTHORITY

AFFDL ltr dtd 8 Jun 1972

AFFDL-TR-66-227

STUDY OF LIQUID METAL NaK-77 FOR APPLICATION IN FLIGHT CONTROL SYSTEMS

R. C. KUMPITSCH

J. R. GRANAN

TECHNICAL REPORT AFFDL-TR-66-227

JUNE 1968

AIR FORCE FLIGHT DYNAMICS LABORATORY
AIR FORCE SYSTEMS COMMAND
WRIGHT-PATTERSON AIR FORCE BASE, OHIO

NOTICES

When Government drawings, specifications, or other data are used for any purpose other than in connection with a definitely related Government procurement operation, the United States Government thereby incurs no responsibility nor any obligation whatsoever; and the fact that the Government may have formulated, furnished, or in any way supplied the said drawings, specifications, or other data, is not to be regarded by implication or otherwise as in any manner licensing the holder or any other person or corporation, or conveying any rights or permission to manufacture, use, or sell any patented invention that may in any way be related thereto.

This document is subject to special export controls and each transmittal to foreign governments or foreign nationals may be made only with prior approval of the Air Force Flight Dynamics Laboratory, FDCL, Wright-Patterson Air Force Base, Ohio 45433.

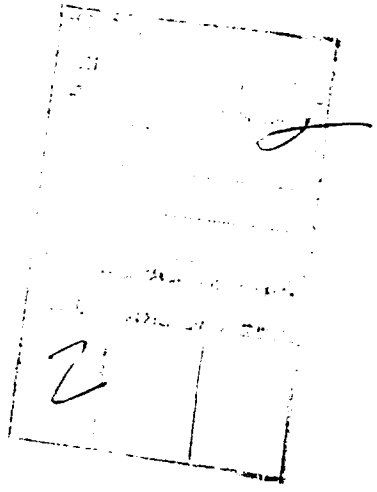

Copies of this report should not be returned to the Research and Technology Division unless return is required by security considerations, contractual obligations, or notice on a specific document.

300- August 1968 - CO455 - 46-990

STUDY OF LIQUID METAL NaK-77 FOR APPLICATION IN FLIGHT CONTROL SYSTEMS

R. C. KUMPITSCH

J. R. GRANAN

FOREWORD

This report has been prepared by the Avionic Controls Department, General Electric Company, Binghamton, New York, as part of U.S. Air Force Contract AF33(615)2263, "Study of Liquid Metal NaK-77 for Application in Flight Control Systems". The contract was initiated under Project No. 8225, Task No. 822510. The work was administered under the direction of the Air Force Flight Dynamics Laboratory, Research and Technology Division, Air Force Systems Command, with Mr. Vernon R. Schmitt, FDCL, as Project Engineer.

The work was performed between September 1964 and April 1967 with Mr. R.C. Kumpitsch as Project Leader.

The authors wish to acknowledge the fine cooperation and support of Messrs. J. Farron, J. Sulich, and A. Kiwior of Bendix Research Laboratories, who participated in the torque motor and position transducer study phases of the program.

This report has been generated and published by the General Electric Company under publication No. ACD-8176.

The manuscript released by authors April 1, 1967 for publication as an RTD Techical Report.

This technical report has been received and is approved.

H. W. BASHAM
Chief, Control Elements Branch
Flight Control Division
AF Flight Dynamics Laboratory

ABSTRACT

A survey of potential aerospace applications and system performance requirements was made. A ten-stage centrifugal pump rated at 3000 psi, 16 gpm, and 1200 F was successfully tested at pressures above 2200 psi, temperatures exceeding 1000 F, and speed above 31, 000 rpm. Flow exceeded the rated capacity of the unit. The total operating time accumulated to date on the test pump has been 50 3/4 hours.

A 1200 F, two-stage servovalve was designed and built, and static tests with oil and NaK-77 were conducted. A linear actuator rated at 15,000 pounds output at 1200 F was re-built and tested with NaK-77 for part of an experimental servoactuating subsystem.

A nuclear testing facility was located and a design layout of an experimental, air-nuclear servoactuating subsystem was made. Design criteria and design layouts for a flight test system suitable for installation in the elevon section of the XB-70 were also established.

The experimental model servoactuating subsystem was assembled and static tests performed. The system was operated successfully at high pressures and with fluid and ambient temperatures in excess of 1000 F. Operating time totaling 9 1/2 hours has been accumulated on the system to date. Fluid seal problems in the high-temperature torque motor forced temporary cessation of the system test effort.

Test data resulting from evaluation of the centrifugal pump, servovalve, and experimental subsystem were tabulated and submitted to the cognizant monitoring agency at R. T. D.

TABLE OF CONTENTS

LIST OF ILLUSTRATIONS

LIST OF ILLUSTRATIONS
(Con'd.)

LIST OF ILLUSTRATIONS
(Con'd.)

SECTION I

INTRODUCTION

This report summarizes the efforts performed under U. S. Air Force contract AF33(615)-2263. The program was a research and feasibility study of the liquid metal NaK-77 for application in flight control servoactuating subsystems. The study involved the following specific tasks:

1. Continuation study of liquid metal flight control applications.

2. Evaluation of an experimental model servoactuating subsystem.

3. Study of an experimental model servoactuating subsystem for air and nuclear radiation environments.

4. Study of design criteria for servoactuating subsystem suitable for flight test.

5. Study of servovalves for servoactuating subsystems.

6. Study of related servoactuating subsystem components.

7. Study of pumps for servoactuating subsystems.

The results of these studies are described in this report and represent a continuation of the effort expended under U. S. Air Force contracts AF33(616)-7794 and AF33(657)-10875. These are described in previous Technical Reports 4.5.6. Background information pertinent to this study is documented in Technical Reports 1, 2.3.

The common and ultimate objective of these programs is the establishment of techniques, capabilities and technology necessary to build liquid metal flight control and power actuation systems capable of reliable operation to temperatures of 1200 F, in air and nuclear radiation environments, for extended periods of time. This capability is to be demonstrated by performing a flight test evaluation with an experimental servoactuating subsystem of this type.

Progress to date has shown a steady evolution, starting with selection of a candidate fluid and elementary feasibility studies. It has progressed through design, procurement and evaluation of various types and configurations of pumps, servovalves, and actuators, to the experimental subsystem described in this report. Extensions of this acquired knowledge has resulted in tentative designs for air/nuclear and flight test subsystems.

Section II

LIQUID METAL FLIGHT CONTROL APPLICATION STUDY

This application study has continued the effort conducted under previous contracts to determine and define, where possible, those advanced flight vehicle system concepts which by their requirements have potential use for liquid metal type hydraulic controls. This effort was performed similarly to the previous studies, in that contacts were made with organizations, cognizant agencies and manufacturers who had interest and a potential future need for wide operating, high-temperature servoactuating subsystems. Whenever maximum benefit could be derived, direct personal meetings and visits were made.

This study included search for the following pertinent flight control actuation subsystem and related control data of each of the various advanced vehicles considered in this investigation:

1. Actuation load and performance specifications.

2. System duty cycle and flight profile requirements

3. Available power supplies for these control systems.

4. Pertinent airframe configuration details for system location and sizing use.

Although the information yield from this search was meager and far too insufficient to enable performing the detailed analysis and sizing of the various specific actuation systems, it has provided information on anticipated future hypersonic aerospace vehicle flight surface and engine actuation system environmental requirements as well as aero-dynamic load and flight system operating performance trends.

The method used to effectively solicit and collect pertinent data involved publication of a brochure for distribution to each of the sources being contacted. The document which was prepared described the liquid metal program goals, both previous and current development efforts, accomplishments which were made, and general status review of this specific technological effort. A supplemental inquiry also accompanied each brochure which described the purpose and intent of the application study and requested specific detailed vehicle application data.

Distribution of this information was made to some 33 agencies and industrial organizations. Responses were received from 10 and visits were made to 5 of this group.

Comments received ranged from: "The present state of the art fluids are adequate for all vehicles which we now have under study.", to "In the area of hypersonics and high Mach number applications, liquid metals appear to be the only practical solution offered to date.". The majority of comments reflected the latter view, which indicates the current realization that new and more advanced systems will be required to meet future needs.

Presentations were made to each of the groups visited. Although no specific, detailed application information was obtained during the course of this investigation, the following general trends and predicted vehicle surface temperature data resulted from the study:

Figure 1 shows the trend of surface temperatures which have been and are to be experienced on manned aircraft up to the 1972 time period. Also shown are the temperature limits of the hydraulic fluids considered for use in flight applications.

It should be noted that the temperatures shown are maximum surface temperatures achieved under the various design flight profiles of these aircraft. In the case of the X-15, the duration of flight was such that conventional hydraulic fluids could be employed in the flight control system. This does demonstrate that flight vehicles can dynamically perform in this high temperature environment. In the future however, systems will eventually be required to operate at these temperature levels for extended periods of time. Presently only those hydraulic fluids identified in Figure 1 have or approach the capability of sustained operation in such an environment.

Current advanced planning studies indicate that hypersonic aircraft and advanced vehicles of the general configurations shown in Figures 2 and 3 will, in the future, be capable of flight in the Mach 6 to 12 speed range at altitudes from 90,000 to 150,000 ft.

Predicted surface temperatures for these vehicles are as indicated on Figures 4 and 5. This trend clearly shows the future need for advanced flight control servoactuating systems capable of reliable operation in such environments.

Representative Fluids	Viscosity Centipoises	Specific Gravity	Pour Point °F	Max. Useful Temperature °F
Typical MIL-H-5606A Hydrocarbon	14.2	0.847	Max. -75	275
Silanes	12.1 (210°F)	---	-15	700
5-p Polyphenyl Ether	13.3 (210°F)	1.20	+40	835-900
Liquid Metal, Sodium-Potassium-Cesium	0.19 (1300°F)	1.69	-95	1300+
Liquid Metal, Sodium-Potassium (NaK-77)	0.14 (1200°F)	0.87	+10	1400+

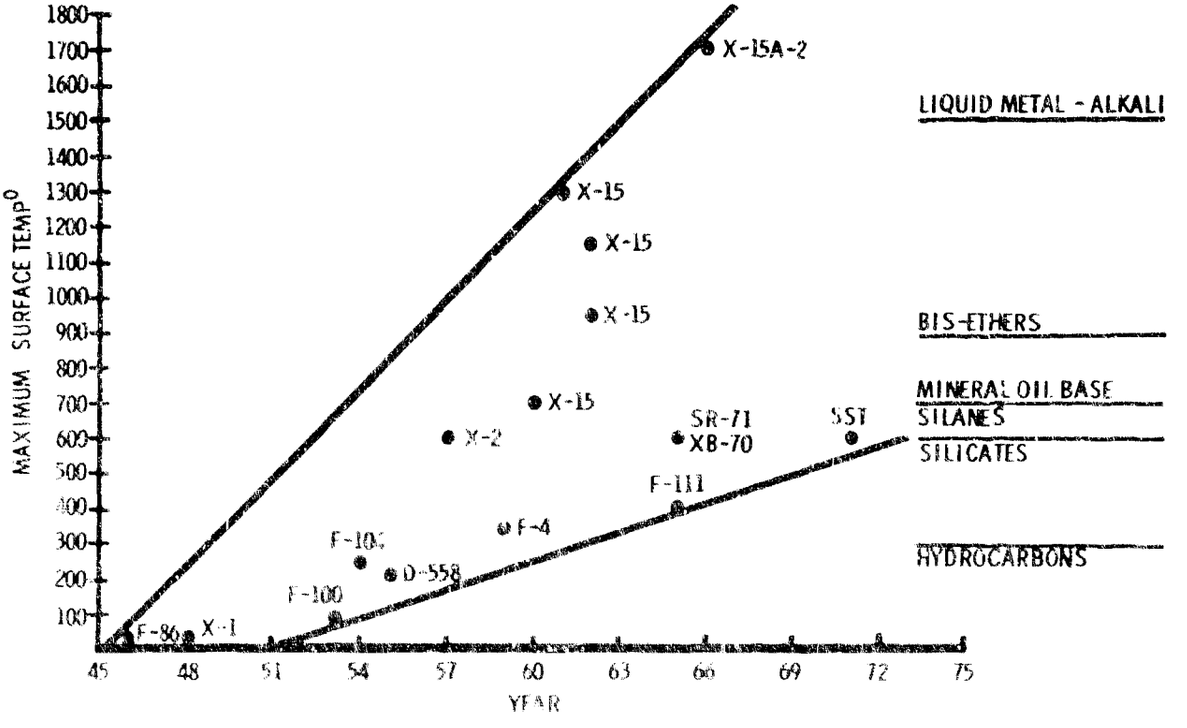

Figure 1 – Temperature Trend for Advanced Vehicles

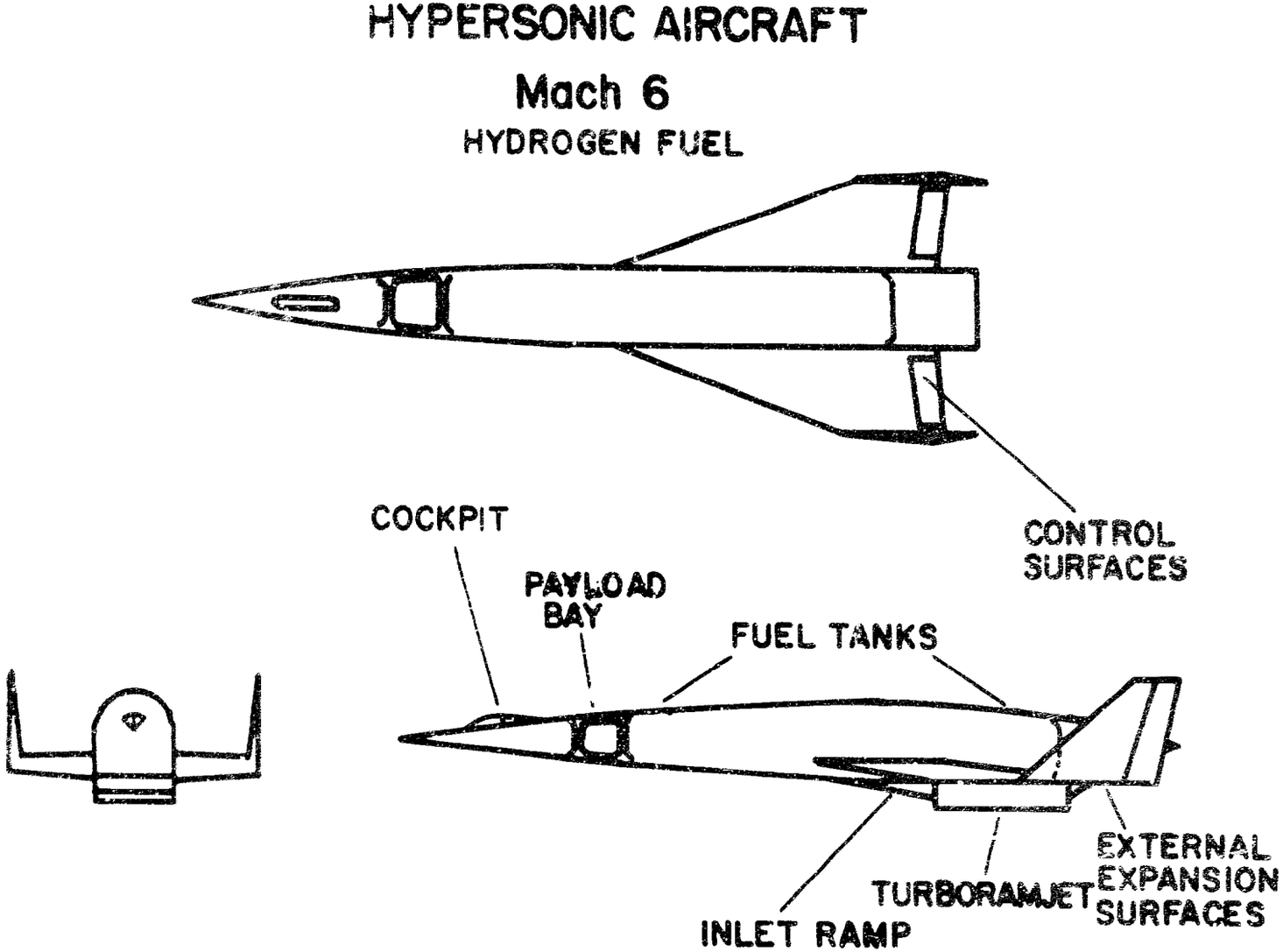

Figure 2 - Typical Configuration of Mach 6 Vehicle

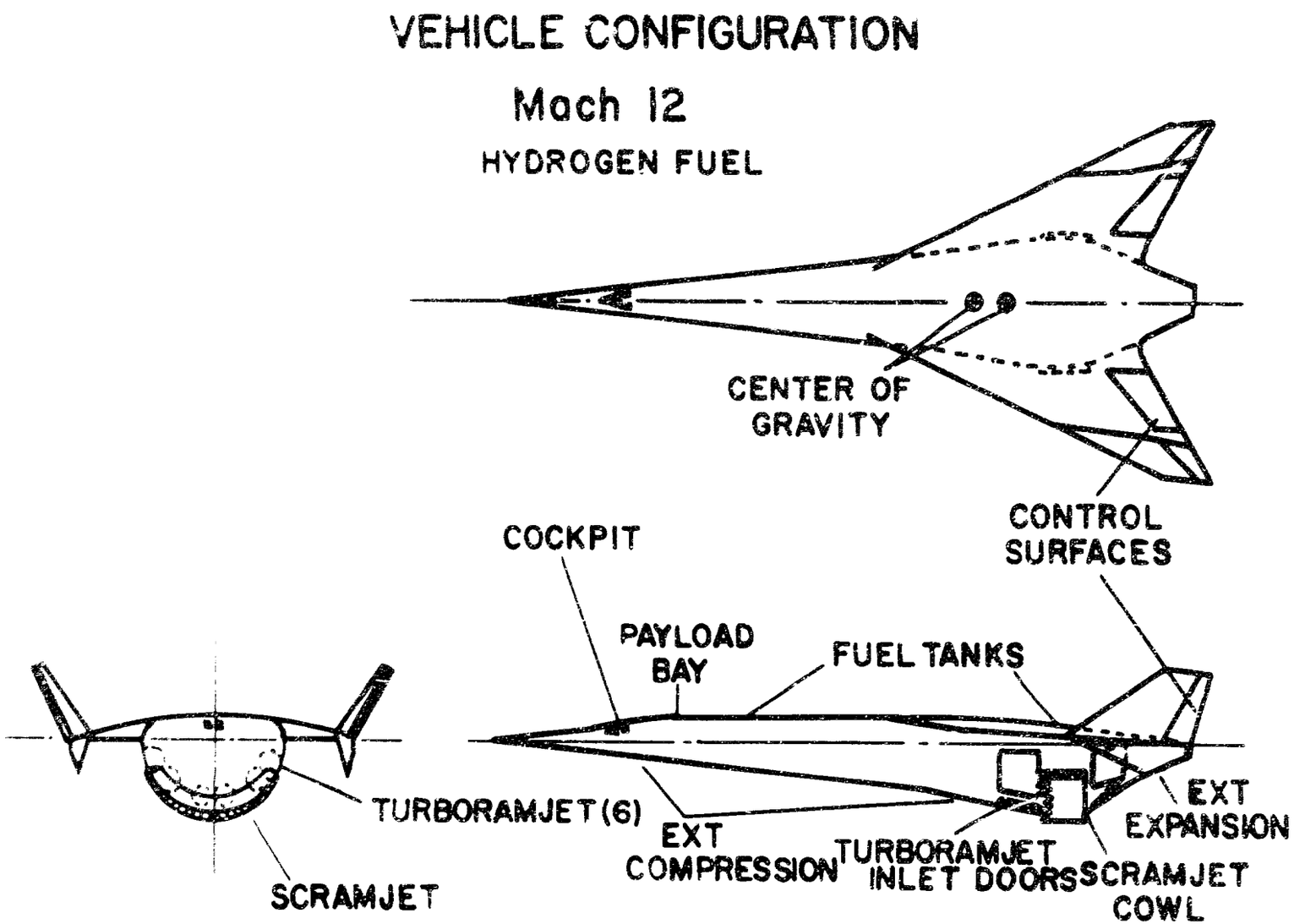

Figure 3 - Typical Configuration of Mach 12 Vehicle

SURFACE TEMPERATURES

M = 6 h = 90,000 ft

DEG. FAHR.

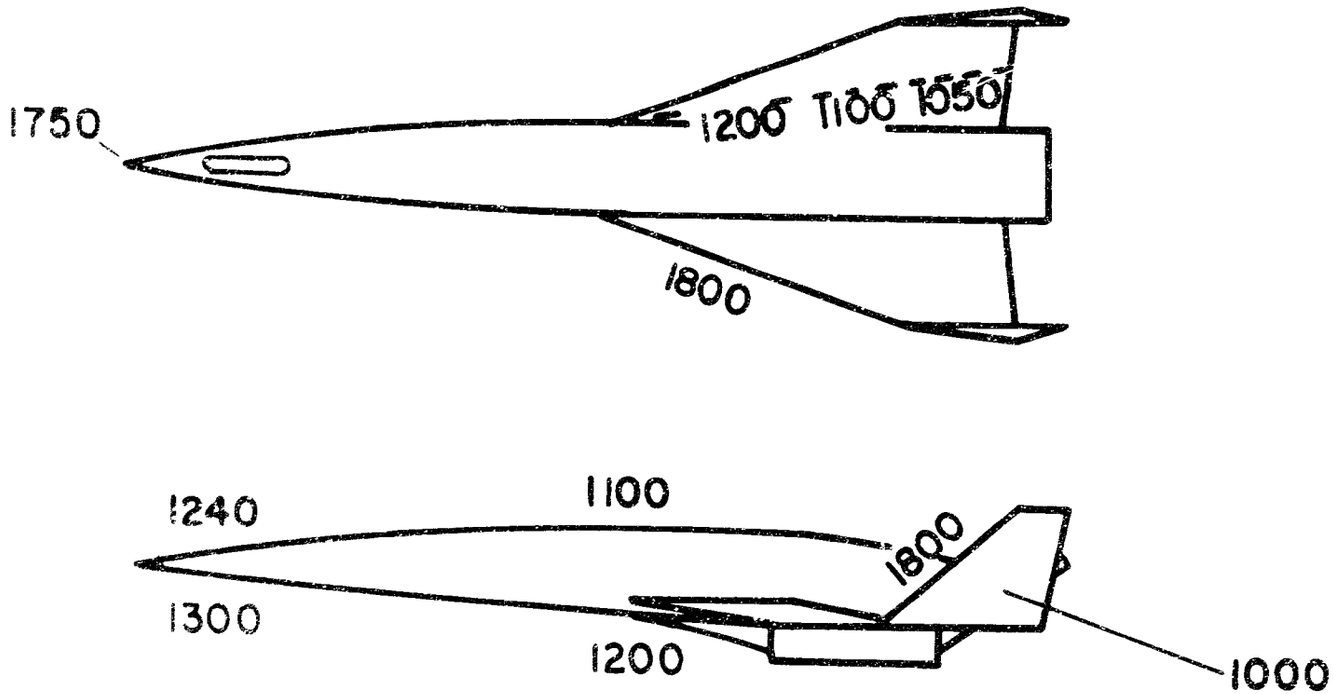

Figure 4 - Predicted Surface Temperatures - Mach 6 Venicle

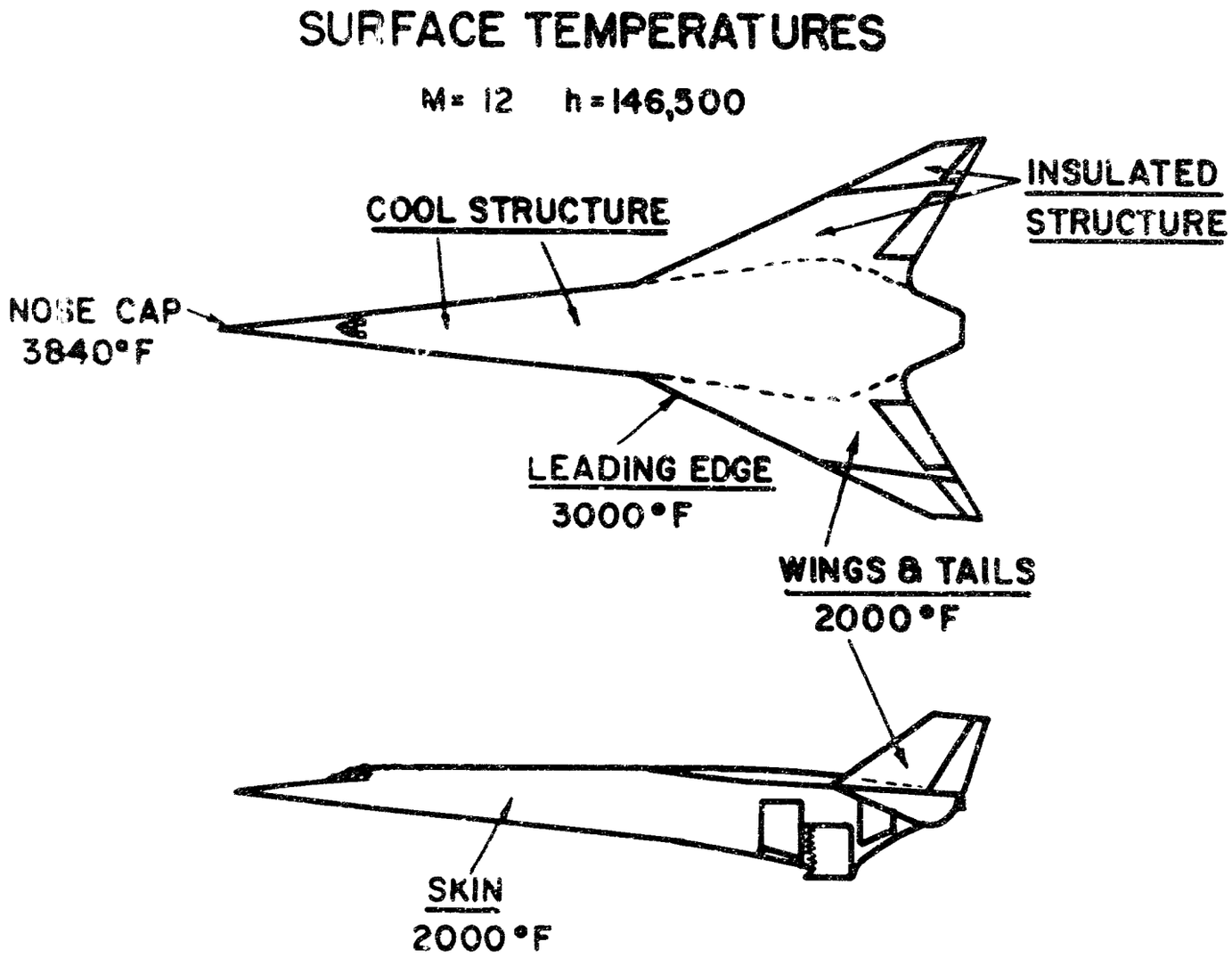

Figure 5 - Predicted Surface Temperatures - Mach 12 Vehicle

This generation of flight vehicles will inherently become much larger in size and weight than its predecessors since much higher thrust propulsion systems are required to operate vehicles in this Mach number speed range. Correspondingly, at these high speeds, higher control surface loadings, more responsive, flight actuation systems having higher positional accuracy will also be demanded for vehicle control.

The results of this study clearly show the need for 1000 F and greater hydraulic systems for future flight control actuation system use if both manned and unmanned hypersonic vehicles are to be realized.

The need for 1000 F systems will also exist in the Mach 3 and above propulsion systems for geometry actuation and other related high temperature control use.

Although a temperature problem has already been encountered in applications where jet engines must operate above Mach 2, this problem is considered by the engine manufacturer to be satisfactorily circumvented by use of cooling in which the vehicle's fuel supply is employed as a heat sink. This and similar methods will continue to be used until the increased system weight and reduced flight profile penalties prohibit further use of such an approach.

A supplemental literature survey was also conducted as part of this study. Two of the vehicles identified on Figure 1 were selected for more detailed investigation because their development status represented the most advanced "state of the art" vehicle designs in regard to both speed and temperature where data was readily available. These vehicles were the X-15 research and the XB-70 experimental aircraft. Technical details regarding the existing flight control servoactuating subsystems of these two vehicles were sought out. As pointed out previously in the case of the X-15 vehicle, it was found that because of the large heat sink available in the fuel supply, the cold soaking prior to flight, and the short flight mission profile, the problem of temperature in the flight surface servoactuating subsystem does not exist. In the case of the XB-70 vehicle system, however, temperature represented a very real problem, which was substantiated by subsequent flight test results. As a result of this study, the XB-70 vehicle was selected as an appropriate vehicle upon which a study of Design Criteria for a Liquid Metal Servoactuating Subsystem for Flight Test Use could be based. Pertinent information on both the elevon subsystem selected for use in this design criteria study, and the proposed liquid metal servoactuating subsystem replacement are described in Section V of this report.

In the XB-70 flight control surface power actuation systems, as in present high Mach engine nozzle actuation systems, heavy reliance upon the fuel supply as a heat sink was used in order to maintain satisfactory operating temperature limits for the system. This has represented a far greater problem in the XB-70 application, since the heat energy level which must be dissipated from the flight actuation system, as well as environmental control for both the crew and temperature sensitive electronic equipment.

The use of liquid metal servoactuating subsystems for both flight surface and engine nozzle actuation applications would considerably reduce the cooling requirements allowing a considerable saving in system weight and an increase in the present mission profile limits on such vehicles. In addition, liquid metal systems would offer higher stiffness and improved response.

The continuation of this application study as part of any further high temperature actuation system investigation is recommended in order to maintain updated assessment of current actuation requirements as well as to keep abreast of changes in these requirements.

Section III

TEST EVALUATION OF EXPERIMENTAL MODEL SERVOACTUATING SUBSYSTEM

In this study, the servoactuating subsystem, represented in the block diagram in Figure 6 and illustrated schematically in Figure 7, was completely assembled and statically tested under various load conditions at fluid and ambient temperatures of 400 F, 750 F and 1000 F in an inert environment. The static tests were performed to evaluate the steady-state positional accuracy, resolution and repeatability of the subsystem. Other tests will also be conducted to ensure that all the system components, instrumentation and auxiliary equipment functioned normally in preparation for future dynamic evaluation of the subsystem.

The initial efforts of this study were directed toward the assembly of the interconnecting plumbing, heating circuits and the related instrumentation requirements between the NaK pump drive enclosure and the servoactuating subsystem components located on the load simulator. Other related efforts requiring re-work and/or additional modification as a result of the previous program efforts were also performed, included:

1. Replacement of the pump heater housing with higher temperature improved heating elements (Figure 8).

2. Installation of supplemental heating elements to the fluid reservoir systems (Figure 9).

3. Fabrication and installation of the torsion bar type spring loading assembly to the load simulator (Figure 10).

4. Replacement of the original NaK to air heat exchanger (cooler) with a new unit of much larger capacity. This modification was required if reasonable temperature control of the servoactuating subsystem is to be maintained.

5. The servoactuating subsystem analysis was updated to incorporate changes resulting from replacement of the pressure control type servovalve (electromagnetic first stage and balanced poppet second state), described in Reference 1, with the flow control valve, (torque motor-jet pipe first stage-spool second stage). This effort also included performing an analog computer evaluation of the final system configuration to determine its predicted performance.

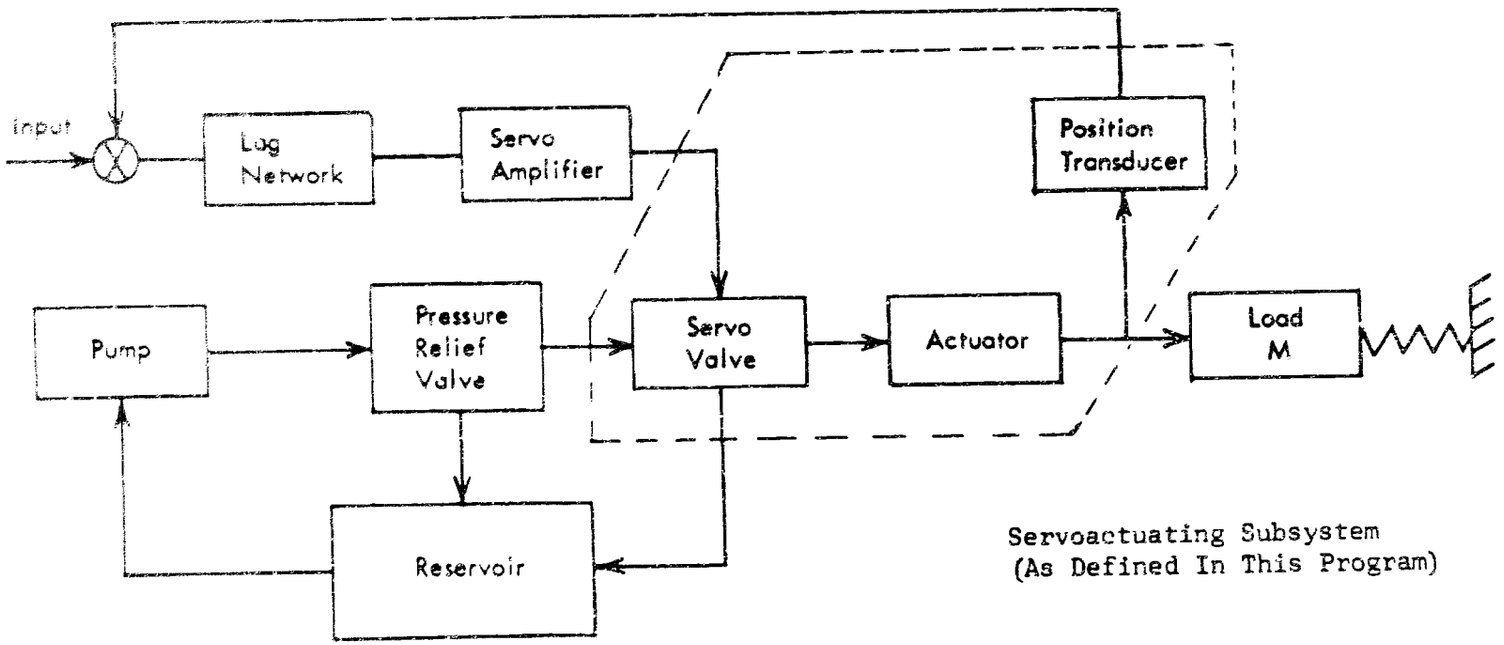

Figure 6 - Block Diagram of Servo Actuating Subsytem

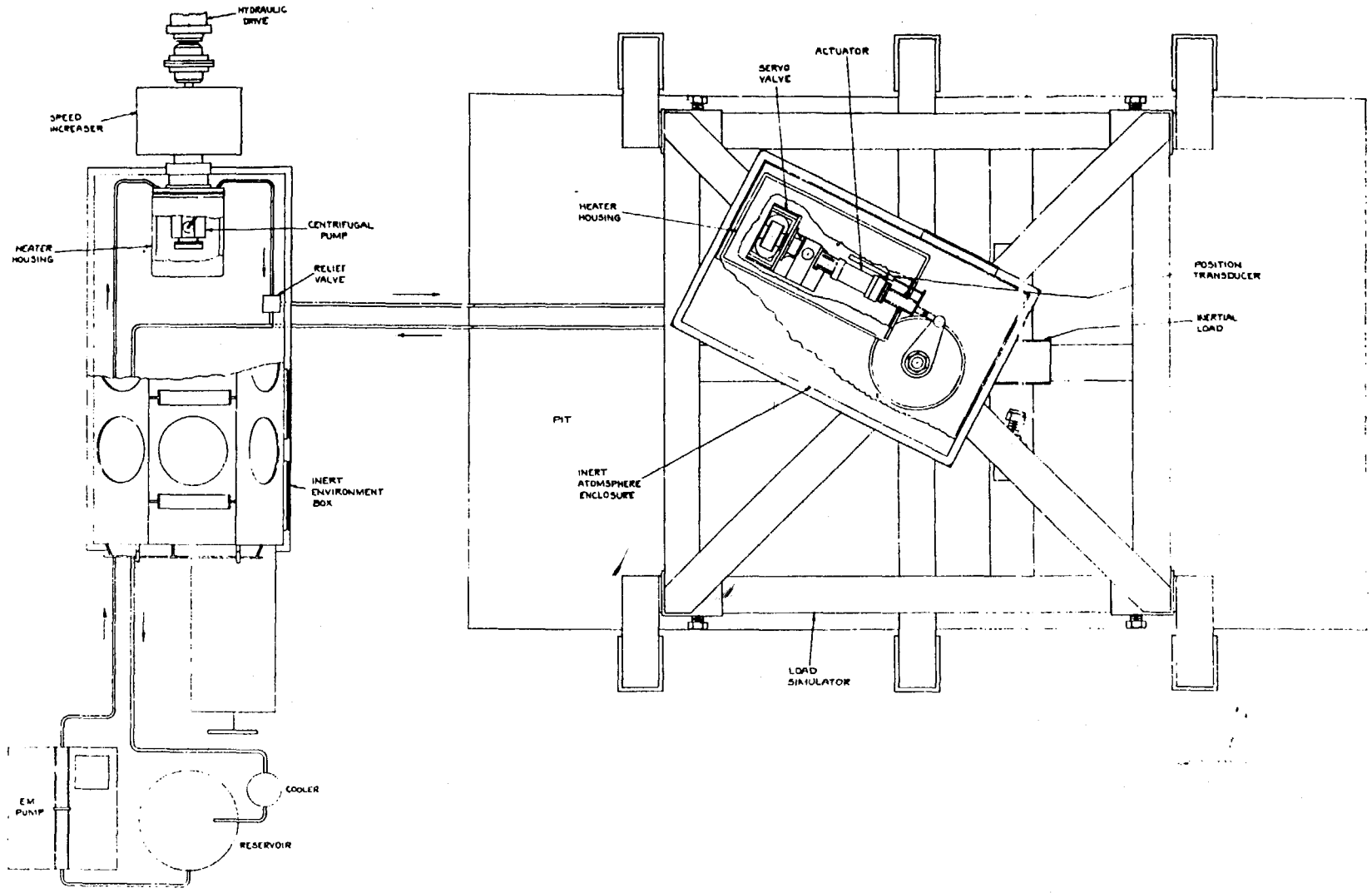

Figure 7 - Schematic of Servo-Actuating Subsystem

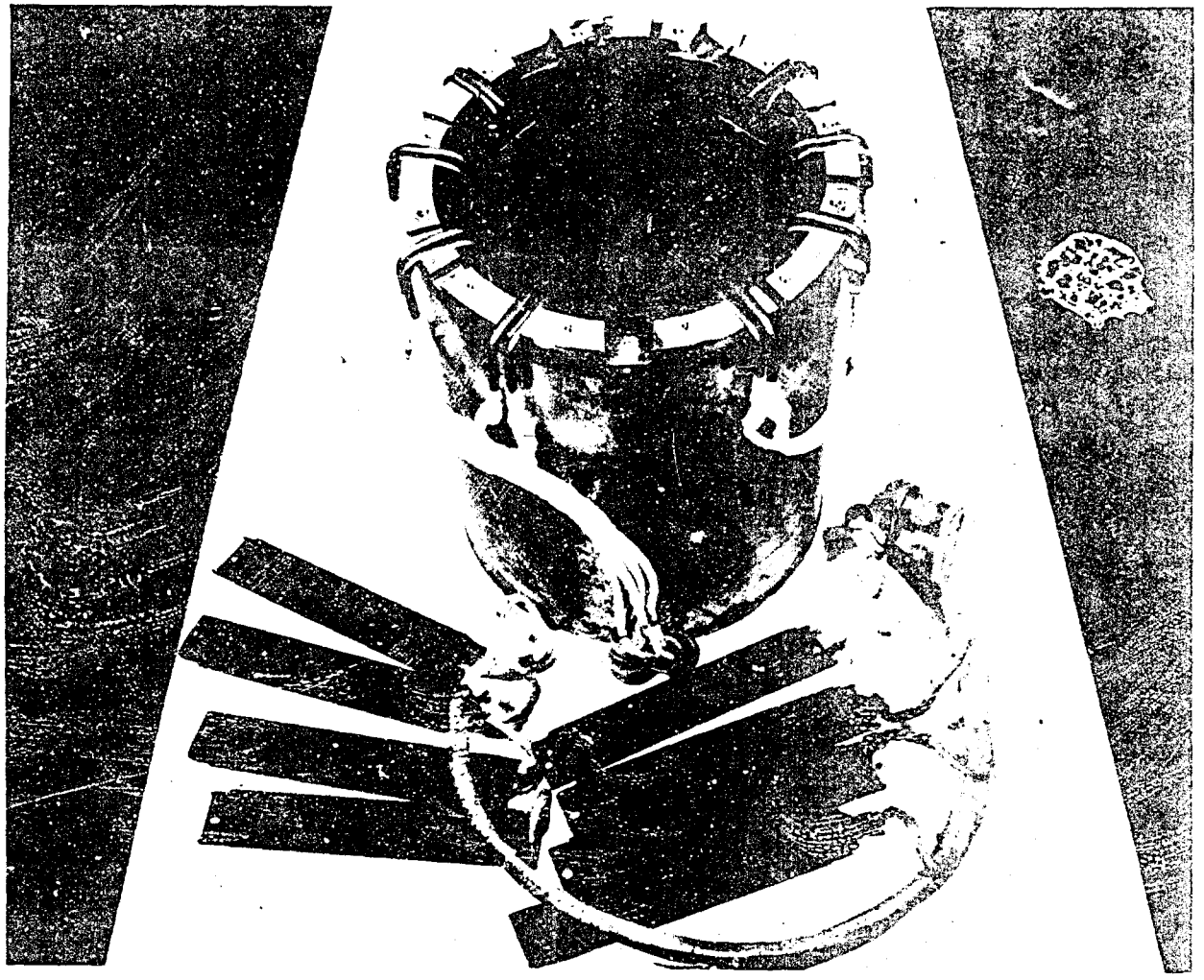

Figure 8 - Pump Heater Housing with Improved Heating Elements

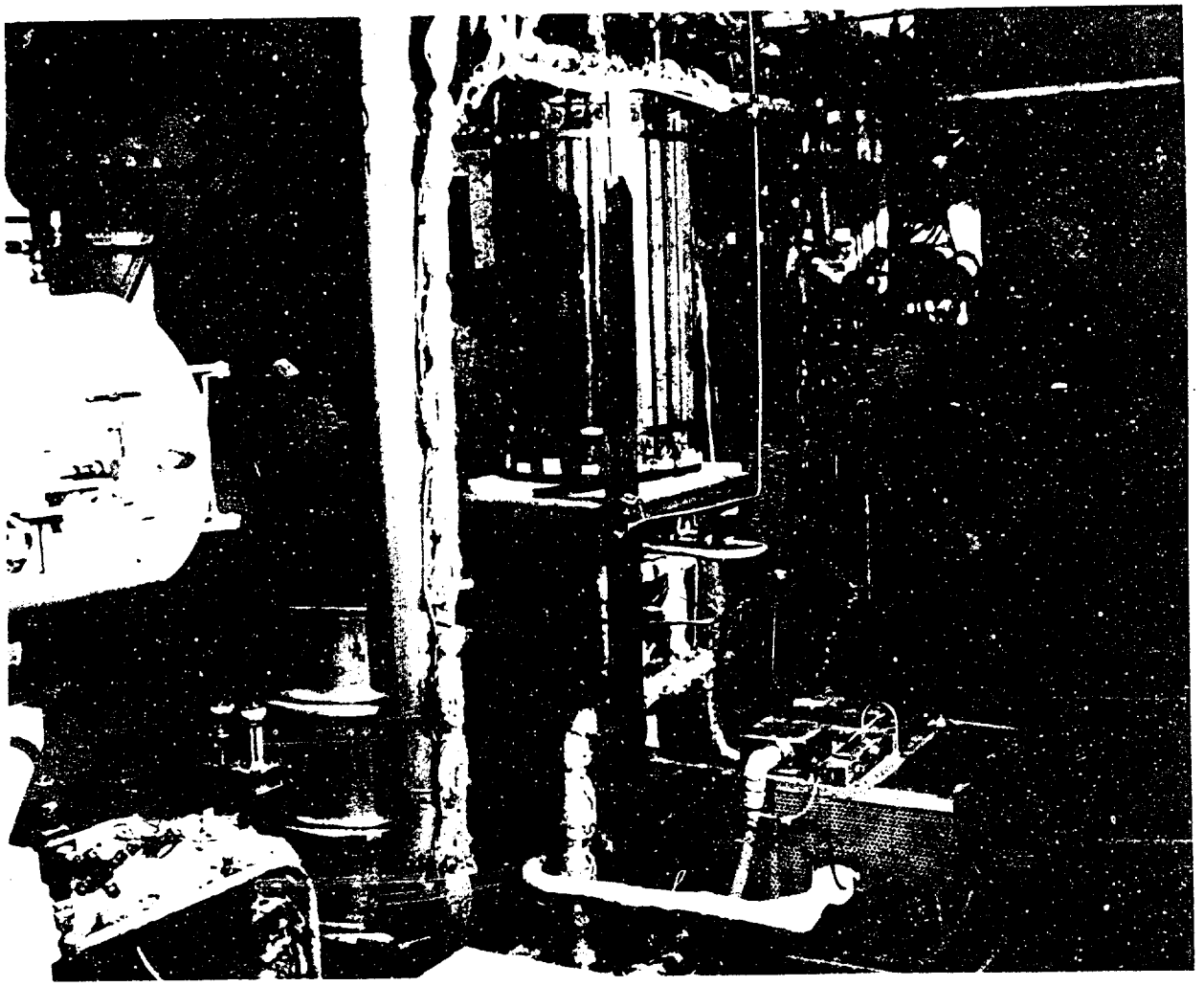

Figure 9 - Fluid Reservoir with Additional Heating Elements

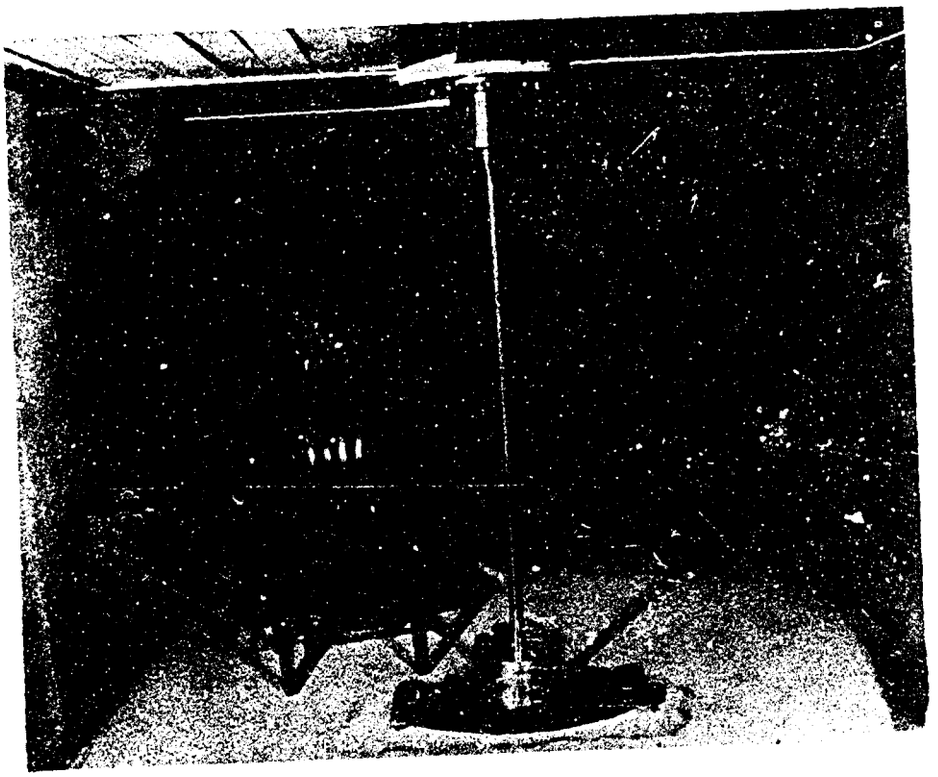

Figure 10 - Torsion Bar Assembly
for Load Simulator

Results of the application study described under Section II indicated that the experimental subsystem design parameters previously established currently remains applicable with one exception, that of system response.

As described in Section II, flight actuation systems possessing higher load carrying capability, improved positional accuracy, and much greater response are the future requirements. Consequently, design changes were made to the experimental servoactuating subsystem to improve its demonstrable response capability from 20 radians/second to 20 cycles/second. Details of this improvement in predicted performance are given in Appendix C.

The revised parameters presently established for this subsystem design are:

1 - System pressure	2200 to 3000 psi
2 - Maximum control flow	7 gpm
3 - Rated load at actuator	Mass 45# Sec.^{2}/ft. Spring 1000#/in.
4 - Maximum load torque	8×10^4 in. - lb.
5 - Closed loop frequency response (20 cycles/sec.)	

The final stages of assembly of the experimental system are shown in Figures 11 and 12. The torque motor and servovalve used in this system are described and discussed fully in Section VI of this report. As mentioned there, some difficulties were encountered with torque motor internal sealing and jet stability under conditions of high pressure. It was expected that these conditions might be aggravated when NaK tests were conducted because of the lower damping value of NaK and the higher temperatures to be attained during test.

Details of the high-temperature position feedback transducer are described in Section VII. Prior to test the transducer was instrumented and checked out and was found to be operating satisfactorily. The linear actuator had been re-designed with a 100-convolution bellows boot, HS-25 high-temperature alloy front bearing, and stepped-type piston rings, after earlier high-temperature tests had shown the need for improvement in these areas.

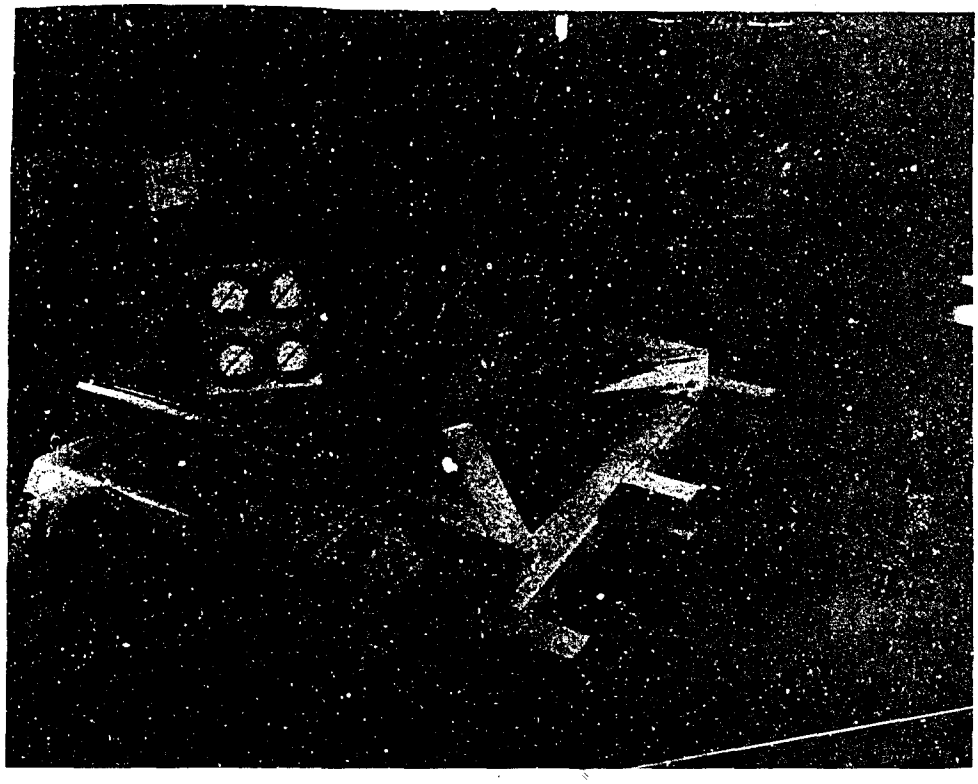

Figure 11 - Overall View of Experimental Servo Actuating Subsystem

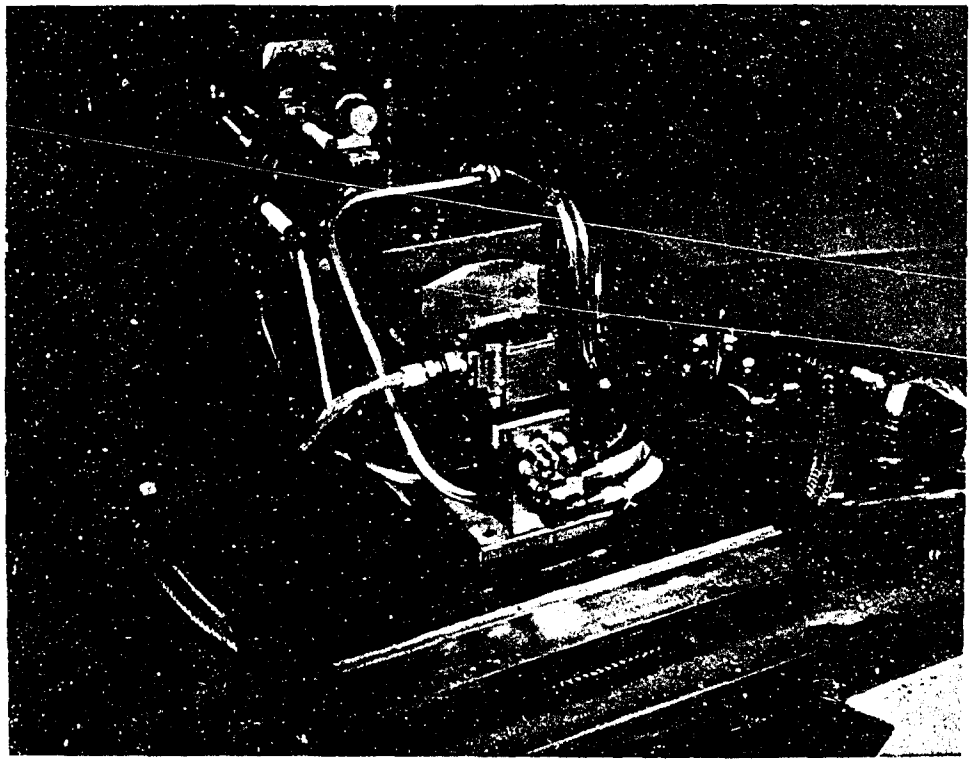

Figure 12 - Assembly of Experimental Servo Actuating Subsystem

Since the primary purpose of these tests was to establish the feasibility of an electro-hydraulic servoactuating subsystem using NaK-77 as the hydraulic fluid, no provisions were made for closed-loop operation. Position control was accomplished by manual adjustment of torque motor differential current. A low-frequency oscillator was included in the circuit to provide cyclic motion of the load.

At the initiation of testing it was found that the torque motor exhibited marked instability at the planned supply pressures and it was necessary to operate at a pressure of 1000 psi. The first test, conducted at approximately 450 F was entirely satisfactory. All components performed well and the load control was excellent. It is particularly significant that this test represents the first time that an electro-hydraulic servoactuating subsystem has been successfully operated with NaK-77. It was noted, however, that an accumulator would have been desirable and will be a necessity before satisfactory dynamic testing can be conducted. At the same time, as would be expected, overall performance is degraded by the necessity of using one-third rated supply pressure in this particular servovalve.

Following this test, temperature was increased while the system continued operating. At 575 F, a sealing flange in the servo supply line began leaking and NaK escaped into the open air. It is interesting that even at this temperature there was no evidence of combustion and the fluid merely dripped onto the steel structure and oxided over. In the interests of safety the test was terminated until the leak could be repaired. The system had operated for over two hours at temperatures approaching 525 F.

In the design of the system NaK leakage past the linear actuator rod seal is conducted through flexible tubing to a weigh tank with an inert gas cover. No leakage was noted during the first test. The shaft seal is of the reed type and is a procurred item. The best available material at the time of procurement was HS-25 alloy which has excellent compatibility with NaK. Its thermal match with the 422 CRE steel piston rod is less than ideal, however, and the optimum amount of pre-stress to be applied to the seal is not known exactly. Previous actuator tests had indicated that normal stressing was not sufficient to maintain a good seal over a wide temperature range. In the present tests, somewhat greater than normal pre-stress was applied, but it was expected that some leakage might occur at temperatures in excess of 750 F.

Upon resumption of tests continuous observation of the weigh tank was made to check seal efficiency. As temperature was increased, the actuating subsystem was operated both manually and cyclically and performance of all components was normal up to 700 F. At this point, seal

leakage was first observed. Operation was continued until the weigh tank filled at around 750 F. Testing was terminated when weigh tank overflow appeared in the inert atmosphere enclosure. At this time, an additional 2 1/2 hours of operation had been accrued. Temperature of the servovalve and torque motor at this time approached 800 F.

Additional tension was applied to the shaft seal. Since it was felt that this might be excessive at lower temperatures and the final test was to be run around 1000 F it was decided not to cycle the actuator until a temperature of at least 900 F was reached. However, the subsystem was gradually heated so that thermal shock would be minimized when the inlet valve was opened. The subsystem is connected to return at all times, so that the shaft seal was exposed to normal drain pressure as it is during operation.

With the centrifugal pump output temperature approaching 930 F and the servoactuating subsystem temperature above 1000 F, 1000 psi was applied to the servo. Within a short time the fuse in the torque motor amplifier opened and NaK was evident in the inert atmosphere enclosure. Since it was obvious that NaK had shorted the torque motor coils the test was terminated.

Upon disassembly of the system it was determined that an internal seal in the torque motor had failed, allowing NaK to penetrate into the normally dry coil enclosure, as shown in Figure 13. Since this enclosure is not tightly sealed the NaK had shorted the coils and oozed out into the inert atmosphere glove box. Examination of all other components, such as the servovalve, actuator and transducer, showed them to be in excellent condition, with no evidence of leakage. Figure 14 shows the tungsten carbide valve spool after oil and NaK tests. There was only minor scratching of the surface and no evidence of erosion around the receiver ports. No shaft seal leakage was observed during this test which was run over a period of 5 hours.

There is reason to believe that the NaK leakage in the torque motor occurred over a long period of time and was not evident until the NaK level reached the top of the enclosure, to short the coil leads. It is reasonable to assume that had this not occurred, the servoactuating subsystem would have functioned satisfactorily at 1000 F or higher.

Although the tests did not reach the design goal of cyclic operation at 1000 F, they represent a significant breakthrough in the actual operation of a NaK-77 hydraulic servo at elevated temperatures. The results fully justify modification of the torque motor to eliminate the questionable areas and resumption of testing at the 1000 F level.

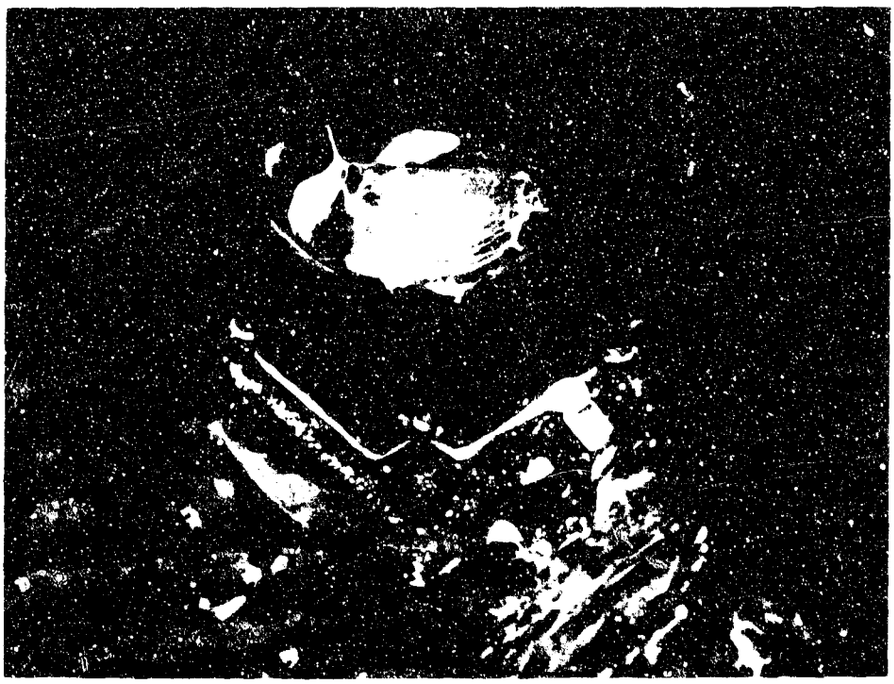

Figure 13 - Torque Motor Showing NaK Leakage Around Coils

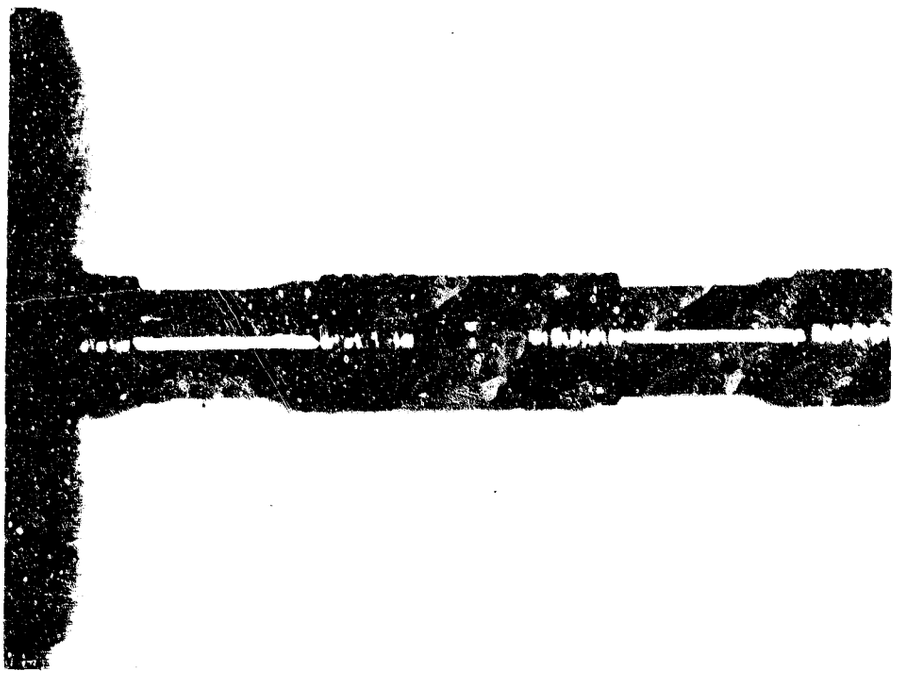

Figure 14 - Servovalve Spool After NaK Tests

Section IV

AIR/NUCLEAR SYSTEMS

Because liquid metal hydraulic systems will be required to operate in an air environment and, very possibly, in the presence of high nuclear radiation, this phase of study considers the design of a system capable of evaluation under these conditions.

The primary objective of the study was to design a test system which, when tested, would provide data to allow evaluation of the following:

a) Steady-state and dynamic performance characteristics.

b) Design criteria relating to system maintenance, servicing, and handling requirements in an air environment.

c) Suitability as to radiation tolerance, life, and reliability in a nuclear environment.

d) Type of equipment malfunction or failure under the specified environmental and test conditions when test evaluations are conducted.

Design criteria and test data generated under Sections III, VI, VII and VIII of this report were used in arriving at a final configuration.

As an initial step, a survey of available nuclear facilities was made and a test site selected. This is the Nuclear Engineering Test Facility of the Air Force Institute of Technology, located at Wright-Patterson Air Force Base, Ohio. The use of this reactor is available without charge for work being done under Air Force contracts.

Table I is a listing of the maximum experimental neutron and gamma fluxes available. The test cell for installation of experiments is 5' x 10' x 4'. Electrical power, compressed and coolant air, and water is also available.

A design layout of the test system is shown in Figure 15 The basic components are a pump, pressure regulator, electro-hydraulic servovalve, linera actuator, and electrical position feedback transducer. The pump is directly driven by a high-speed air turbine.

Tentative system parameters are as follows:

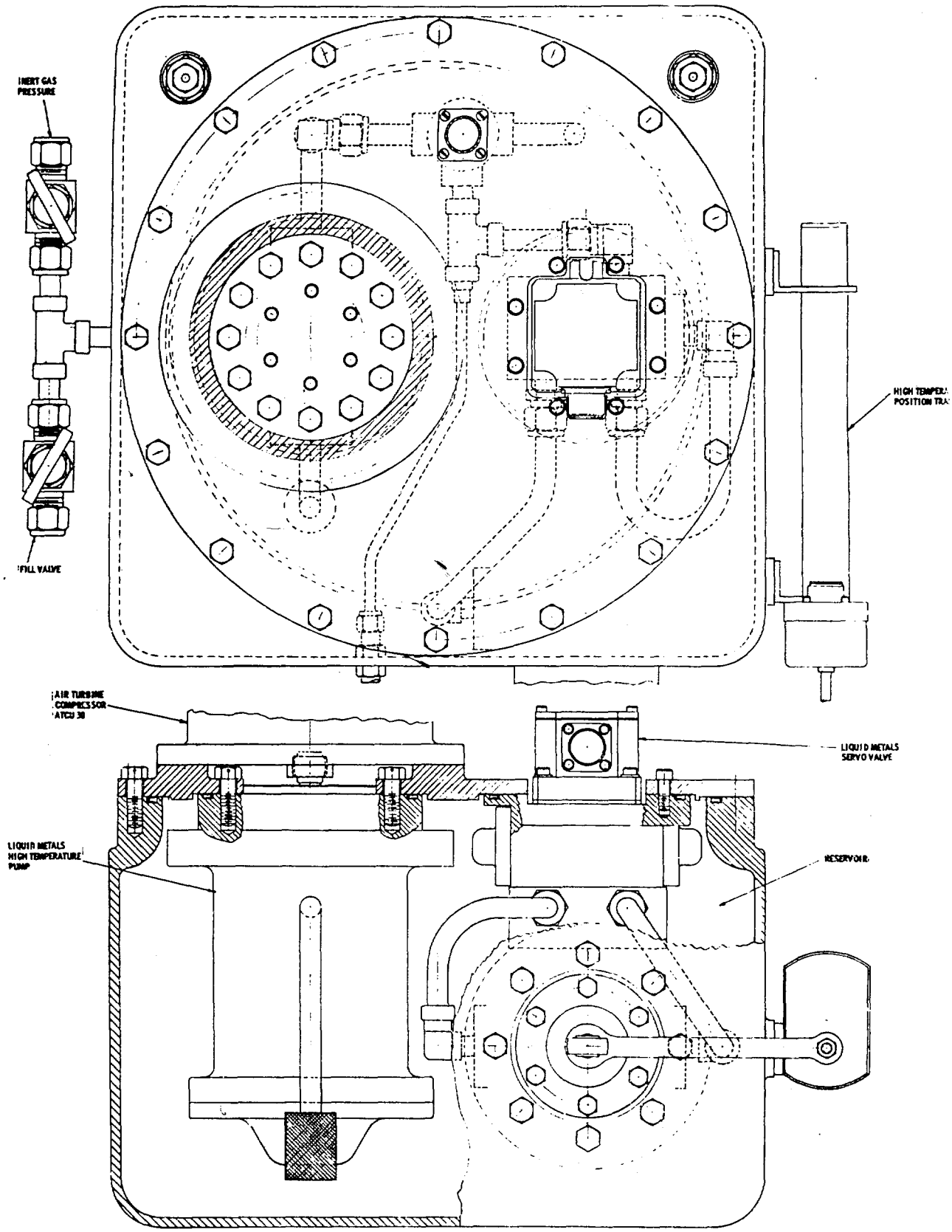
INERT GAS
PRESSURE
FILL VALVE
HIGH TEMPER
POSITION TRA
AIR TURBINE
COMPRESSOR
ATCU 30
LIQUID METALS
SERVO VALVE
LIQUID METALS
HIGH TEMPERATURE
PUMP
RESERVOIR

Figure 15

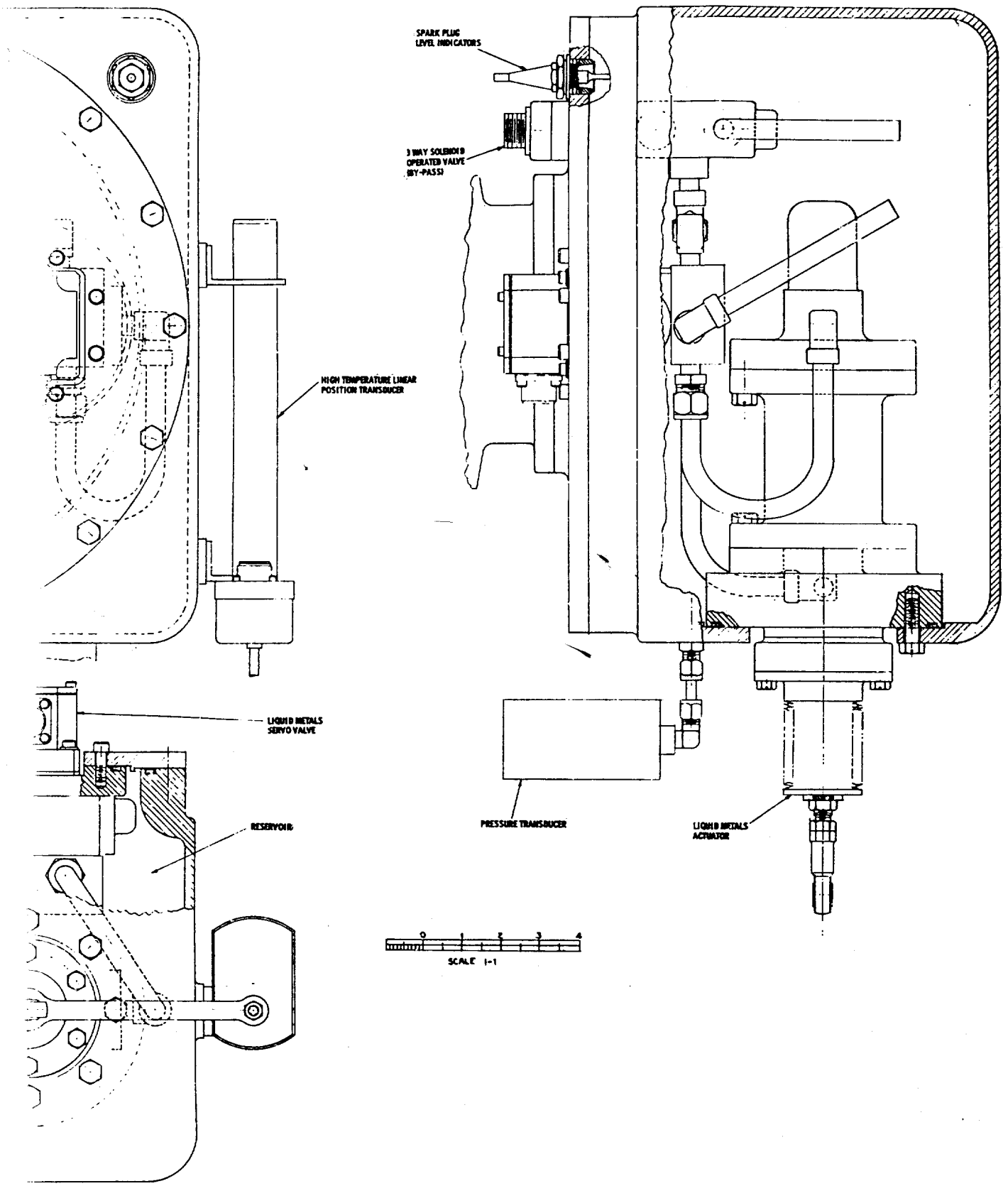

Figure 15 - Layout of Air/Nuclear Test System

B

Fluid - NaK-77

Pump output pressure -	2200-3000 psi
Pump Flow -	10-15 gpm
Pump Speed -	35,000-40,000 rpm
Servovalve flow, maximum-	5-7 gpm
Fluid temperature - maximum -	1000^{O}F.
Ambient temperature - maximum -	-1200^{O}F. *

*Does not include air turbine or electronic equipment.

DETAIL DESIGN

The pump drive, shown in Figure 16 is the turbine section of an AiResearch Mfg.. Company air turbine compressor unit Model ATCU30. This unit can be operated with a large number of combinations of total pressure ratio and nozzle area to provide a range of power and speeds.

Assuming pump speed of 40,000 rpm, output pressure 2500 psi, output flow 15 gpm, and pump efficiency of 60 percent,

$$\text{Pump input power} = \frac{2500 \times 15}{1714 \times 0.60} = 36.5 \text{ HP}$$

For the turbine, assume,

Turbine inlet total pressure	187 in. Hg. abs.
Turbine inlet total temperature	746.5^{O}R.
Horsepower	40
Speed	40,000 rpm
Turbine outlet total pressure	29.92 in. Hg. abs.
Pressure ratio	6.25/1

From AiResearch Mfg. Co. report AAC - 3827-R

$$\delta_1 = \frac{187}{29.92} = 6.25$$

$$\theta_1 = \frac{746.5}{518.4} = 1.4400 \qquad \sqrt{\theta_1} = 1.20$$

$$\frac{HP}{\delta_1 \sqrt{\theta_1}} = \frac{40}{(6.25)(1.20)} = 5.333 \text{ HP (corrected)}$$

$$\frac{N}{\sqrt{\theta_1}} = \frac{40,000}{1.20} = 33,300 \text{ rpm (corrected)}$$

BLANK PAGE

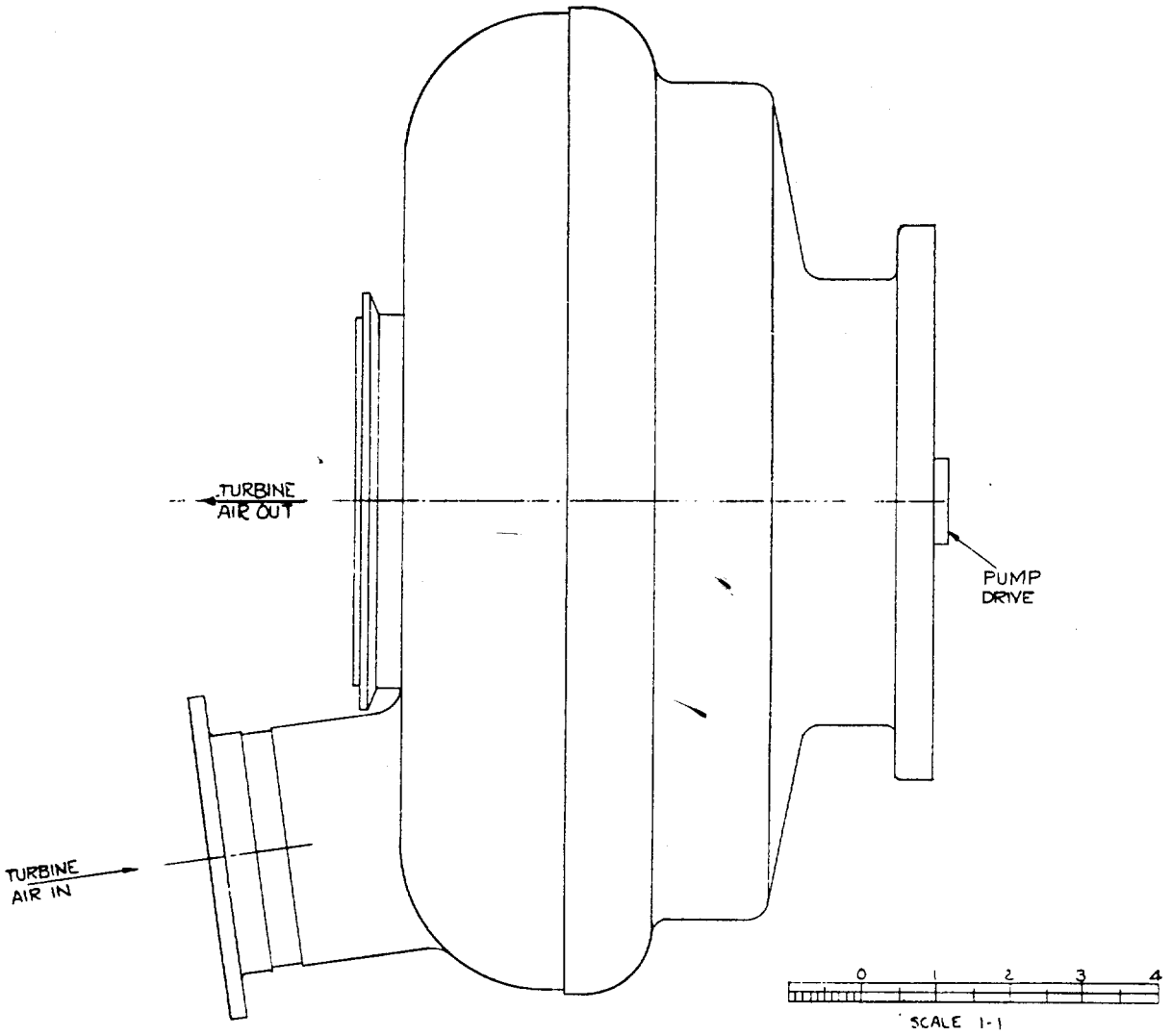

Figure 16 - Air Turbine Pump Drive - Air/Nuclear Test System

For $P_{IT}/P_{2T} = 6.25$ ($A_G = 0.5$ in^2) and

$N/\sqrt{\theta_1} = 33,300$, $HP/\delta_1\sqrt{\theta_1} = 7.2$

Taking A_G as 0.5 in^2 and referring to Figure 10 of the report, for

$P_{IT}/P_{2T} = 6.25$ and $N/\sqrt{\theta_1} = 33,300$ read off

$W_t\sqrt{\theta_1}/\delta_1 A_G = 18.65$

$$\frac{W_t\sqrt{\theta}}{\delta_1} = 18.65 \times 0.5 = 9.33 \text{ lb/min.}$$

$$W_t = \frac{9.33 \times 6.25}{1.20} = 48.6 \text{ lb/min.}$$

This will be the weight flow required from the compressor at approximately 90 psi pressure.

The pump is a four-stage, balanced centrifugal unit with hydrostatic journal and thrust bearings, and a bellow-type shaft seal. It is mounted vertically and the pump inlet is submerged. Supercharge pressure is supplied by pressurizing the stainless steel reservoir with inert gas. The pump is built of TZM molybdenum alloy with the exception of bearings and shaft seal.

The servovalve is identical with the unit described in Section VI except that the spool diameter is somewhat smaller due to the lower flow requirement. The valve is mounted in the reservoir, eliminating the need for a return line. The torque motor portion, as shown in Figure 15, is external to the reservoir because of the need for isolating the electrical connections from NaK.

The general configuration of the actuator, including the bellows shaft seal, is of the type described under Section VII. A probable modification would be the substitution of a borided molybdenum cylinder for the present stainless steel cylinder with titanium carbide liner, and a borided moly shaft for the present tungsten carbide flame plated stainless steel.

The position transducer, also described in Section VII, must be externally mounted. It is, however, designed for the maximum ambient temperature of 1200°F.

Since pump capacity is considerable in excess of the maximum flow requirements, no accumulator is included in the system. The pressure regulator is a conventional, high-temperature type which has been in use for several years in the NaK test loops.

The philosophy in the design of this system was to provide an integral package which would be capable of operation in an air environment. Due to the nature of the working fluid it is not practical to have interfaces such as shaft seals directly exposed to an air environment. Isolation of the fluid must be provided by means such as actuator boots or an inert gas interface at points such as the exit of rotating shafts. Consequently, the test system described in this Section may be considered as a developmental model of a working system such as that covered in Section V.

Test evaluation of the system would involve operation at room temperature and elevated temperatures to assess the effect of temperature on such parameters as positional accuracy, resolution, repeatability and frequency response. Similar tests would be conducted in a nuclear environment to determine material changes and heating effects. At present, no time duration for these tests has been established. A post-test examination would be made after radioactivity has decayed to an acceptable level.

TABLE I

MAX. EXPERIMENTAL FLUXES[1] AVAILABLE (PRELIMINARY CALCULATIONS)[2]

LOCATION	FAST ABOVE 0.2 MEV N/CM^2 - SEC	INTERMEDIATE 0.6 EV TO 0.2 MEV N/CM^2 - SEC	THERMAL BELOW 0.6 EV N/CM^2 - SEC	GAMMA DOSE RATE ERGS/GM. CARBON-HR.
IN-CORE	2×10^{15}	1×10^{15}	1×10^{15}	2×10^{11}
TEST CELLS	8×10^{13}	7×10^{13}	6×10^{12}	
BSF	2×10^{13}	4×10^{13}	8×10^{13}	4×10^{10}
THERMAL COLUMN VOID WITH H_2O	2×10^{9}	8×10^{9}	2×10^{10}	4×10^{8}
HORIZONTAL BEAM TUBES (AT CORE END) WITH H_2O	1.0×10^{13}	2×10^{13}	5×10^{13}	4×10^{10}

(1) Variations of flux intensity and ratios can be affected by offset fuel loading of the core and/or the use of temporary shielding.

(2) To be confirmed during checkout and reported through the Radiation Effects Information Center publications.

Section V

DESIGN CRITERIA FOR FLIGHT TEST SYSTEM

Since the ultimate application of the high-temperature liquid metal system being developed in this program is flight control, this phase of effort is concerned with the selection of an appropriate vehicle and the delineation of design criteria for a flight testable sub-system.

There are no vehicles available which operate at sustained surface temperatures above 1000 F. In lieu of this, the XB-70 operates with a bulk oil temperature around 450 F and requires cooling to maintain this temperature. It was felt, therefore, that a reasonable evaluation might be made by substituting an uncooled liquid metal system in one of the XB-70 control channels. Further, the elevon sub-system of the XB-70 has a configuration which would allow substitution of a liquid metal actuator without significantly affecting overall operation in the event of a malfunction of the liquid metal equipment.

The elevon control consists of 12 panels, each of which has two hydraulic actuators in parallel. The actuators have a 4.8" bore and a 2.0" rod, a stroke of 7.375" and operate with a nominal hydraulic pressure of 3600 psi. Servovalves are mechanically actuated, with mechanical feedback. Synchronization is maintained by operating all valves with a common linkage.

Based on similar dimensions, but with an electro-hydraulic servovalve and electrical feedback, an actuator design was evolved as shown in Figure 17. The actuator is fabricated of TZM molybdenum alloy with cylinder bore and piston rod borided. The rod is protected from atmosphere by a welded bellows boot filled with inert gas. An annulus internal to the rod seal, and the tail rod housing are connected to drain pressure. The servovalve is mounted directly on the actuator and manifolded to minimize external piping.

The original input linkage is used to actuate a high-temperature potentiometer whose output is combined with the feedback transducer signal to produce an error signal to drive the servovalve torque motor. The servovalve is a two-stage, jet pipe design similar in construction to the valve described in Section VI.

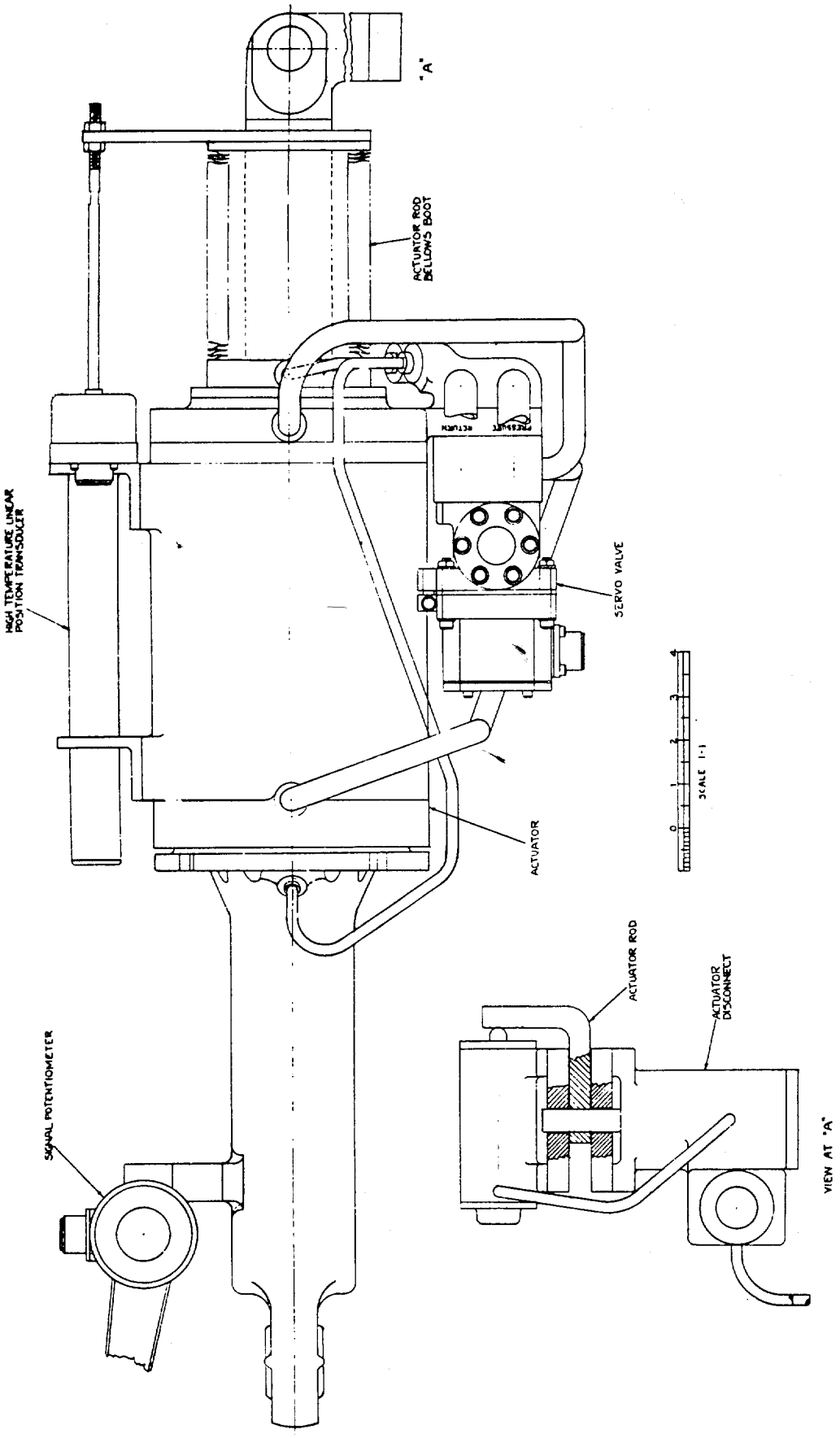

Figure 17 - Actuator for XB-70 Elevon Control

The original #4 (right side or left) hydraulic actuator is removed and the liquid metal actuator substituted. The installation is shown in Figure 18. In order to disable the liquid metal actuator in case of failure, a hydraulic disconnect is provided. This is manually operated through a solenoid valve. In the event of failure, hydraulic pressure is applied to withdraw the pin from the hinge bearing. Additional motion pushes the piston rod free of the hinge so that the actuator drops out of the way. The elevon panel can still be moved, with reduced capability, by the remaining hydraulic actuator.

The liquid metal pump and reservoir are located in the fuselage. Consideration was given to APU, air turbine, or hydraulic motor drives for the pump. The APU was ruled out on the basis of size and complexity. Air turbine drive would have required the installation of considerable ducting as well as bleeding a large quantity of air from the engine compressors.

Since theXB-70 has adequate installed hydraulic horsepower it was decided to use hydraulic drive coupled to the pump through a gear-type speed increaser. Information was obtained from Vickers, Inc., indicating that a B-70 PV-175 utility pump could be converted to a hydraulic motor, The operational data on this unit is as follows:

Displacement	2.69 in^3/rev.
Pressure	2500 psi
Speed	5000 rpm
Temperature	400 - 450 F (maximum)
Weight	60 $\pm$ 5 pounds
Fluid	Oronite 8515

The motor would have an output of approximately 72 HP which would be adequate for the system.

The pump is a four-stage centrifugal rated at 16 gpm and 4000 psi at 40,000 rpm. It has an estimated efficiency of 60 $^{o}/o$ or a power input of 62 HP.

Maximum required flow to the servovalve, including jet pipe flow and valve leakage, is approximately 15 gpm. For this reason the flight test hydraulic system does not have an accumulator.

The pump-reservoir is similar to that described for the air/nuclear tests (Section IV), using an inert gas pressurized reservoir to supply inlet pressure for the pump. The liquid metal power supply is shown in Figure 19.

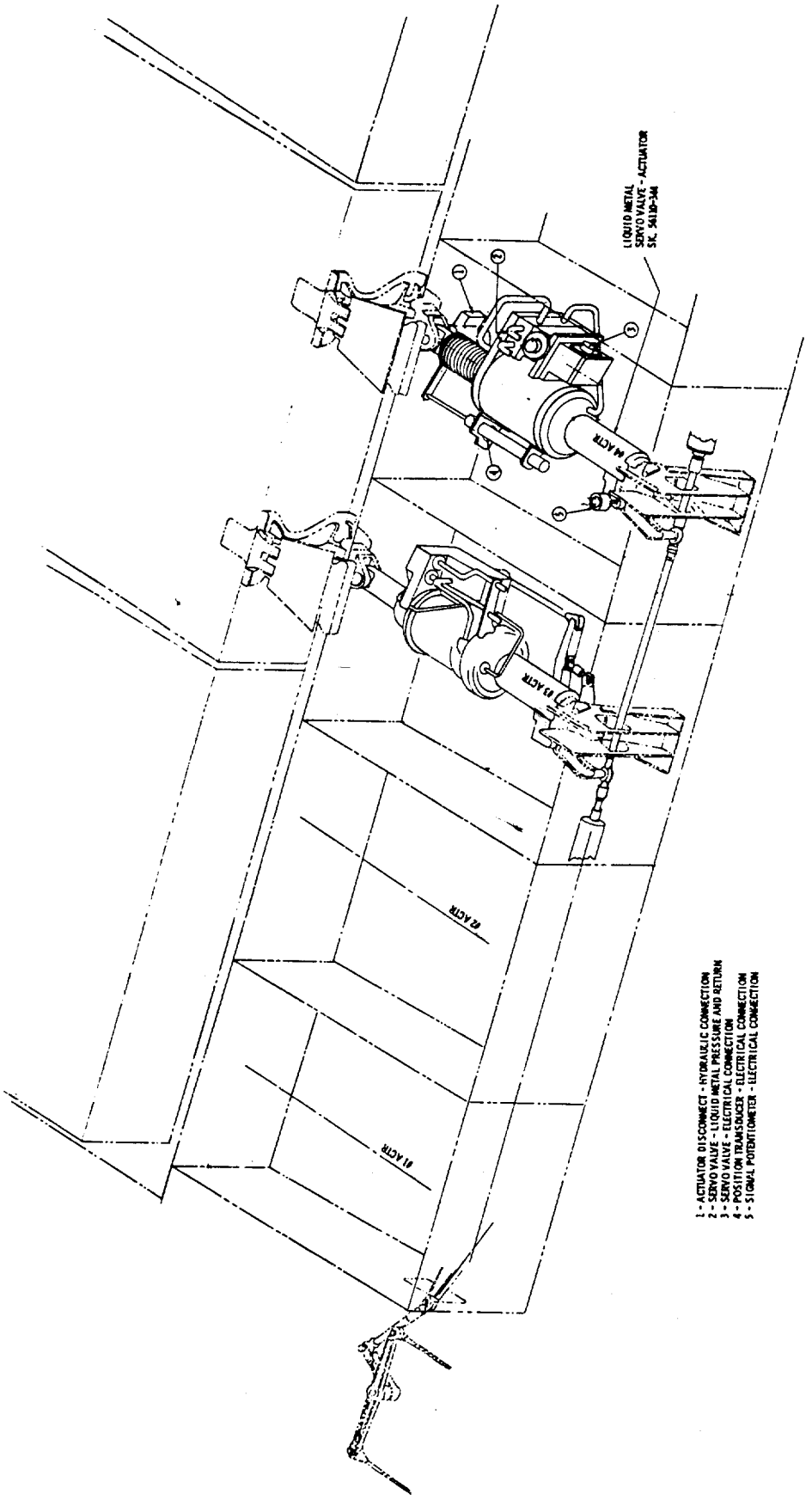

Figure 18 - Installation of Actuator in XB-70

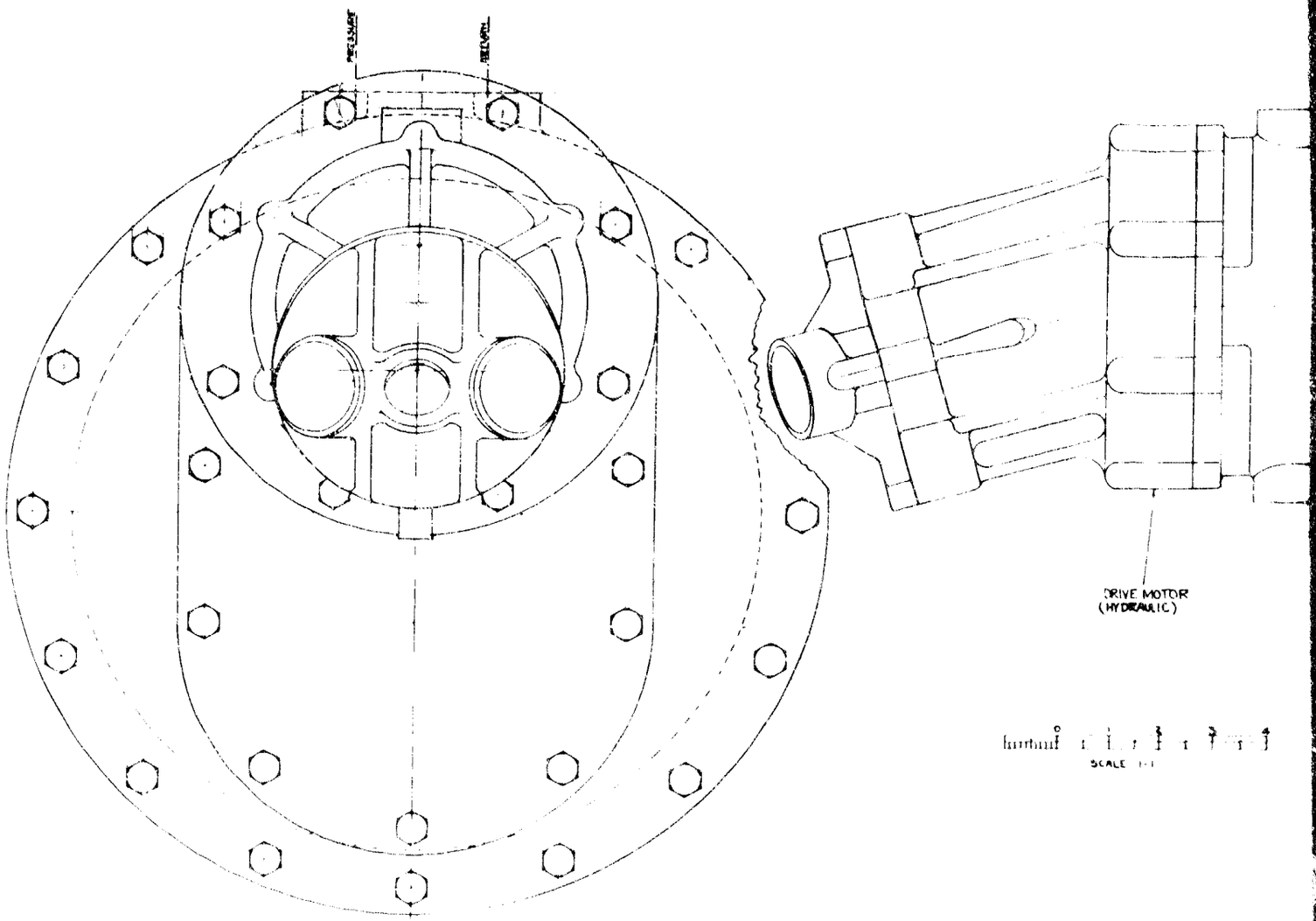
DRIVE MOTOR
(HYDRAULIC)

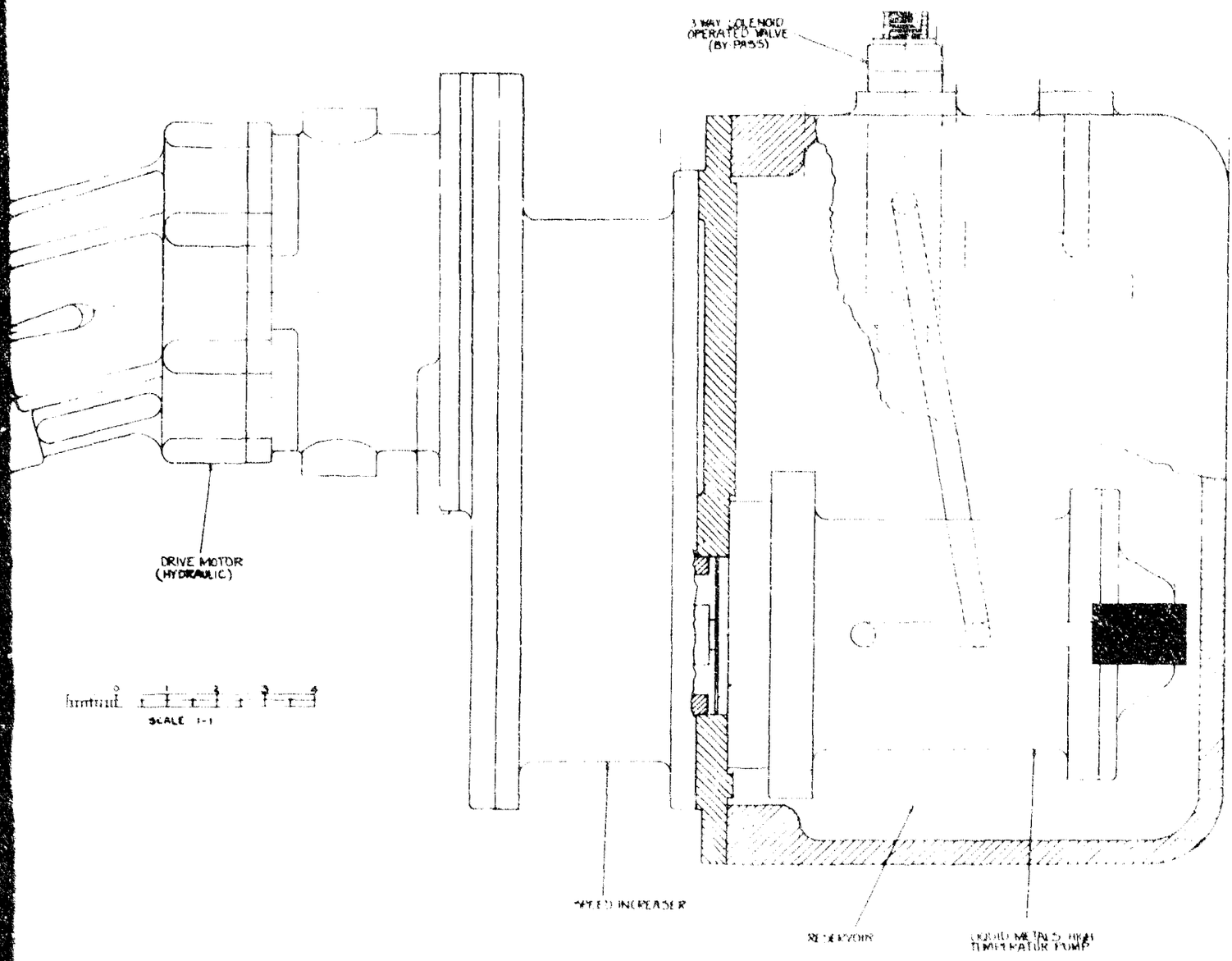

Figure 19 - Hydraulic Power Package for XB-70 Elevon Control

Section VI

SERVO CONTROL VALVES FOR SERVOACTUATING SUBSYSTEM

The successful development of an electro-hydraulic servovalve is an essential prerequisite for the evaluation of a high temperature, liquid metal servoactuating subsystem. The object of this study was to produce a practical servovalve to be used in the test evaluation of the experimental model servoactuating subsystem described in Section III.

During previous contacts a unique, high temperature servovalve was developed and tested for feasibility. This valve utilized a miniature electromagnetic pump as a combined transducer and pilot stage, driving a poppet-type second stage through differential bellows. The valve was a pressure control type rather than the more common flow control servovalve.

Testing of this valve revealed several shortcomings. In particular, it was found that the poppets, being unguided, failed to provide controlled modulation around null. This is illustrated in the curves of Figure 20 which shows that no repeatable flow data round null could be obtained. In addition, it was decided that a flow control design should be pursued as being more universally applicable to hydraulic servo systems.

It was therefore recommended that the valve be redesigned while rataining the electromagnetic pump pilot stage if possible.

PROGRAM OBJECTIVE

This phase of the liquid metal program had as a prime objective, the study of two-stage, flow control valve designs suitable for use in high performance, high-temperature-pressure liquid metal servoactuating subsystems. If at all possible, the electromagnetic first stage and balanced poppet second stage concept was to be utilized. At the same time however, other concepts were to be examined and a critical comparison made.

In order to broaden the technical base for this study, arrangements were made with the Battelle Memorial Institute, Columbus, Ohio , for consultation services. The results of these consultations are contained in Appendix D. Their past experience, both in liquid metals and servovalves, was to be utilized to review design concepts and suggest modifications or improvements.

BLANK PAGE

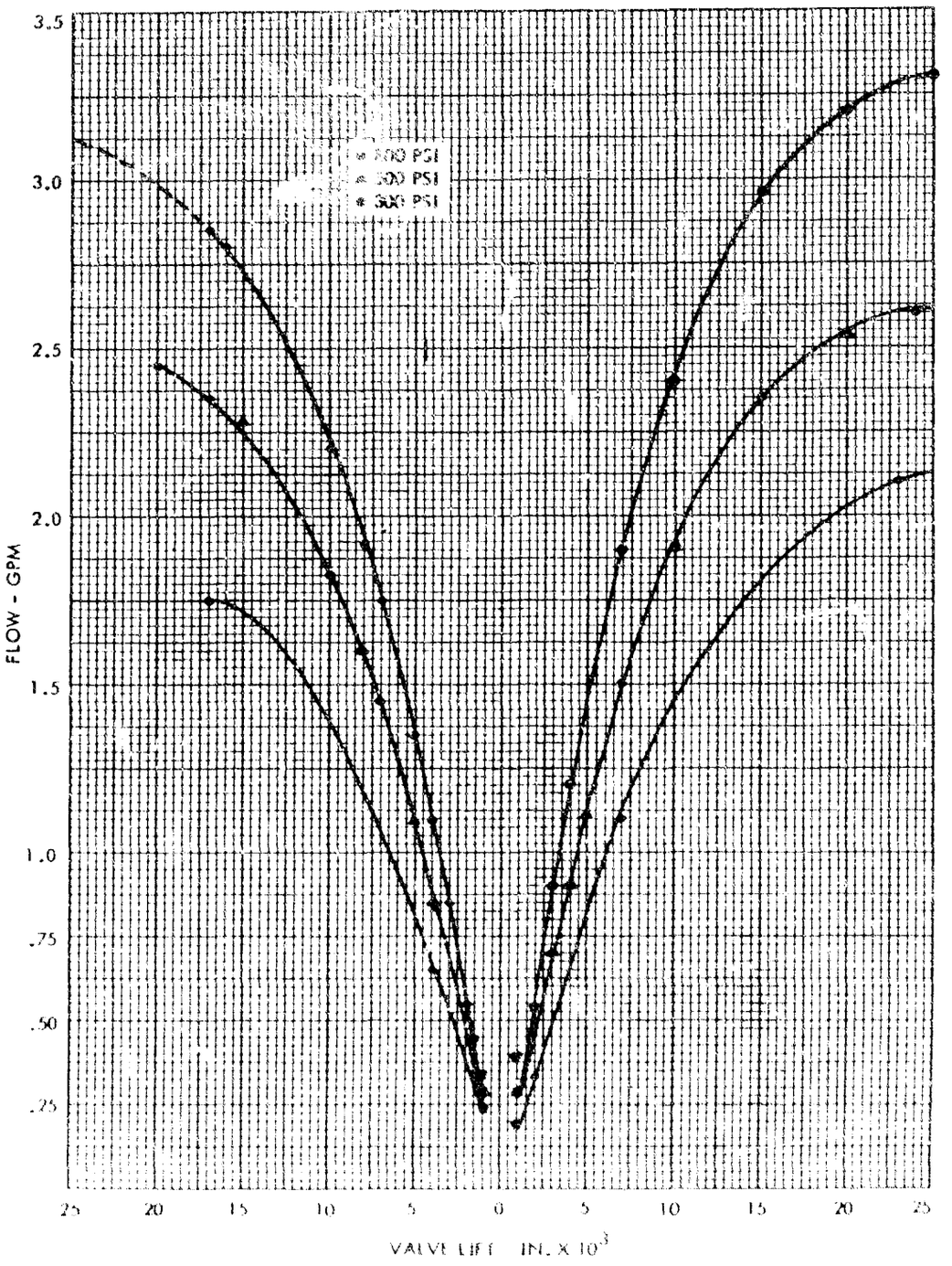

Figure 20 – No-Load Flow Curve Original Poppet Valve

Following selection of a design, two valves were to be built; one for use in the experimental servoactuating subsystem, the other for valve test use and as a replacement in the event of difficulty with the first unit.

These valves were to be evaluated with a monitor fluid such as petroleum ether to obtain preliminary performance characteristics to be used in a theoretical analysis and determination of the valve transfer function.

Finally, a complete schedule of static and dynamic tests with NaK-77 were to be conducted to establish valve performance at high pressure-temperature with liquid metal as the working fluid.

VALVE DESIGNS

Assuming that the electromagnetic pump pilot stage would be retained, it was determined that a re-design was necessary to obtain hermetic sealing and convert pressure to output motion, through opposed bellows. This arrangement would eliminate contamination and effectively average out unequal bellows extensions due to manufacturing tolerances or expansion of the sealed NaK in the pump.

It was realized that the relatively low force available from the E-M pump would not be sufficient to shear contaminant particles in a spool-type second stage. The alternative of using the E-M pump primarily as a transducer driving poppet valves to control a spool second stage was ruled out as being unnecessarily complex.

The more direct approach, which retained the contamination tolerance of poppet valves, consisted of using poppet valves in the second stage, controlled by theE-M pump output pressure operating a bellows-sealed rocking beam.

The success of this approach was dependent on satisfactory flow modulation around null. Since no such information was available, it was decided to design and build a breadboard of one-half of a complete poppet-type second stage in conjunction with the overall valve design.

A layout of the second stage valve is shown in Figure 21. Flow enters at port A, between the two halves of a double beat poppet valve. Opening the valve allows fluid to enter the chambers above and below the poppets. These chambers are inter-connected internally and, through B, to the servoactuator.

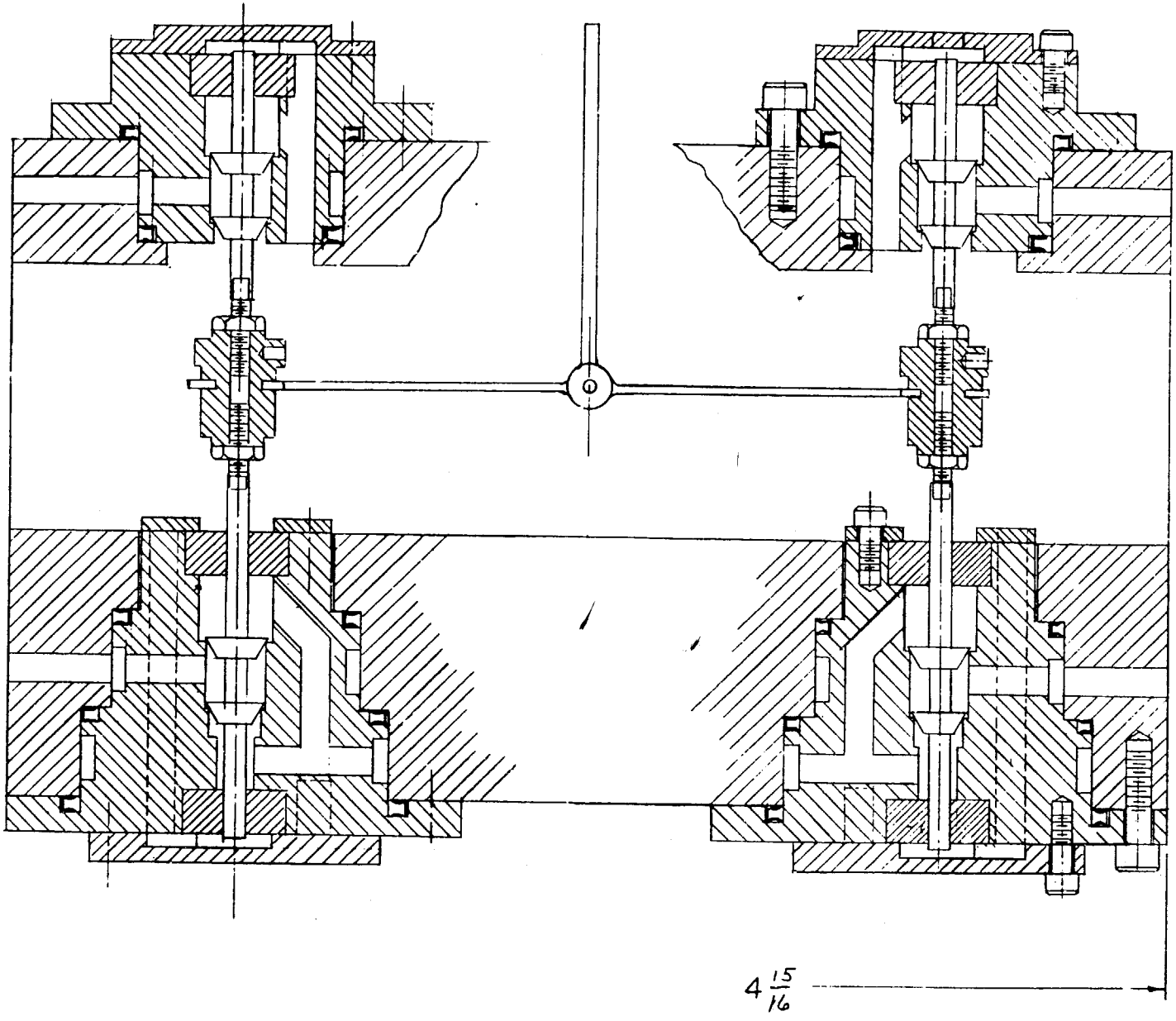

Figure 21 - Layout of Poppet-type, Second-Stage Servovalve

Flow returns to the valve from the second servo line through port C, and thence to the valve housing through the upper poppets. The housing is maintained at drain pressure. The rocking beam, shown schematically by the heavy lines, is actuated from outside the valve block, motion being transmitted through a bellows seal. The E-M pump and control bellows can be removed as a separate assembly without opening the main housing. The bellows seal is required to withstand drain pressure only.

Leakage from servo line B to drain is sealed by close-clearance capillary seals as shown. The original plan was to provide positive sealing at these points by using miniature bellows. Quotations from vendors indicates that these bellows would be extremely expensive. More disturbing was the fact that manufacturers will guarantee such high pressure-temperature bellows for 10^4 partial or complete cycles only. Under dynamic operating conditions this represents only a few hours life at best.

The breadboard valve is actually one-half of the valve shown in Figure 21. It was designed with a degree of underbalance so that there would be no reversal of force as valve reaction increases with opening. Valve travel was regulated by dead weight loading. Position was measured with a 0.0001 inch dial indicator. An exploded view of the test model valve is shown in Figure 22. The double-beat poppets are shown in Figure 23. The complete assembly, mounted on a MIL-0-5606 hydraulic test stand is illustrated in Figure 24 . The photograph shows the loading beams and weight pans, and the dial indicator resting on the valve stem extension.

Static tests, consisting of zero flow pressure gradient, zero load servo flow, and flow vs. servo load, were conducted at 1000, 1500, 2000 and 3000 psi supply pressures. Null leakage in this type of valve is negligible, but leakage through the valve stem capillary seals was measured at the various pressure levels. Representative curves are shown in Figures 25 to 27.

The general results of the tests showed that satisfactory modulation of flow around null could be achieved,and that the poppet-type valve had the high pressure gain and flow characteristics required for precise hydraulic control.

It was recognized, however, that the poppet valve design had several disadvantages. The extremely high gain of these valves causes minute distortions of valve stems and seats caused by pressure or temperature changes to exert a considerable effect on flows around null. With round

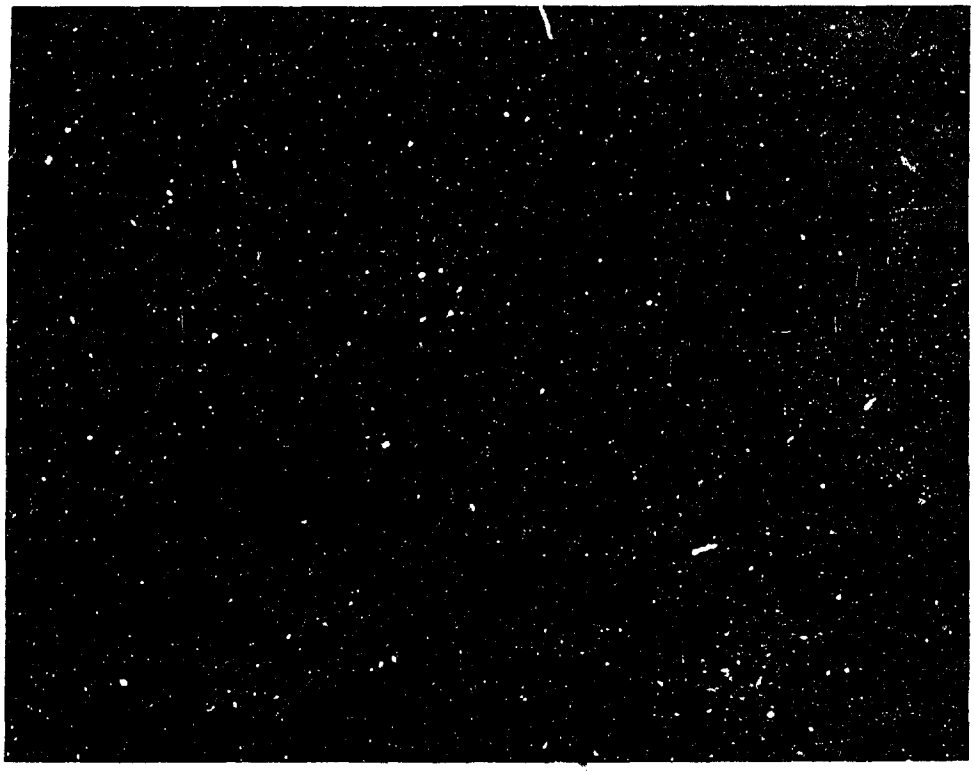

Figure 22 - Experimental Model Poppet Valve - Exploded View

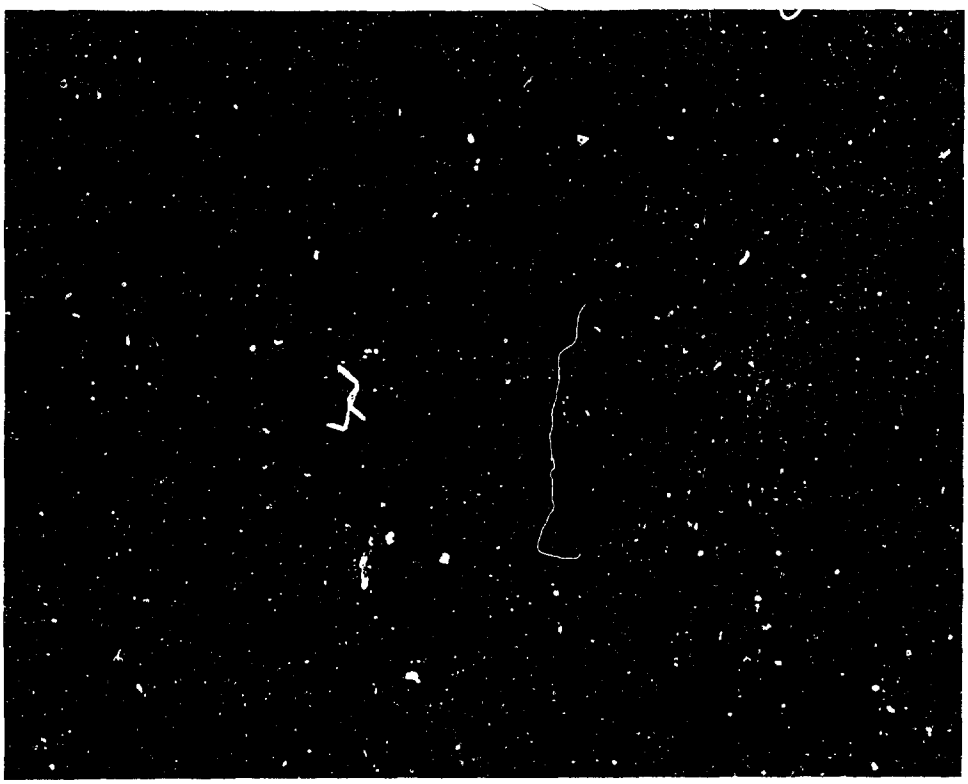

Figure 23 - Detail of Double-beat Poppet

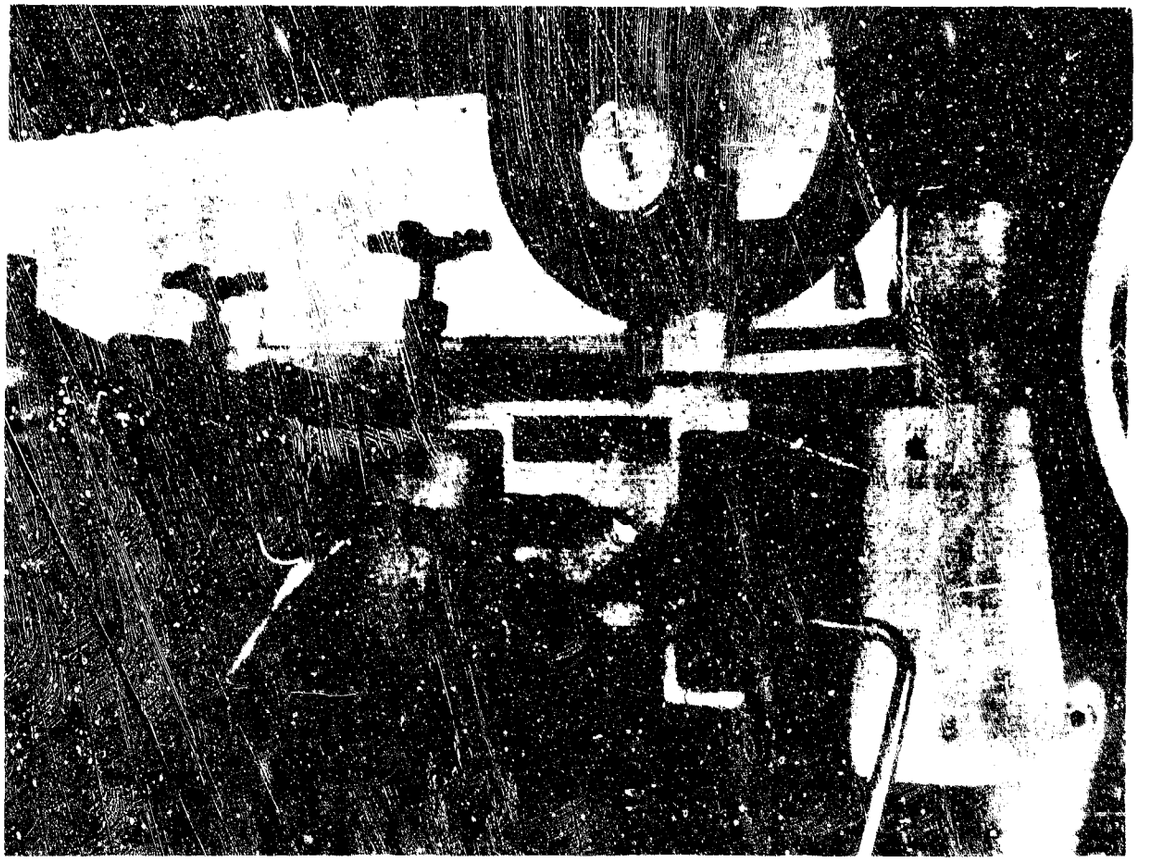

Figure 24 – Poppet Valve Test Setup

ports, the metering areas do not increase linearly with valve opening. As a result, flow versus opening is non-linear, which could be undesirable for certain servo applications.

The poppet-type valve is inherently complicated and requires a very high degree of workmanship. While this configuration is desirable from the standpoints of contamination tolerance and reduction in the number of rubbing surfaces, it is not as simple a design as a spool valve. In addition, the poppet valve requires a bellows seal which has very limited reliability at high temperature.

These findings were reviewed and confirmed by consultation with personnel from the Aerospace Components Division of Battelle. In order to obtain a practical operating servovalve within a minimum development time, it was decided that a conventional servovalve design approach be adopted. This approach would include a high-temperature transducer operating either a flapper-nozzle or jet pipe pilot stage, and a balanced spool type second stage. Successful performance would, of course, obviate the necessity for the more complex poppet valve.

This conclusion was based on the following considerations:

1. A high-temperature torque motor had been developed and was available for trial.

2. Considerable experience exists with the design, manufacture, and operation of balanced, spool-type second stage valve units.

3. Both mechanical and hydraulic interstage feedback has been developed and successfully applied.

Direct actuation of a spool valve by an E-M pump pilot stage is not feasible because of the low force output of the E-M pump, the necessity for using bellows to transmit motion and the difficulty of providing interstage feedback.

The simplest and most direct means of actuation for a liquid metal valve is the jet pipe. Configurations such as the flapper-nozzle, requiring small orifices in series, would probably compromise valve performance and reliability. Some type of feedback between stages is essential. In view of the high temperatures involved, this feedback should preferably be hydraulic.

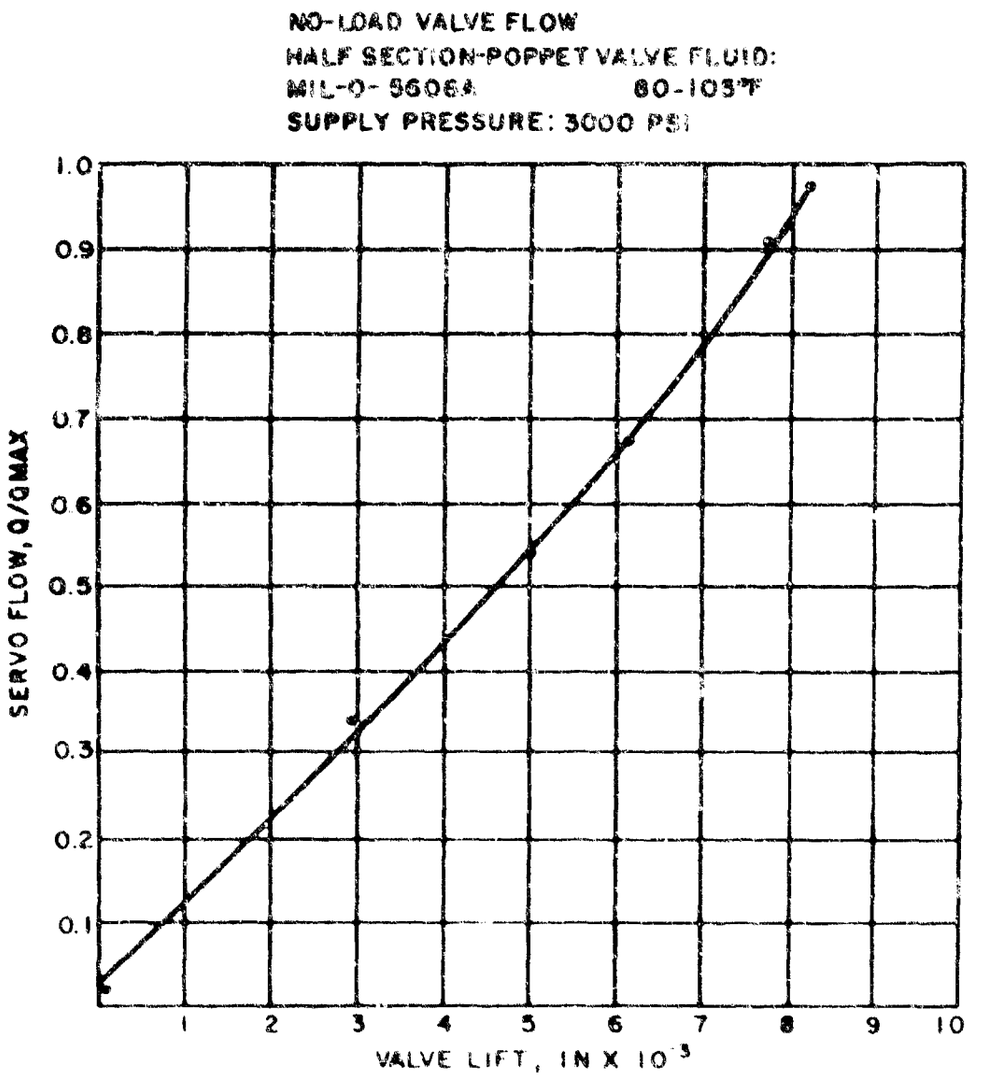

Figure 25 – No-Load Flow Curve – Poppet Valve

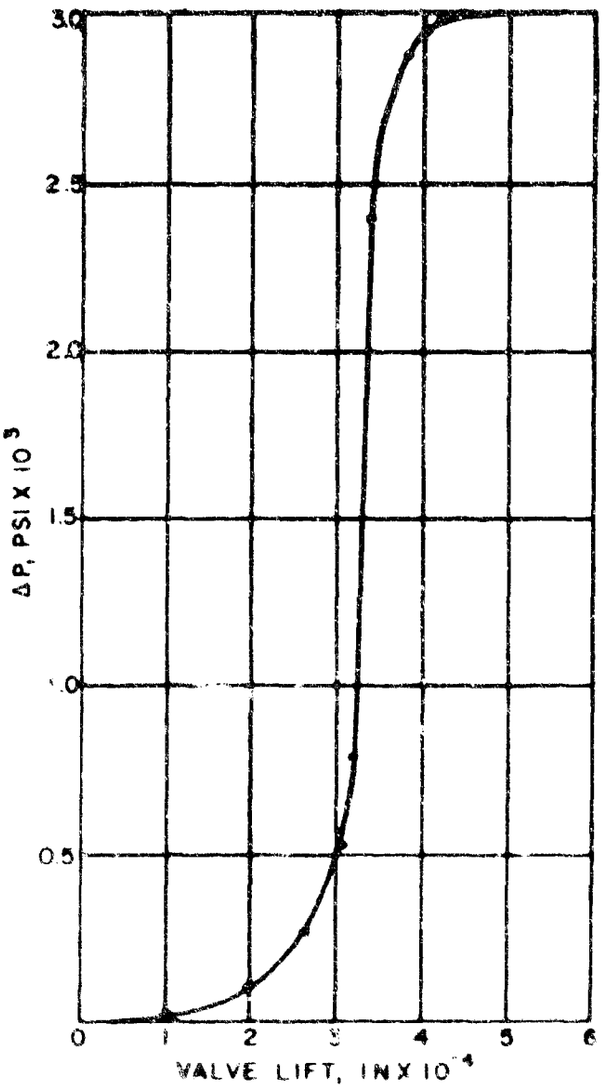

BLOCKED SERVO PRESSURE GRADIENT
HALF SECTION-POPPET VALVE FLUID:
MIL-O-5606A 80 - 105°F

Figure 20 Blocked Servo Pressure Curve – Poppet Valve

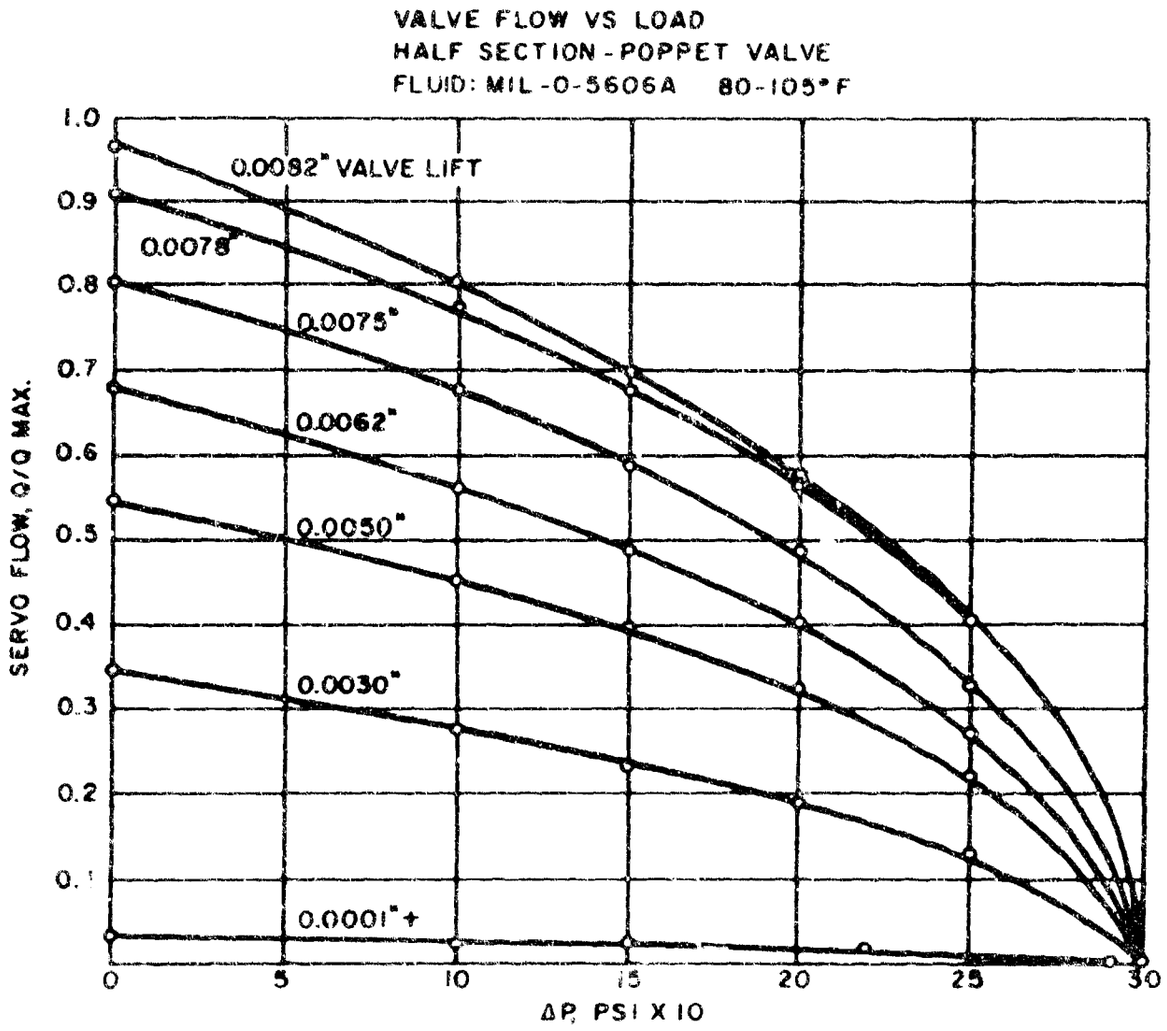

Figure 27 - Load-Flow Characteristics - Poppet Valve

Since this approach reduces the E-M pump to the function of a transducer, a comparative study of this unit vs. a high-temperature torque motor was initiated. Tests were conducted on the original E-M pump pilot stage over an input signal frequency range of 0.5 to 50 cps, and at various quiescent pressure levels in the control loop. Analysis of test results to determine frequency response showed that, with a zero psig quiescent pressure, an initial break occurred at approximately 1 cps, followed by a 20 db slope to beyond 50 cps. It was also noted that the initial break point moved out as quiescent pressure was increased, indicating gas entrapment in the control loop.

Revision of previous servo calculations to include the effects of fringing loss and back emf showed that the test pump and pressure transducer combination should have a flat response to 12.7 cps. This limitation is primarily due to the bellows gradient and entrained fluid volume. Since a response of 12.7 cps is too low for satisfactory servovalve operation, considerable development would be required to produce a pump-bellows combination with optimum characteristics.

The operational characteristics of E-M pumps are readily calculated, and it can be shown that pump efficiency is significantly reduced by electrical losses in the metallic pumping section. This can be circumvented by substituting an insulating material in that part of the pump.

As part of the study, the feasibility of using high-purity alumina (Lucalox), for the pumping section was investigaged. This would require the joining of Lucalox and niobium tubing and electrical connections. The techniques for joining these materials is not well developed although examples of successful joints have been reported. The main problem is the differential expansion at the joints between the two materials when exposed to high temperatures.

An example of a fabricated pumping section is shown in Figure 28. It will be noted that cracks developed in the ceramic during brazing. Since that time, considerable progress in joining techniques has been reported but additional development effort would be required to provide reliable joints.

Past experience showed that there would also be problems with high-temperature bellows. Only very limited design data are available for bellows that are subjected to high-frequency fatigue loading. Also, if the bellows were made of conventional materials such as stainless steel or Inconel, the weldment of niobium tubing to the bellows materials could be a source of trouble.

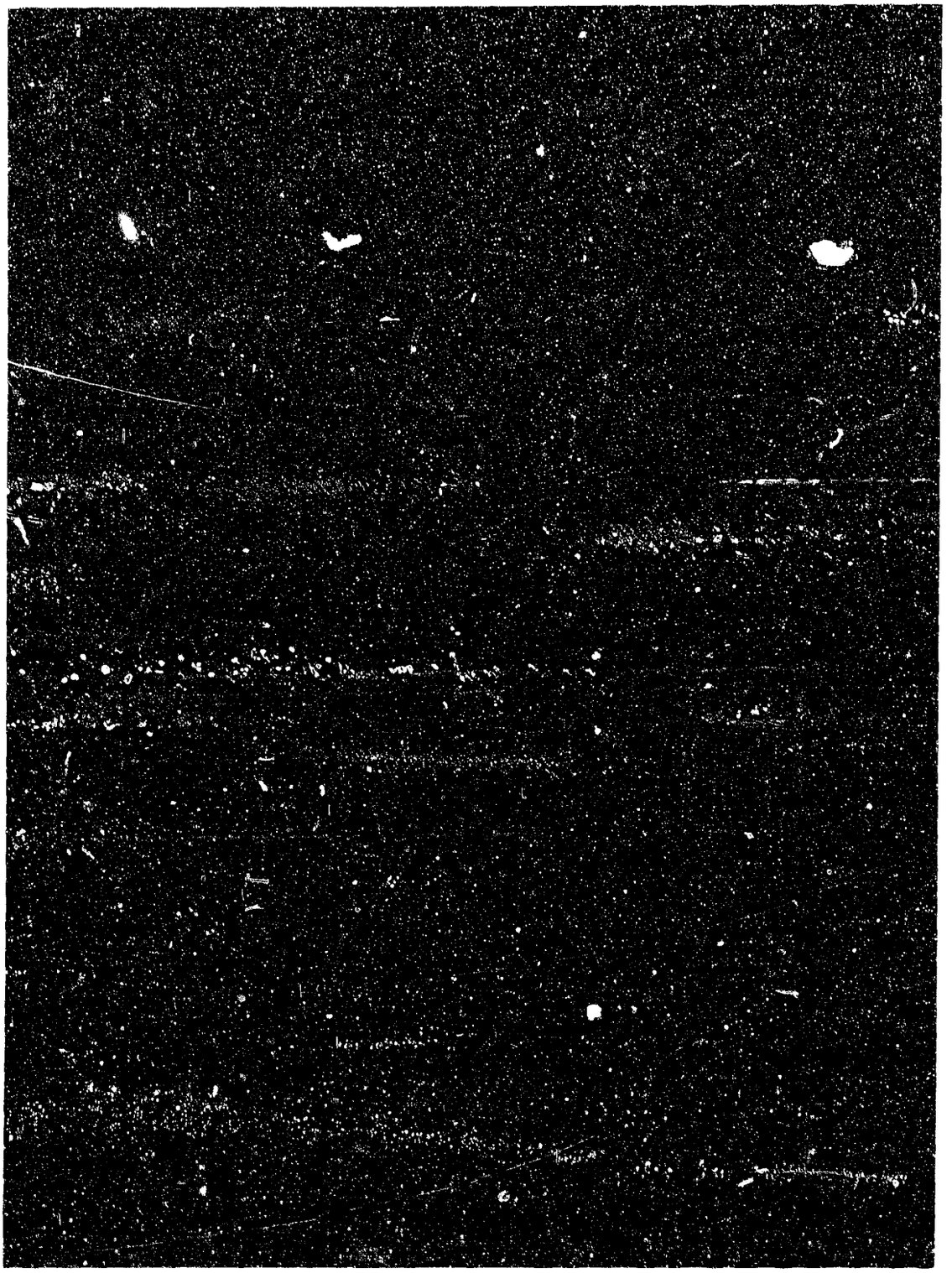

Figure 28 Lucalox Pumping Section for Miniature EM Pump

On the other hand, Bendix Research Laboratory had developed and built a 1200° F torque motor for a high temperature servovalve application. This motor, with modifications, could be used to actuate a jet pipe.

The result of this study was a decision to develop a two-stage servovalve using a high-temperature torque motor, a jet pipe pilot stage, and a spool-type second stage, designed to operate at fluid and ambient temperatures up to 1200 F. Two methods of incorporating hydraulic feedback were also investigaged.

The first approach envisioned a spool valve contoured to form a cusp at the center to split the jet pipe stream. A diffuser slot allowed the stream to impinge on the sharp edge while sealing the rest of the periphery. A groove on either side of the cusp converted the velocity head to pressure which was transmitted to the ends of the spool by longitudinal passages. With the spool centered under the jet the flow divides equally on each side of the cusp and pressures on each end of the spool are equal. If the jet is deflected more flow enters one chamber than the other and a corresponding pressure differential appears across the spool. The spool then moves in a direction to again center the jet, at which point the pressures equalize. There is, thus, a one-to-one correspondence between jet deflection and spool motion.

In this type of valve, the required pressure differential must be maintained by the sealing action of the cusp which, ideally, approaches a knife edge. In high-temperature, liquid metal valves it is necessary to provide higher than normal spool clearance to reduce the tendency to bind or jam. Because of the extremely low viscosity of NaK-77 it is difficult to fulfill this second requirement and still maintain satsifactory sealing. Test reresults indicated that optimum performance could not be achieved with this valve.

In order to expedite design and manufacture of a working servovalve, effort was directed toward a more conventional jet pipe-receiver port configuration, retaining however, the concept of hydraulic feedback.

The general characteristics of this servovalve are as follows:

Supply Pressure	3000 psi
Maximum Flow	7 gpm
Torque Motor Response	300 cps
Torque Motor Power, maximum	7 watts
Fluid	NaK-77
Fluid temperature, maximum	1200 F
Ambient Temperature, maximum	1200 F

Both jet pipe diameter and spool-sleeve clearance are larger than those normally employed in servovalves. While these have a significant effect on valve losses and response time, it was felt that the first valve should be designed for maximum reliability rather than optimum performance.

The original torque motor had been designed with a flapper on the output shaft, and had a calculated maximum output of 0.5 pound. The revised design provided a clevis which engaged the jet pipe. It was determined that 0.5 pound was inadequate and the design was further revised to provide a theoretical force of one pound by reducing armature travel from 0.012 to 0.010 inches. However, the vendor pointed out that actual maximum force of 0.75 pound would be more realistic.

Much of the design difficulty and requirement for high force output came about because of using a torque motor designed for a flapper-nozzle application without any changes in configuration. It was determined that the torque motor could be re-designed so as to incorporate the jet pipe into the armature and thereby reduce the required output force.

The final design was a modification of the original Bendix torque motor developed for a pneumatic application at temperatures up to 1200^{0}F. Figure 29 (a) shows the original configuration of two coils and a spring-centered armature arranged as an E dot type of magnetic circuit. Figure 29 (b) utilizes a flexure tube and reverses the torque motor so that the mature is at the bottom, submerged in the fluid. High pressure NaK is introduced into the jet pipe, which is the flexural member, at the pivot point, so that the entire assembly is specifically designed for jet pipe actuation without intermediate linkages.

The torque motor assembly, shown in Figure 30, is mounted on top of the valve body with the jet pipe nozzle extending through a hole in the body, positioning the nozzle over the two receiver ports of the valve spool.

The torque motor is positioned on the valve body by two dowel pins. One pin, secured to the body, fits between two adjusting screws in the torque motor mount. By adjusting these screws, the torque motor can pivot about the second dowel pin, allowing exact positioning of the jet nozzle over the receiving ports.

The basic unit is a dry coil type torque motor with two coils to provide both polarizing and control flux. Each coil is wound with 300 turns of AWG No. 28 nickel-jacketed, ceramic insulated copper wire. Figure 31

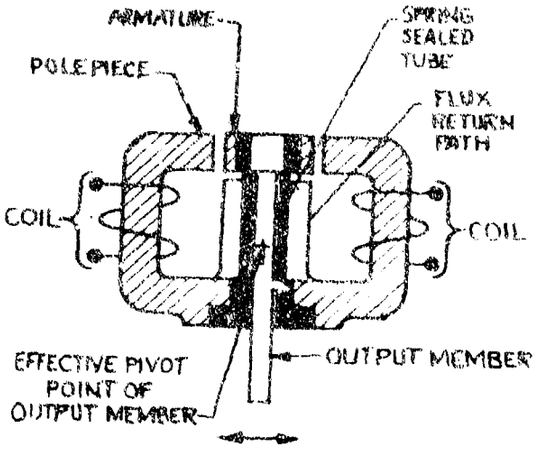

Figure 29(a) - Schematic of Original Torque Motor

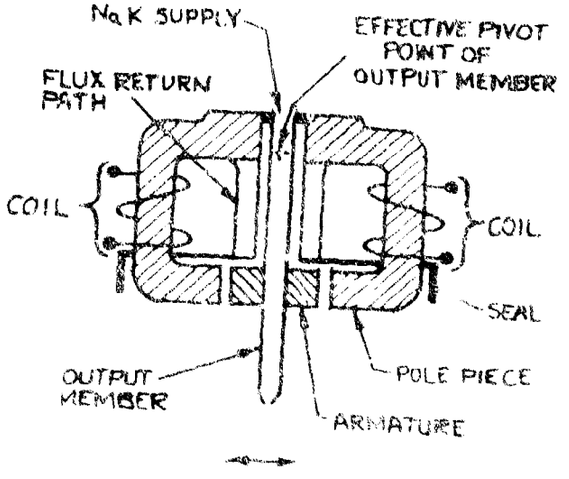

Figure 29(b) - Schematic of Modified Torque Motor

Figure 30 - Torque Motor Assembly

Figure 31 - Fabrication of Torque Motor Coils

shows the steps used in fabricating the coils. The coils fit over two posts in the torque motor body made of silicon iron (Relay No. 5), which serve as magnetic cores for the coils. Two additional posts extending up from the body, also made of silicon iron, serve as magnetic return paths.

The various parts of the torque motor such as cover housing, coils, pole pieces, core posts, return posts, and jet pipe spring tube assembly are all fastened to a TZM molybdenum body. The requirement to provide hermetically sealed joints between materials having greatly different coefficients of thermal expansion created the most serious problems in the design of the torque motor.

A joint fabrication development was initiated to obtain zero leakage joints between the molybdenum body structure and the silicon iron magnetic path. Development involved structural analysis of the joints as well as fabrication and testing of numerous sample joints. This also included development of plating procedures to protect the silicon iron from corrosion during high temperature material stabilization and performance testing of the torque motor. Material combinations that required joining were molybdenum to molybdenum, molybdenum to silicon iron, and molybdenum to Inconel - X. Electron beam welding was used mainly in making these dissimilar metal joints.

Upon receipt of the two torque motors pressure tests were made with both Argon and MIL-H-5606A fluid. Despite successful fabrication of sample joints, the torque motors themselves exhibited leaks in several areas. Each torque motor has seven cross-drillings in the molybdenum body which were sealed by molybdenum plugs electron beam welded in place. Practically every joint was found to be porous. Repairs were made by brazing with a nickel-manganese alloy. The upper end of the Inconel-X jet pipe was joined to the molybdenum center post by electron beam welding, as shown in Figure 32. One torque motor leaked badly at this point. Microscopic examination showed a definite crack at the interface between the two metals. Since re-welding was not a practical solution this leak was also repaired by brazing.

It was also determined that the welded joints between the molybdenum body and the silicon iron core and return posts were not leak-tight, which would allow fluid to penetrate to the coil enclosure. Because, again, welding was not satisfactory, brazing was attempted but did not result in a good joint.

A considerable amount of development was involved in making this repair. Of several approaches considered, the one finally selected consisted of welding 0.005 thick molybdenum diaphragms to the molybdenum body, covering the lower ends of the core and return posts where they penetrated

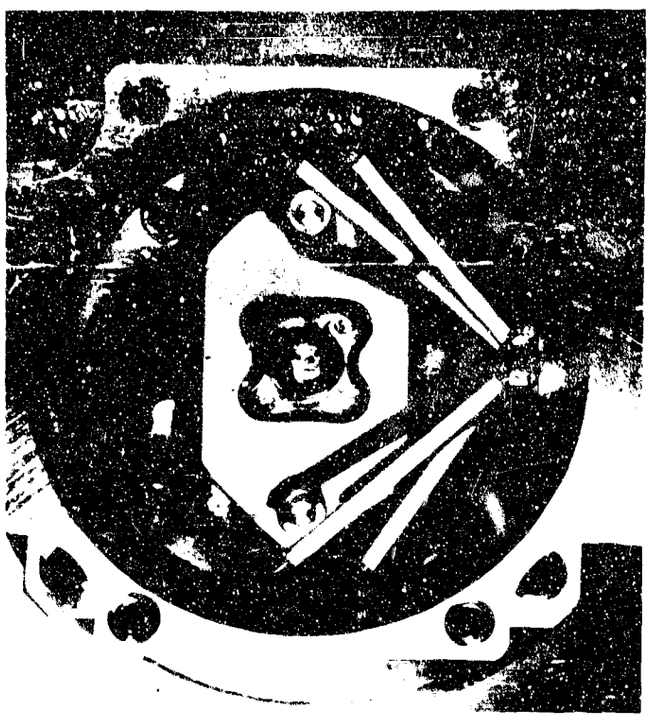

Figure 32 - Welding of Inconel-X Jet Tube to Molybdenum Body

the molybdenum base. This approach also proved unsuccessful, due to porosity and pin holes in the welds. Nickel-manganese brazing was then tried but a completely integral joint could not be obtained. At the same time, the introduction of the 0.005 diaphragms in the magnetic circuit increased the effective non-magnetic gap and affected the operating characteristics of the torque motors.

Repeated heating of the structure during brazing operations also permanently loosened the return leg posts and partially annealed the Inconel-X jet tube so that the spring gradient was drastically reduced below design specifications.

It became apparent that a completely satisfactory repair would involve re-design and replacement of major parts of the torque motor. This was not feasible at this point due to time and funding limitations.

Emergency repairs were effected by removing the coil core posts, which are threaded, and machining the molybdenum base to accept soft copper gaskets. At the same time the 0.005" molybdenum disks were removed and the recesses machined so that silicon iron disks could be forced into place. All threads and interstices were filled with a resin-base enamel. While this material has only very limited high-temperature capabilities, it has been used successfully in joints in heat treating furnaces and it was expected that it would afford sealing long enough to complete the high temperature NaK tests.

The return leg posts were knurled and pressed into position. Adjustments were made to compensate for the silicon iron disks which now replaced the 0.005" molybdenum diaphragms in the magnetic circuit. The torque motors were then tested with MIL-H-5606A fluid and no leaks could be detected.

Development and optimization of the jet pipe-receiver assembly was done by flow-checking a series of jets and received blocks over a pressure range of 1000 to 3000 psi, using MIL-0-5606 as the test fluid. Because the valve spool, although constrained to move longitudinally, has some slight rotational freedom, both round and square receiver ports were investigated. Tests of square ports were not satisfacotry and exhibited instability, possibly due to corner effects. Tests of round ports showed no variation in performance when jet pipes and receiver port center lines were misaligned by several thousandths of an inch. Accordingly, the round port configuration was used in the final servovalve design.

The jet pipe flow is approximately 0.75 gpm at 3000 psi pressure drop. Receiver ports have a nominal diameter 25 per cent greater than jet pipe diameter. Maximum static pressure recovery at 3000 psi input was approximately 97 per cent.

Following the completion of oil tests, the assembly was re-tested with NaK-77 at room temperature. Flow and pressure data were as predicted and no plugging was observed although the NaK supply had a high level of oxide contamination.

The principal structural material used in the construction of the torque motor, valve block and second stage valve sleeve is TZM molybdenum alloy. The jet pipe is Inconel-X and the second stage spool is tungsten carbide (WC 94 per cent - Co 6 per cent).

Before making final material selections, considerable study was given to compatible material combinations for the sleeve-spool assembly. Previous liquid metal components had generally utilized dissimilar carbides in areas of sliding contact. In the present case, the situation was complicated by the use of molybdenum, which has a very low coefficient of thermal expansion for the valve block.

Earlier material evaluations had shown that untreated molybdenum vs. various carbides in a NaK environment was reasonably satisfactory but generally resulted in some wear of the molybdenum member. The Research & Development Center of General Electric has recently developed a process for forming a diffusion bonded, boride coating on TZM molybdenum. Since this is an extremely hard, adherent layer, it was decided to test samples in NaK at elevated temperature to determine its compatibility with tungsten carbide.

Several sets of test specimens consisting of rotating tungsten carbide cylinders and stationary V-blocks of borided TZM were prepared and run in a modified Falex wear tester. Specimens were immersed in NaK-77 at 1000 F and run under load for 30 minutes. Results generally showed good compatibility, with minimum wear and no evidence of material transfer, welding, or scoring. A representative set of specimens is shown in Figure 33.

These material tests produced some very interesting results. The first set of specimens showed excellent performance for a running time of 30 minutes. The second set was also satisfactory, although wear was somewhat greater. This set was re-run for a total time of 60 minutes. At the conclusion of this test it was apparent that the borided case had worn

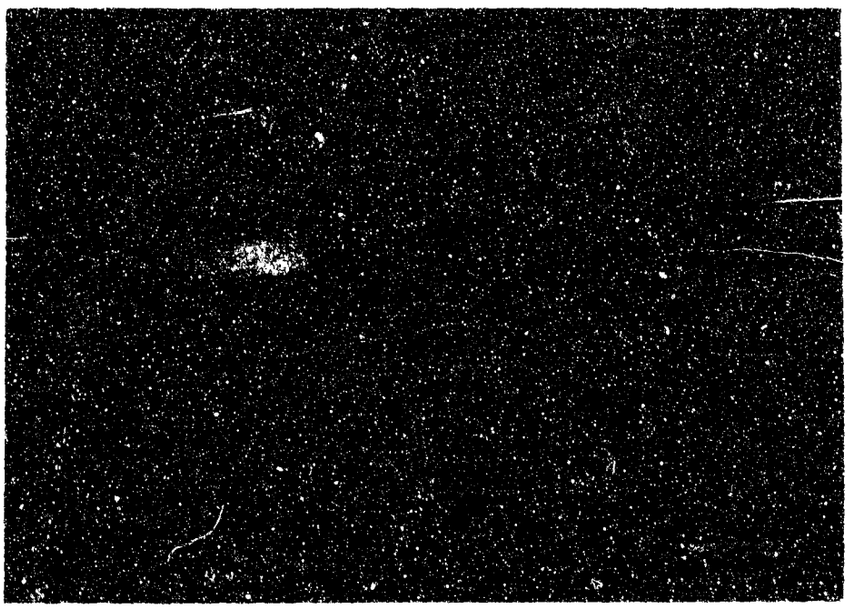

Figure 33 - Wear Test Specimens - Borided Mo vs. WC

through although no pickup on the carbide could be noted. A third set was unsatisfactory. After 30 minutes, the case had worn through, considerable wear of the substrate was apparent, and slight pickup was evident. Performance of a fourth set was almost identical with the first. Microphotographs of these specimens are shown in Figures 34 to 37.

The boriding process history showed that the first and fourth specimens were treated at a lower temperature and for a longer period of time than the second and third specimens. There are several possible reasons for the observed conditions. The longer processing cycle for specimens 1 and 4 can affect the base material by re-crystallization. Second, the bath used for processing may initially have impurities. Third, depending on time and temperature, there are several different borides which may be formed. Without a wet analysis this cannot be confirmed, but it could have a significant effect on surface wear.

Following these tests, dummy valve sleeves were made to determine if boriding could be successfully applied to long internal bores. Two sleeves were sectioned after boriding and subjected to metallographic examination. It was found that one sleeve had a very thin boride layer while the second was approximately 5 times as thick. Figures 38 and 39 show the outside diameters of the two sleeves. In each case, adhesion was excellent. Figure 40 shows the thin coating on an inside diameter. The dark band results from shrinkage of the nickel plate and epoxy compound used in preparing the sample. Figure 41 is an inside diameter of the heavier coating. Figure 42 illustrates how the boriding follows the intersection of a drilled cross hole and the inside bore. In the section shown in Figure 43, a small burr was left after drilling. Growth and fissuring of the boride is quite evident in this view, and indicates that extreme care must be taken in machining before boriding.

A layout of the final servovalve design is shown in Figure 44. Operation of this valve is conventional with the exception of the hydraulic, interstage feedback. With the spool centered under the jet pipe, the control flow divides equally into each receiver port and the velocity heads are converted to equal pressures on each end of the spool. If the jet is deflected to the right, more flow enters the right receiver port and pressure on the left end of the spool rises correspondingly. This forces the spool to the right until it is again centered under the jet and the pressures are equalized. Returning the jet to center reverses the operation and the spool valve returns to its original position. Thus, follow-up is accomplished without mechanical connections. The springs shown at each end of the spool are very light and are intended only to keep the spool near center when no hydraulic pressure is applied to the valve.

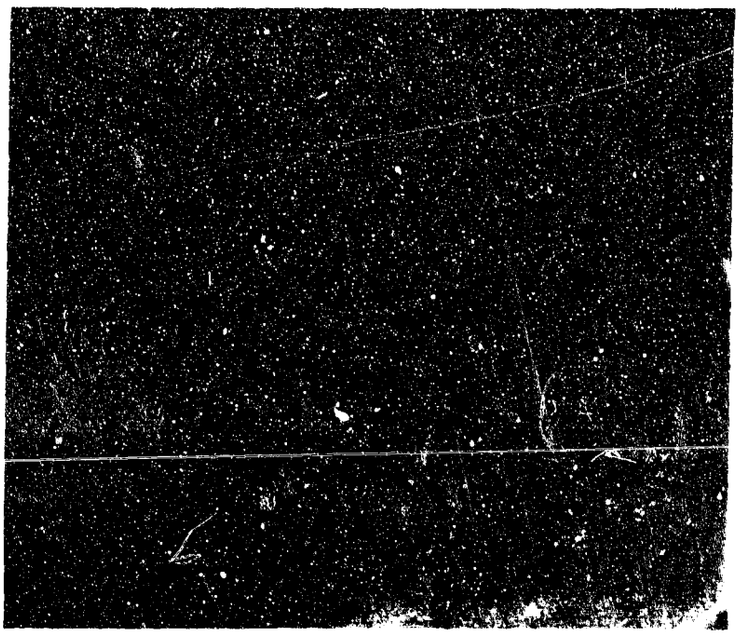

As borided

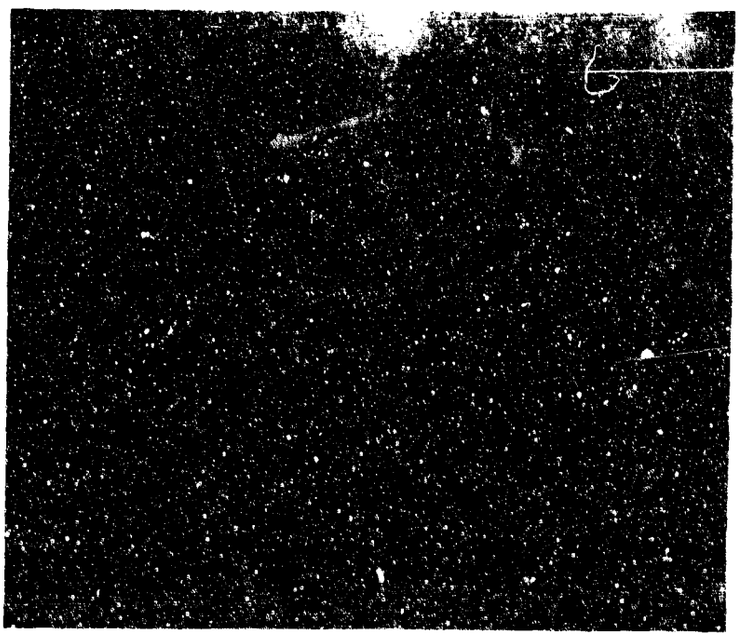

After test

Figure 34 Microphotograph of Borided Mo
First Specimen

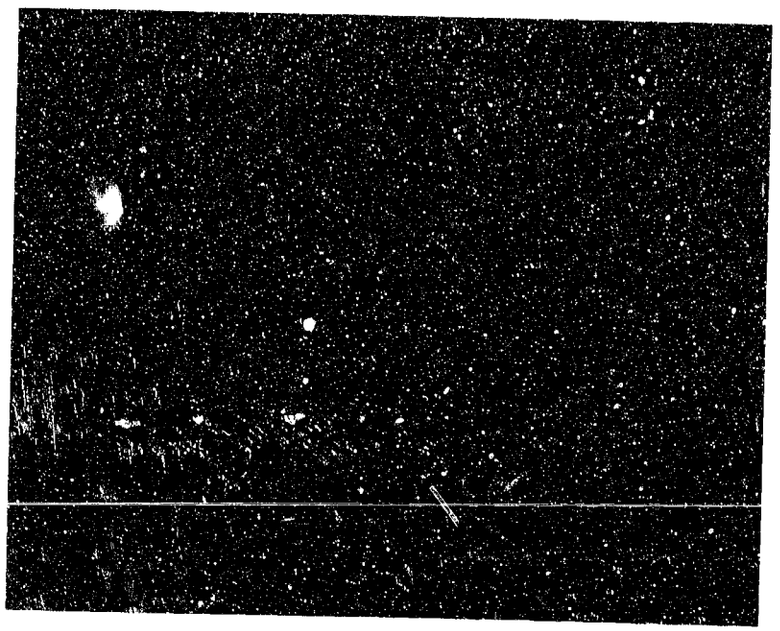

As Borided

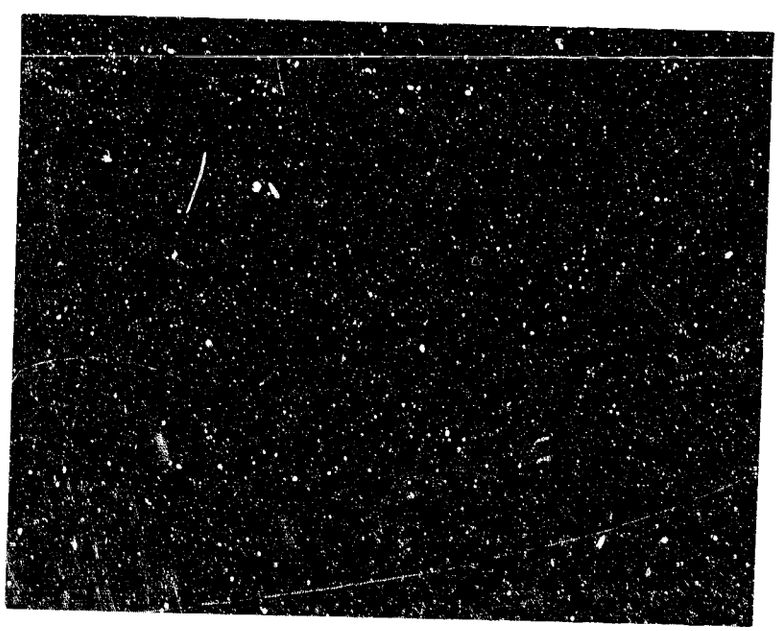

After Test

Figure 35 – Microphotograph of Borided Mo – Second Specimen

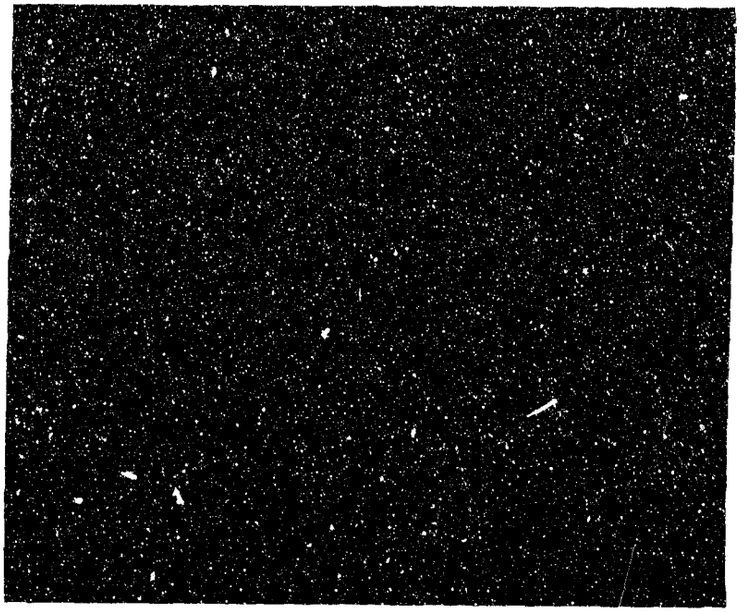

As Borided

After Test

Figure 36 - Microphotograph of Borided Mo - Third Specimen

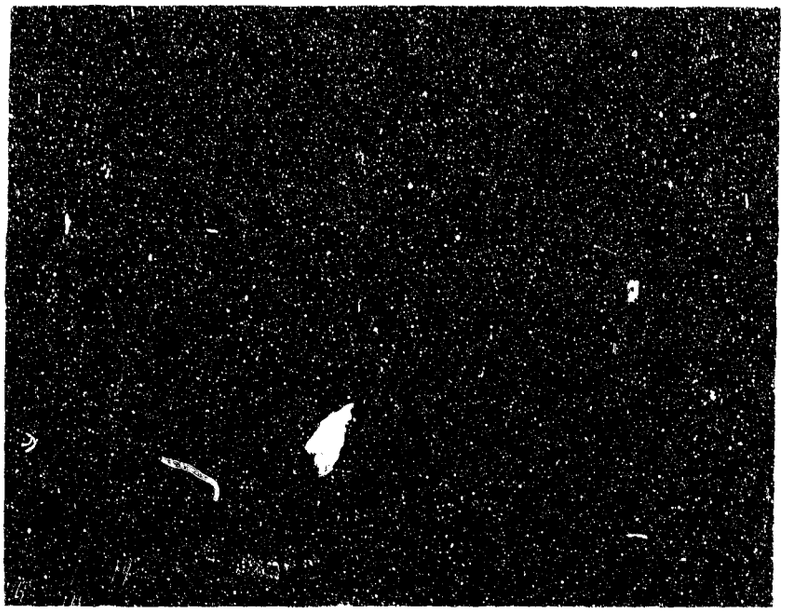

As Borided

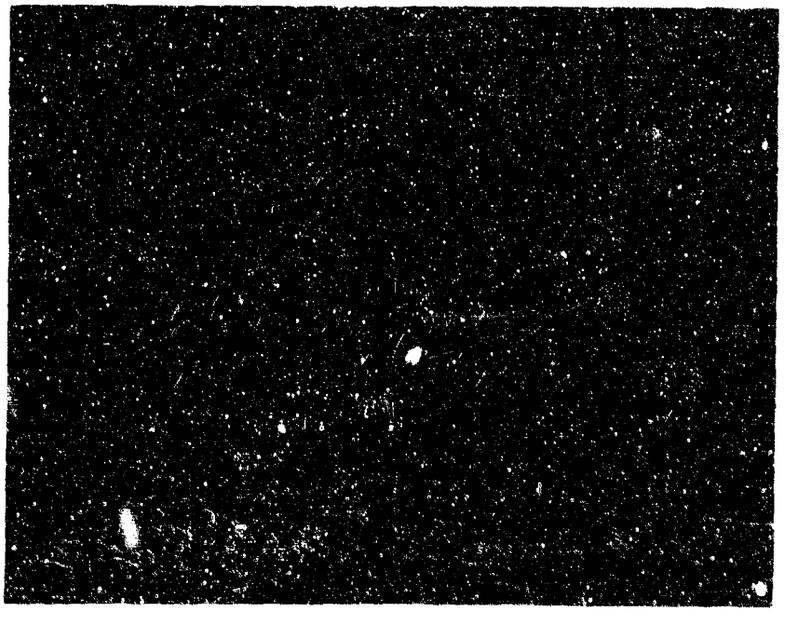

After Test

Figure 37 – Microphotograph of Borided Mo – Fourth Specimen

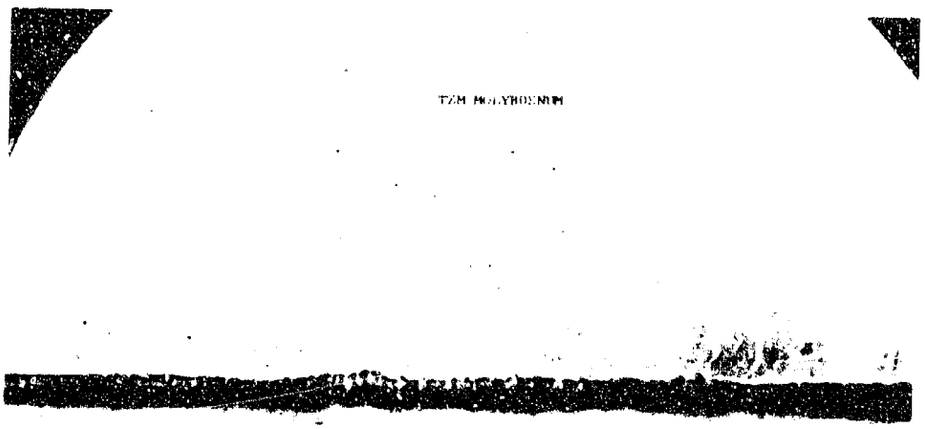

Figure 38 - Microphotograph of Borided Valve Sleeve - thin layer

Figure 39 - Microphotograph of Borided Valve Sleeve - heavy layer

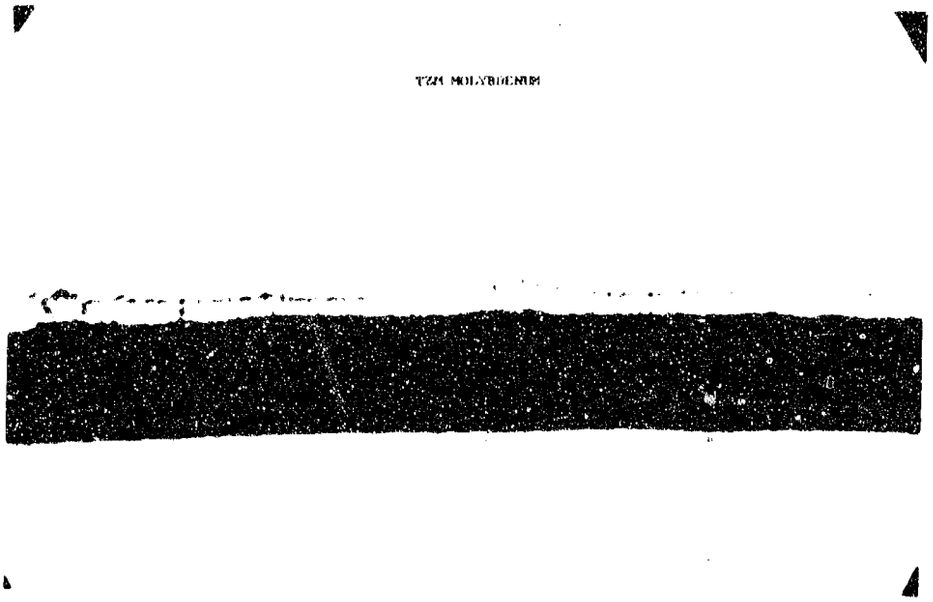

Figure 40 - Thin Borided Coating on Inside Diameter

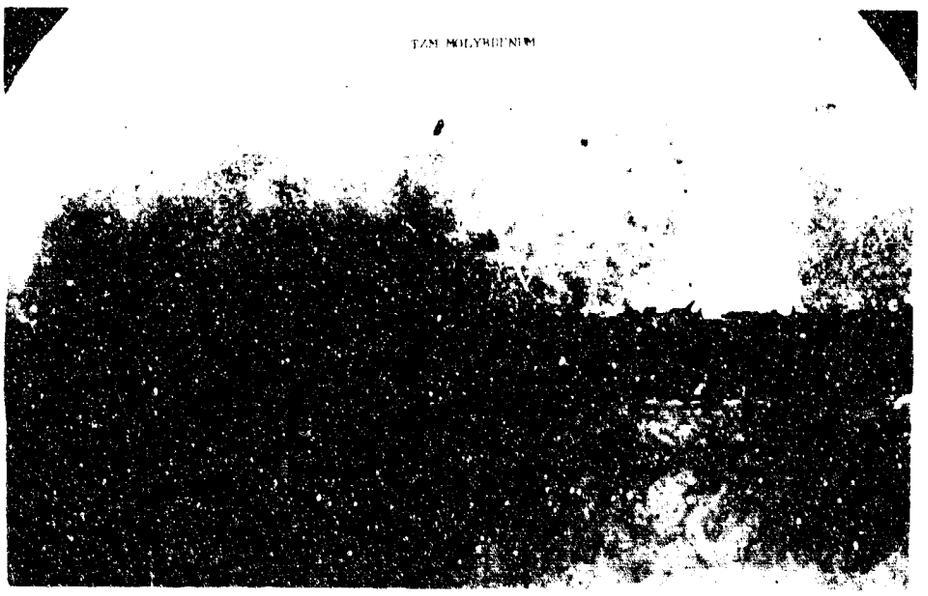

Figure 41 - Heavy Borided Coating on Inside Diameter

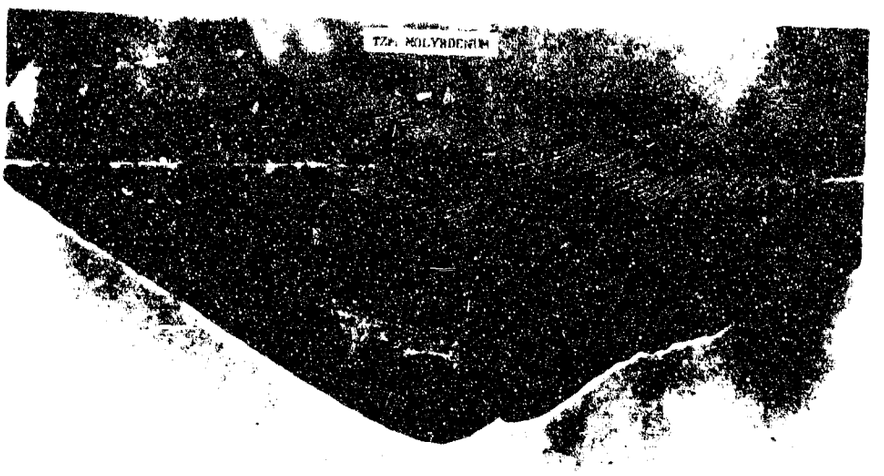

Figure 42 - Borided Coating at Intersection of Bore and Cross Hole

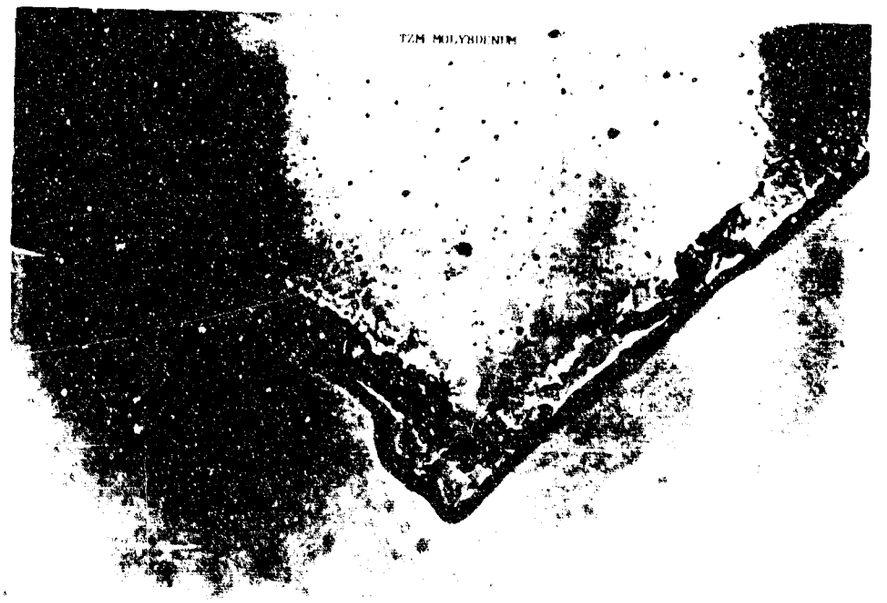

Figure 43 - Effect of Burr on Borided Coating

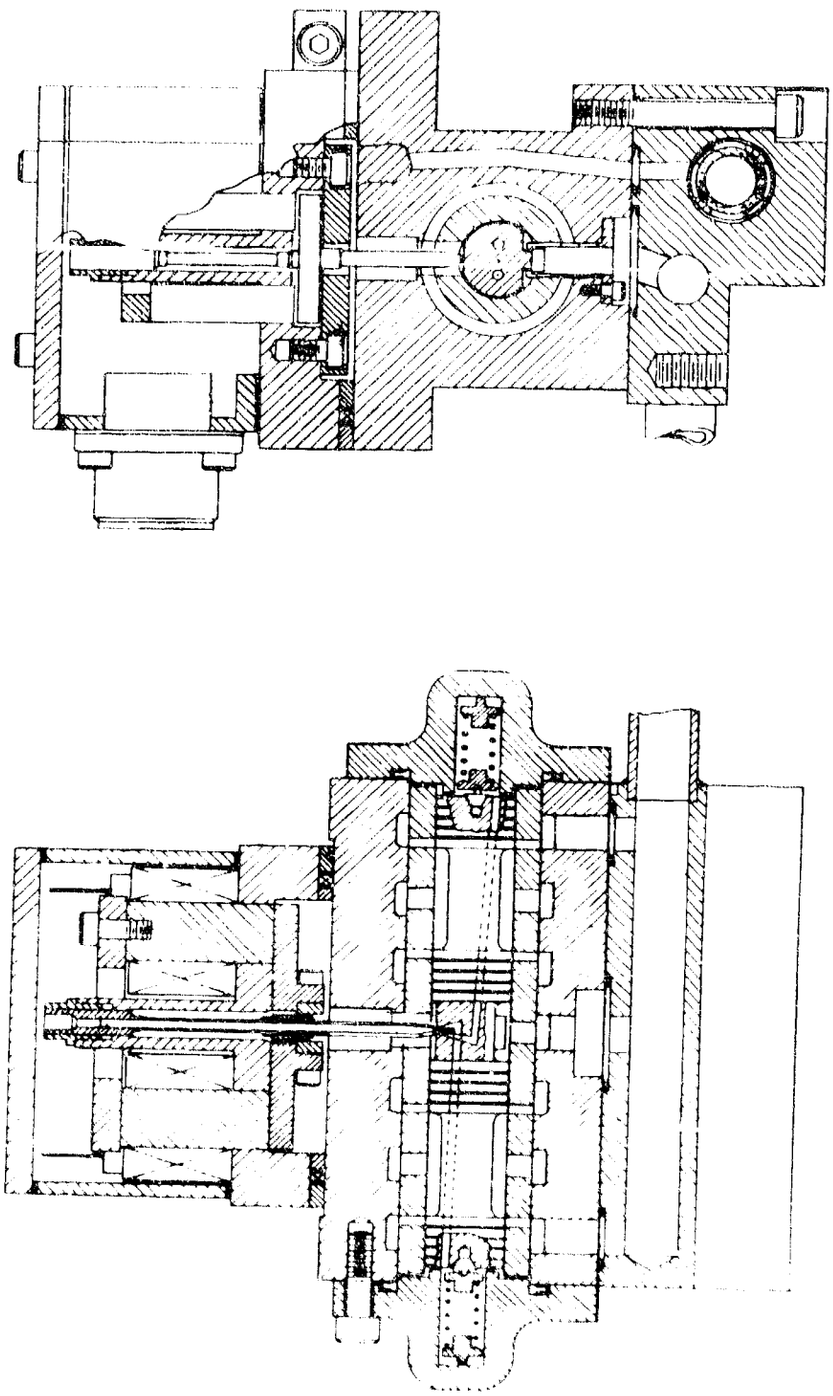

Figure 44 – Layout of Two-stage Servovalve

Figure 45 shows a borided TZM valve sleeve after machining. The rectangular ports are generated by electrical discharge machining. Figure 46 shows the configuration of the tungsten carbide valve spool. The spool is ground from the solid. Receiver ports and axial passages are put in with the EDM process. The lower ends of the receiver chambers are then sealed with tungsten carbide plugs brazed in place. Figure 47 is an exploded view of the second stage and manifold, while Figure 48 shows the assembled valve and torque motor.

Prior to receipt of the torque motors, a duplicate of the jet pipe was fabricated and a test fixture made to position the jet pipe mechanically as shown in Figure 49. The valve was then tested with petroleum ether at 1000 psi, and with MIL-H-5606 at 1500, 2000 and 3000 psi. These tests included measurement of jet pipe flow and internal valve leakage, determination of flow and pressure gradients, and a family of load-flow characteristics at rated pressure. Representative curves are shown in Figures 50 to 52.

Concurrently, preparations were made for NaK-77 testing by constructing the valve test loop shown schematically in Figure 53. The actual loop, as illustrated in Figure 54 is designed to permit a duplication of the above tests at temperatures to 1000^{O}F.

After making repairs to the torque motors, they were mounted on the servovalves and tested with MIL-H-5606A at pressures of 1500, 2000 and 3000 psi. As mentioned previously, there was evidence of jet instability at pressures over 2500 psi, and it was expected that this might be aggravated when NaK testing was conducted.

Standard static valve tests, consisting of jet pipe flow and internal valve leakage, determination of flow and pressure gradients, and a family of load-flow characteristics at rated pressure were conducted. Representative curves are shown in Figures 55 to 57. The difference in flow characteristics between Figures 50 and 55 is due to the fact that the servovalve was trimmed to reduce overlap after the test shown in Figure 50.

Upon completion of oil tests, the valves were dismounted and thoroughly cleaned to remove all traces of oil. One unit was then installed in the test setup of Figure 54.

The first NaK test was conducted at approximately 450^{O}F. It was found that the valve exhibited random instability at a supply pressure of 1000 psi. Both flow and pressure could be controlled by manual adjustment of torque motor differential current but fluctuations were too severe to obtain significant data. At pressures above 1000 psi the instability became progressively worse.

A second attempt to secure data was made at 750^{O}F but it was found that instability increased, probably due to the lower density of the NaK at increased temperature. At this point, valve testing was terminated in order to concentrate on testing of the servoactuating subsystem.

The primary cause of difficulty appears to be too low a spring gradient in the jet tube, combined with the low damping of high temperature NaK. Before the completion of the current contract preliminary re-design of the torque motor was initiated to provide, among other things, a stiffer jet pipe spring tube assembly.

Upon disassembly, it was found that the weld joining the Inconel-X jet pipe and the molybdenum center post had broken, allowing NaK to enter the torque motor, as shown in Figure 58. This joint had been cracked when received and had been repaired by furnace brazing. Oil tests at 3000 psi after brazing had shown no evidence of leakage. Under high temperature, however, the dissimilar coefficients of thermal expansion had apparently induced stresses which resulted in re-opening the crack.

The tests, incomplete though they are, demonstrate the feasibility of the servovalve with hydraulic feedback operating with high-temperature liquid metals. Since the problem areas have been pinpointed, re-design should result in a practical component capable of operation at temperatures to 1200^{O}F.

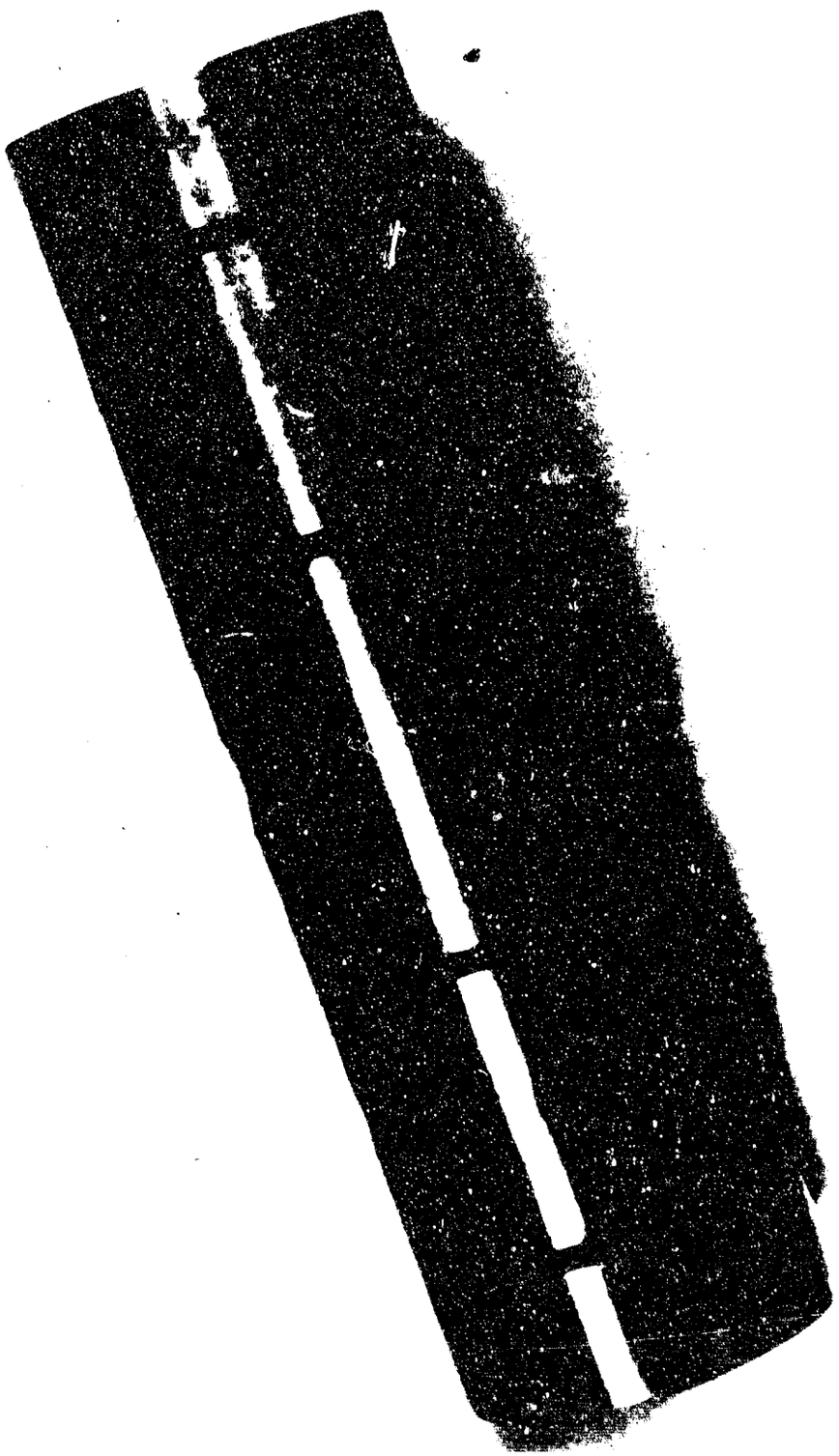

Figure 45 Borated TZM Valve Sleeve

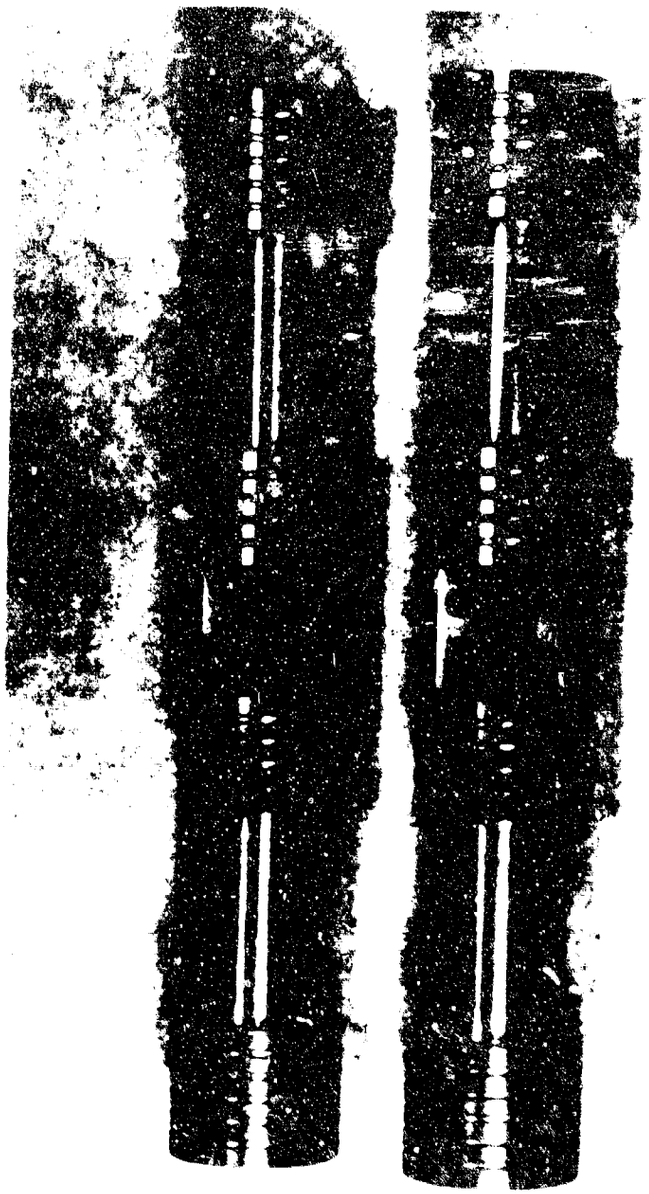

Figure 46 - Tungsten Carbide Valve Spools

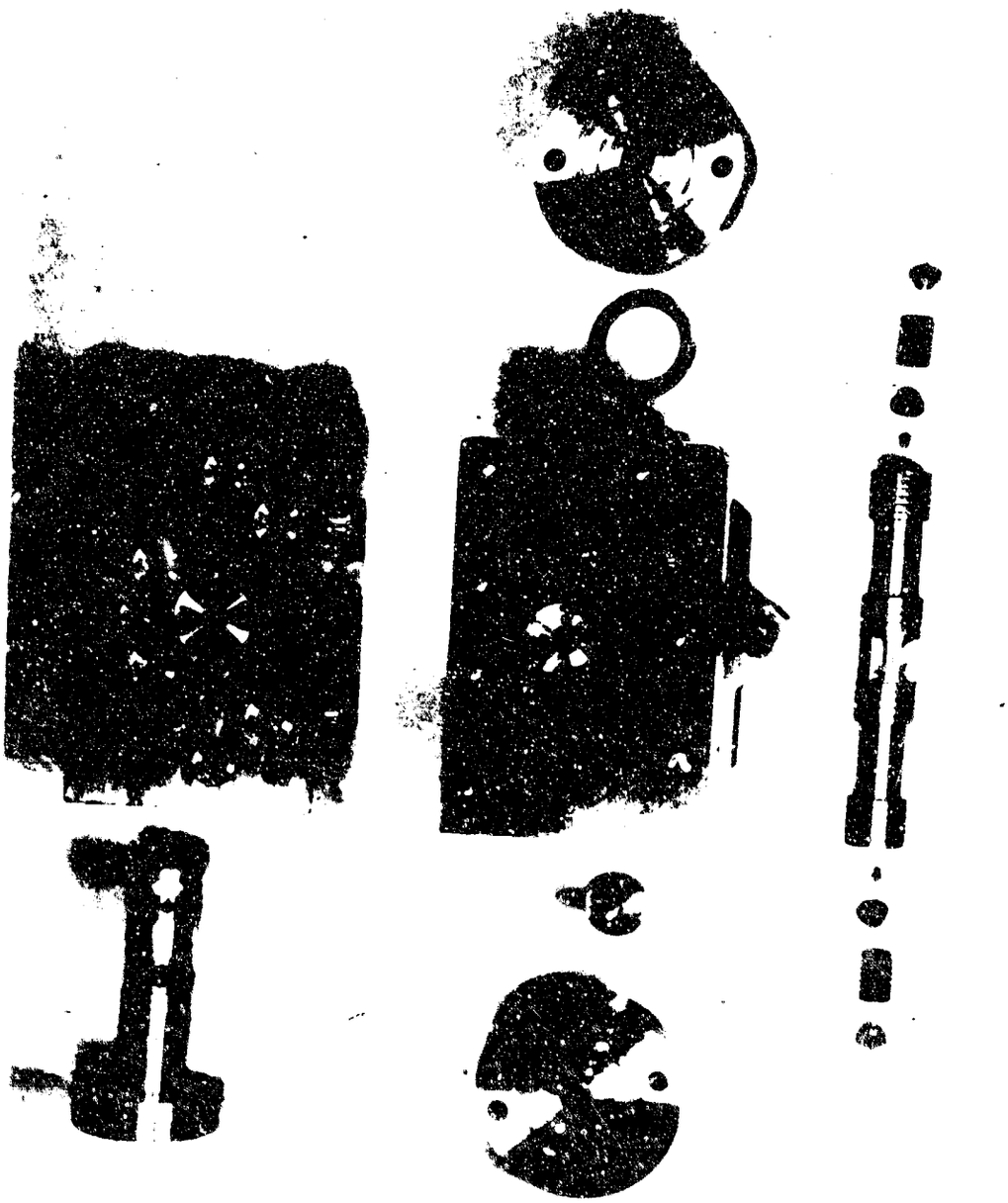

Figure 47 - Servovalve and Manifold - Exploded View

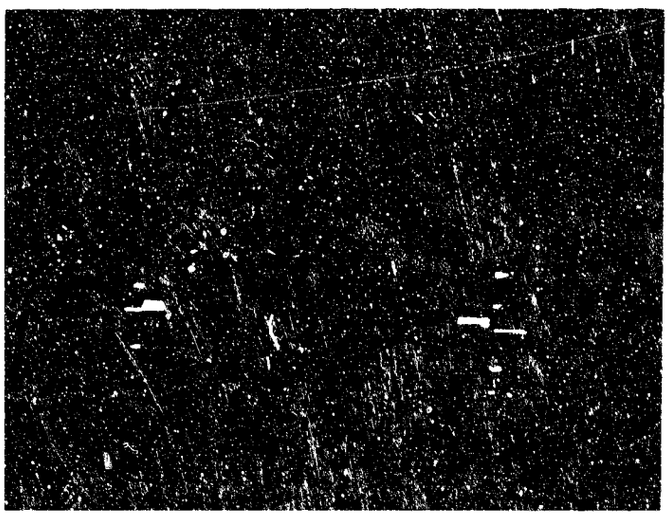

Figure 48 - Servovalve and High-temperature Torque Motor

Figure 49 - Jet Pipe Test Fixture

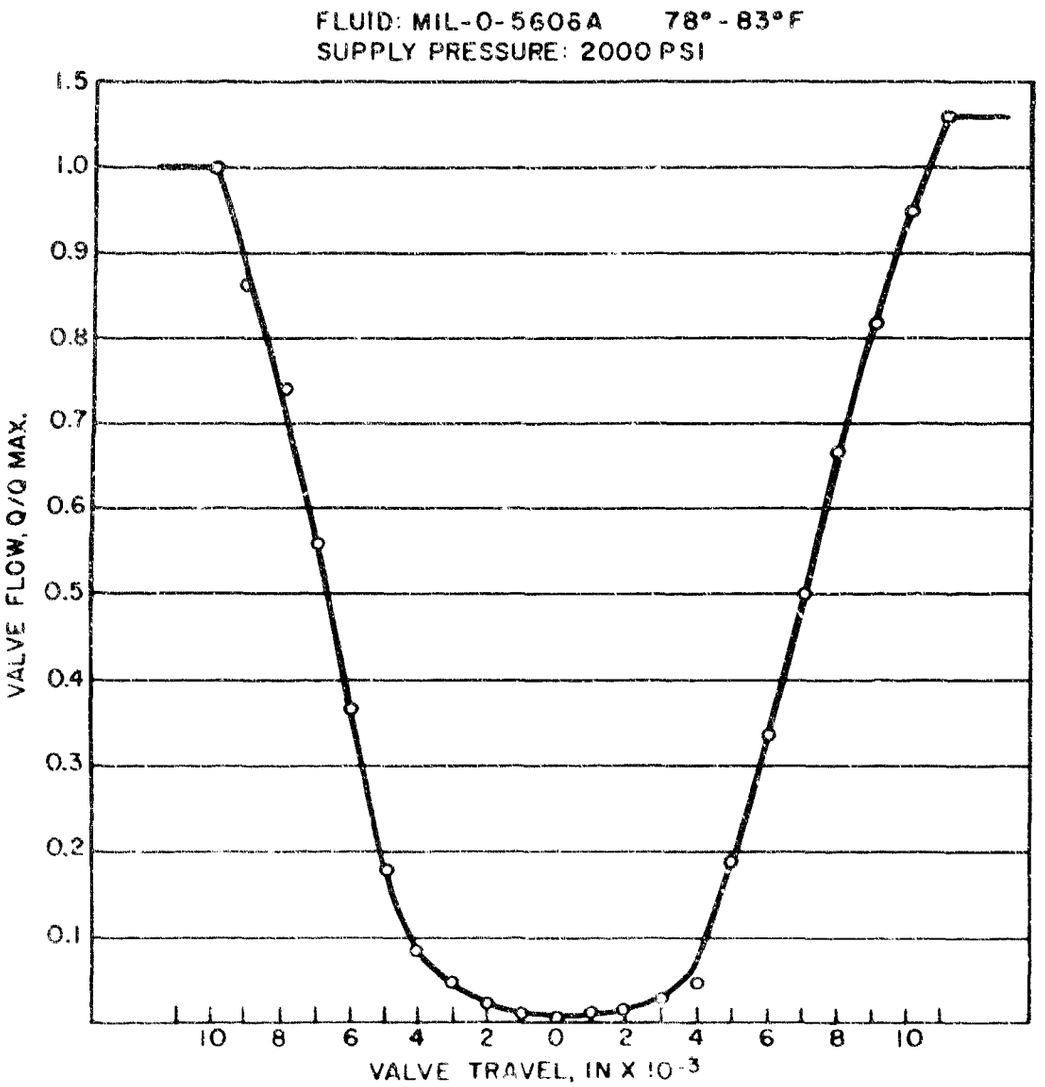

Figure 50 - No-Load Flow Curve - #1 Servovalve

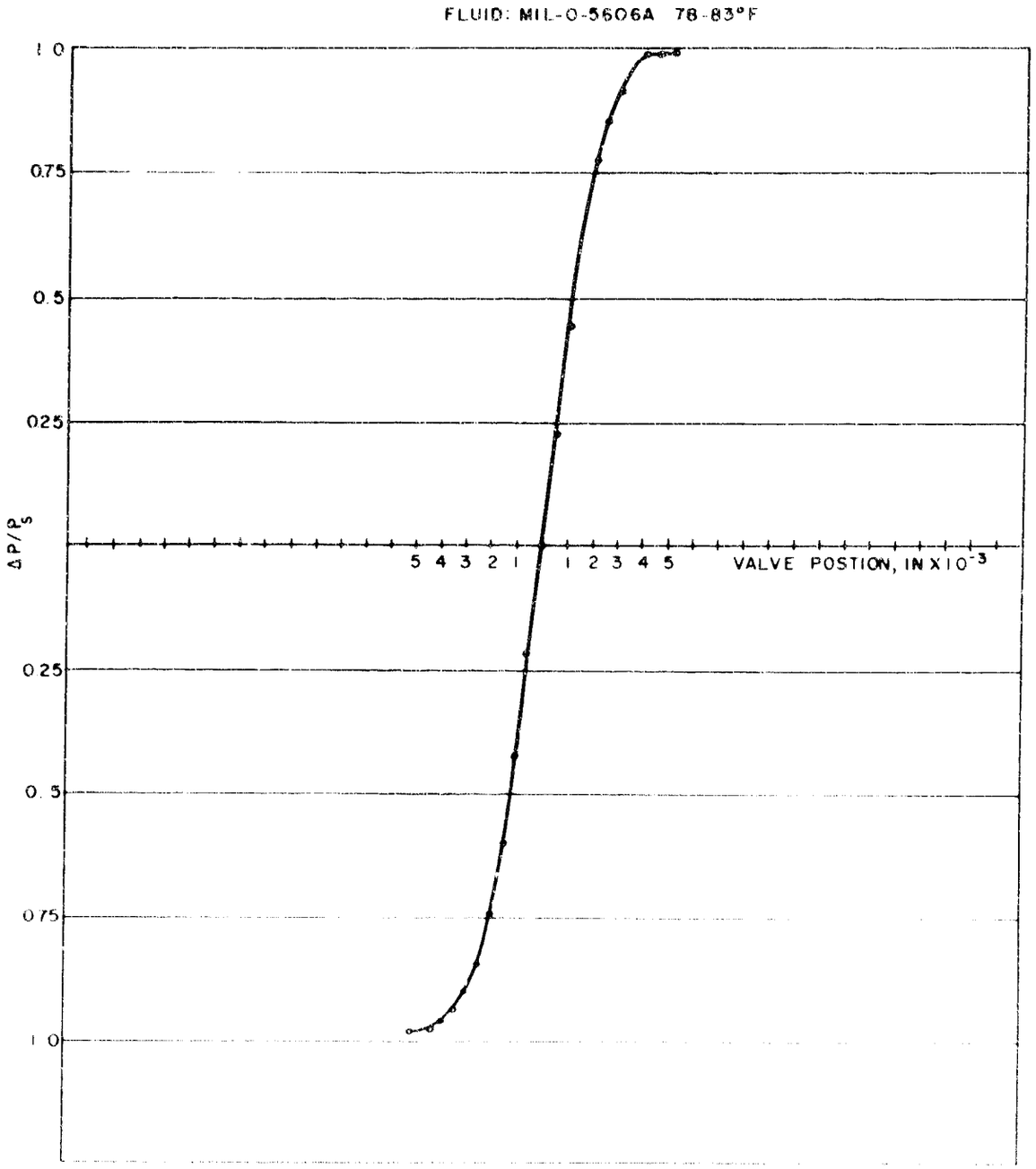

Figure 51 - Pressure Gradient - # 1 Servovalve

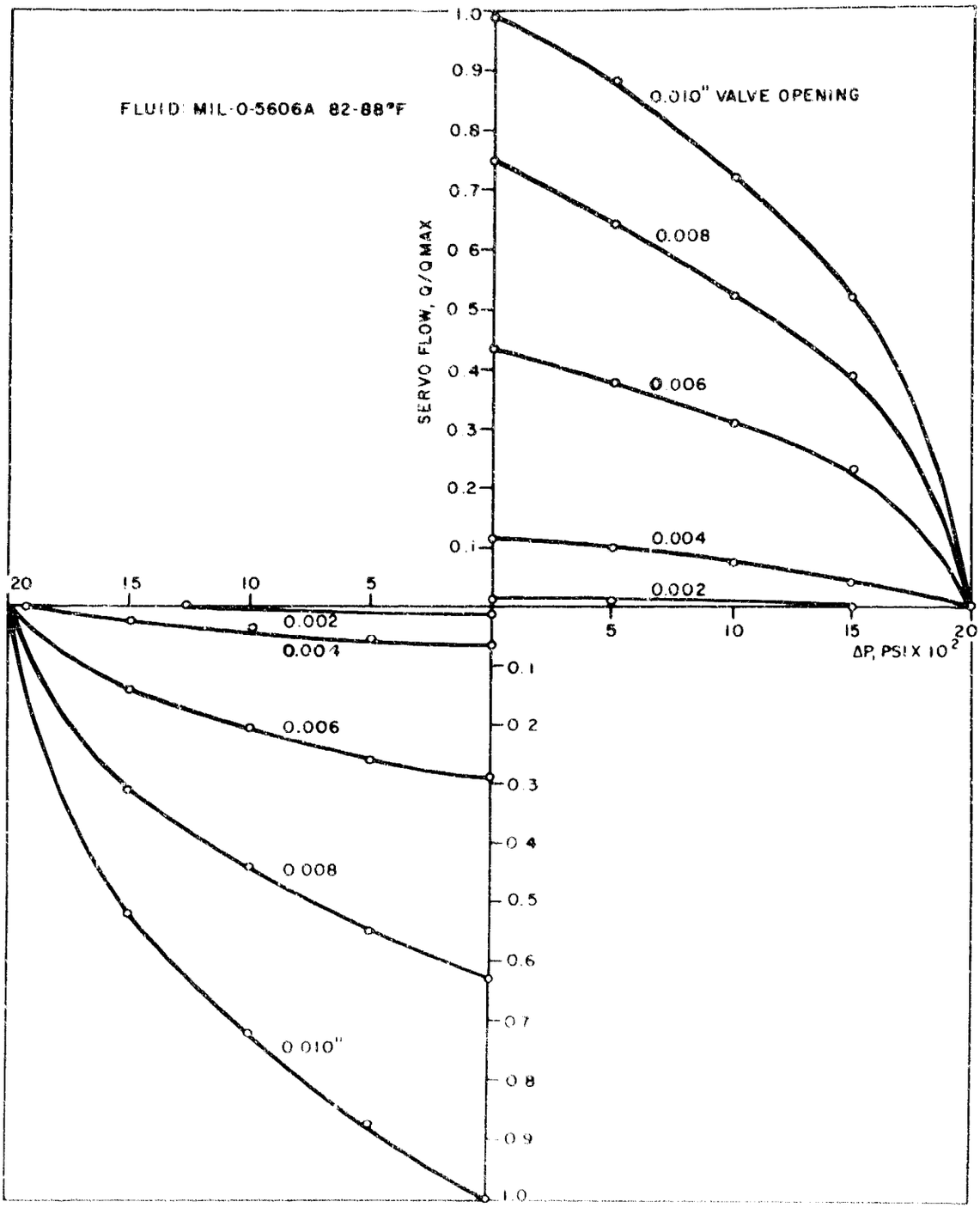

Figure 52 - Load-Flow Curves - # 1 Servovalve

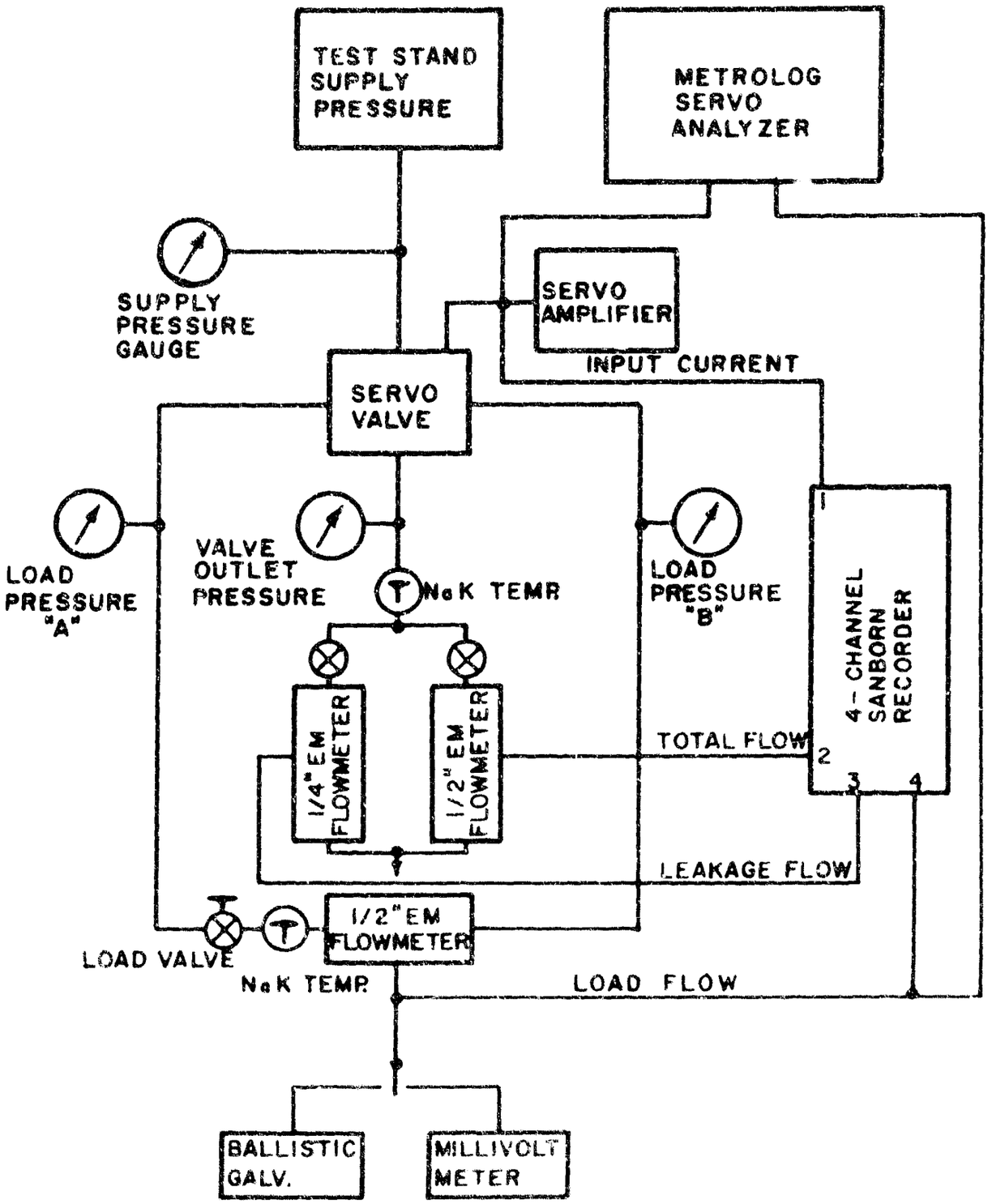

Figure 53 - Schematic of NaK Valve Test Loop

Figure 54 - NaK Test Loop with Servovalve Installed

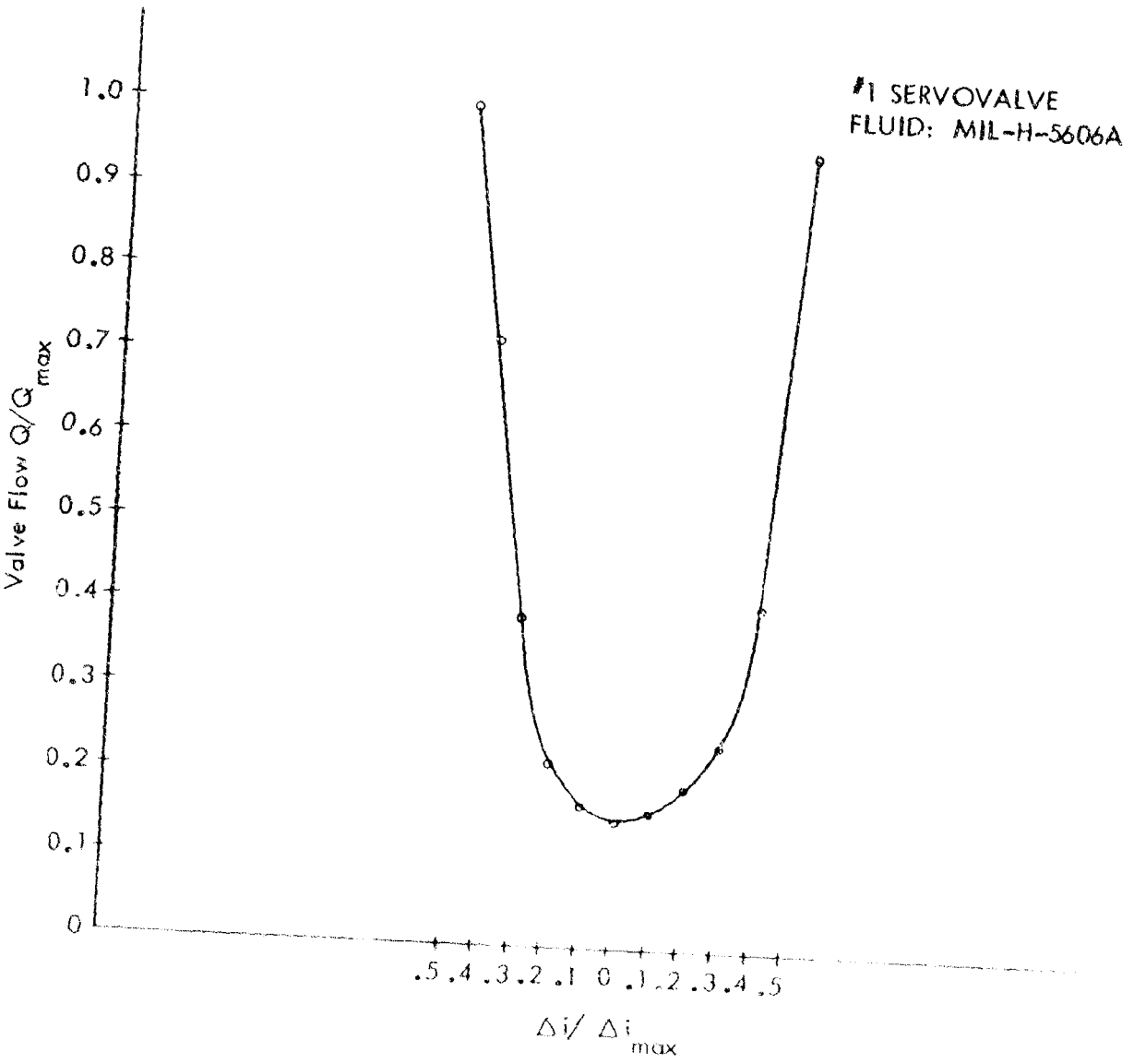

Figure 55 - No-Load Valve Flow-Servovalve Oil Test

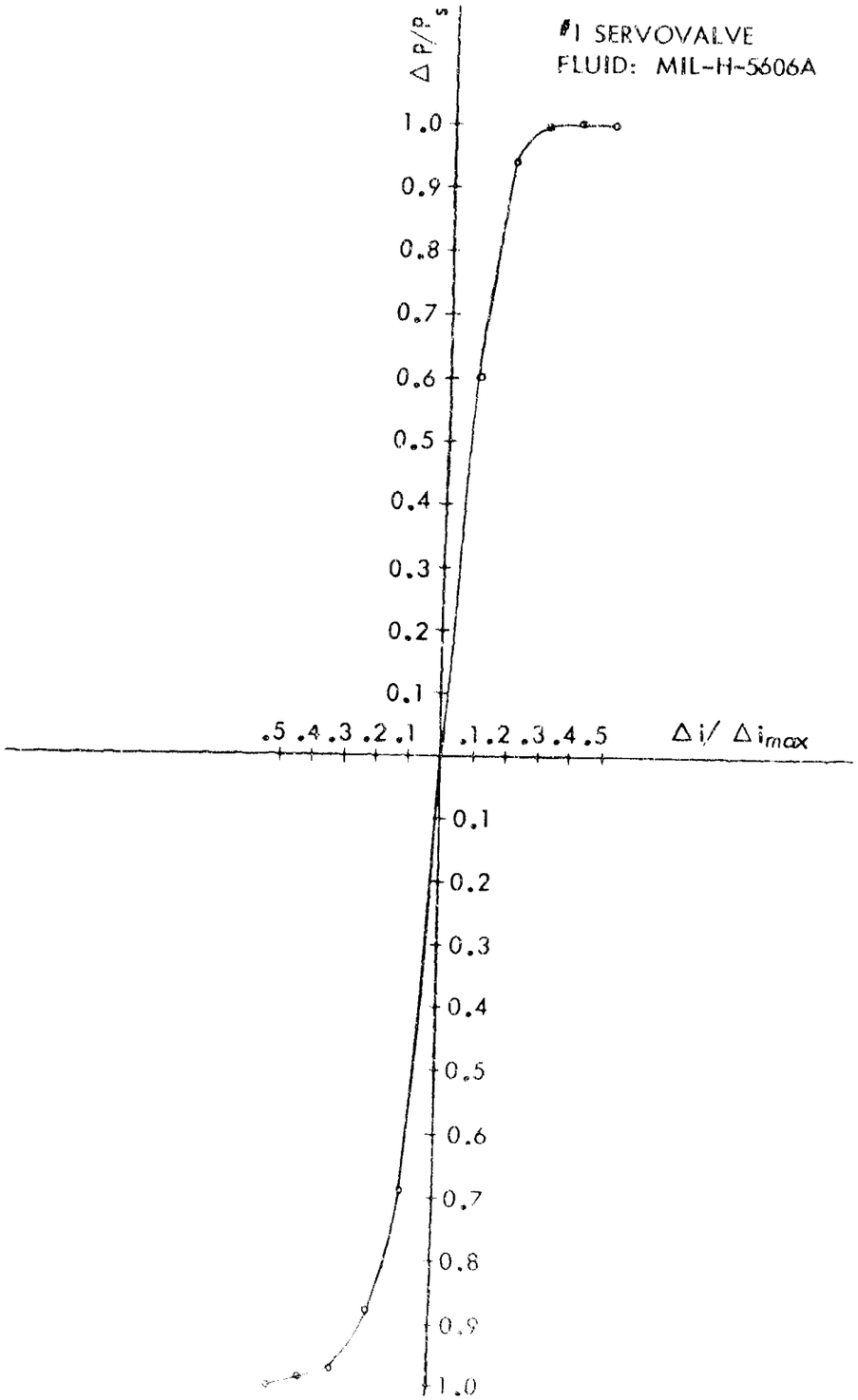

Figure 56 - Blocked Servo Pressure Gradient - Servovalve Oil Test

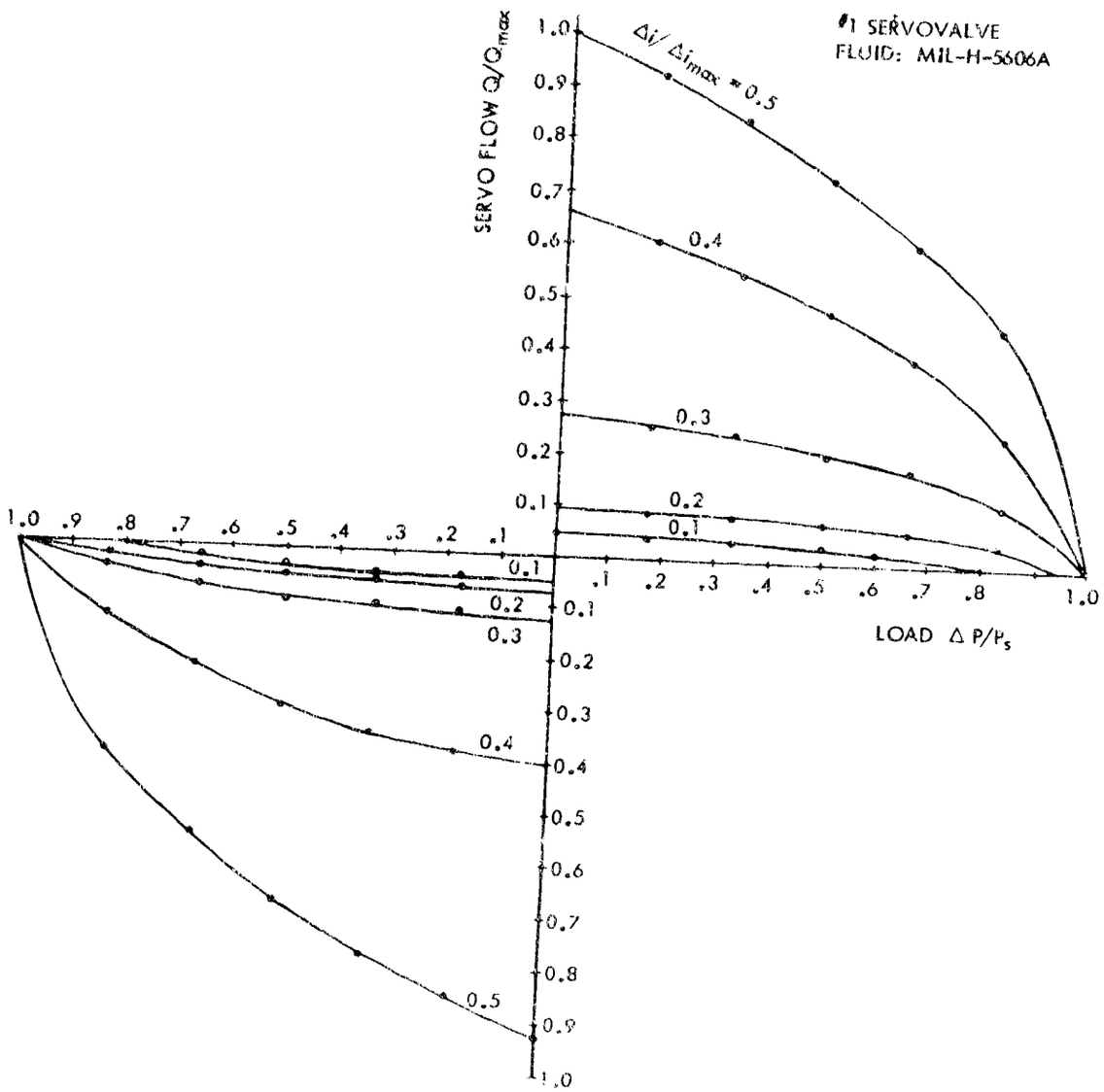

Figure 57 - Servo Flow-Load Characteristics - Servovalve Oil Test

Figure 58 - Nak Leak in Torque Motor after Servovalve Tests

Section VII

RELATED COMPONENTS

The basic objective of the present liquid metal program is the confirmation of liquid metal feasibility through test evaluation of a servoactuating subsystem at elevated temperature. Concurrently, effort has been devoted to the preliminary design of an experimental system capable of operation in both atmospheric and nuclear environments. In consequence, the major portion of the work has been concentrated in the areas of pumps, servovalves and actuators because these are essential to the operation and evaluation of the system. While seemingly subordinated to these components, such accessories as pressure regulators, transducers, accumulators, filters and fittings are clearly recognized as necessities in the final design of a flight control subsystem.

In order to achieve economy in the expenditure of effort, priorities have necessarily been imposed. Thus, specific work phases have been assigned to the study of servovalves and pumps. While not occupying a separate section, it will be noted that similar concentrated effort has been devoted to actuators. To a lesser degree, this is also true of transducers. Supplementary studies of accessories have, in general, consisted of a compilation of design criteria and probable requirements, together with some specific data on what equipment is currently available or capable of modification to fit tentative specifications.

ACTUATOR

Under contract AF33(657)10875, a high-temperature liquid metal actuator was designed and built. An assembly drawing of this unit is shown in Figure 59. All structural members, as well as piston and rod, were of 422 CRE steel. Piston and rod were hardened to 50 Rc to provide a hard substrate for the LW-1 tungsten carbide flame plate on the running surfaces of each. Piston rings were HS-25 flame-plated with LW-1 on the periphery. Cylinder liner and piston rod bearing were K-163B1 titanium carbide.

Sealing of the rod is accomplished in part by the carbide bearing which acts as a capillary seal. The outer seal is an all-metallic, reed type developed by the B. F. Goodrich Co., with a HS-25 sealing member. The space between the seals is connected to drain so that the outer seal normally sees only return pressure.

An additional feature of the design is the welded bellows boot which covers the piston rod. This boot is normally connected to an inert gas supply so that the rod is protected from atmosphere. This precaution

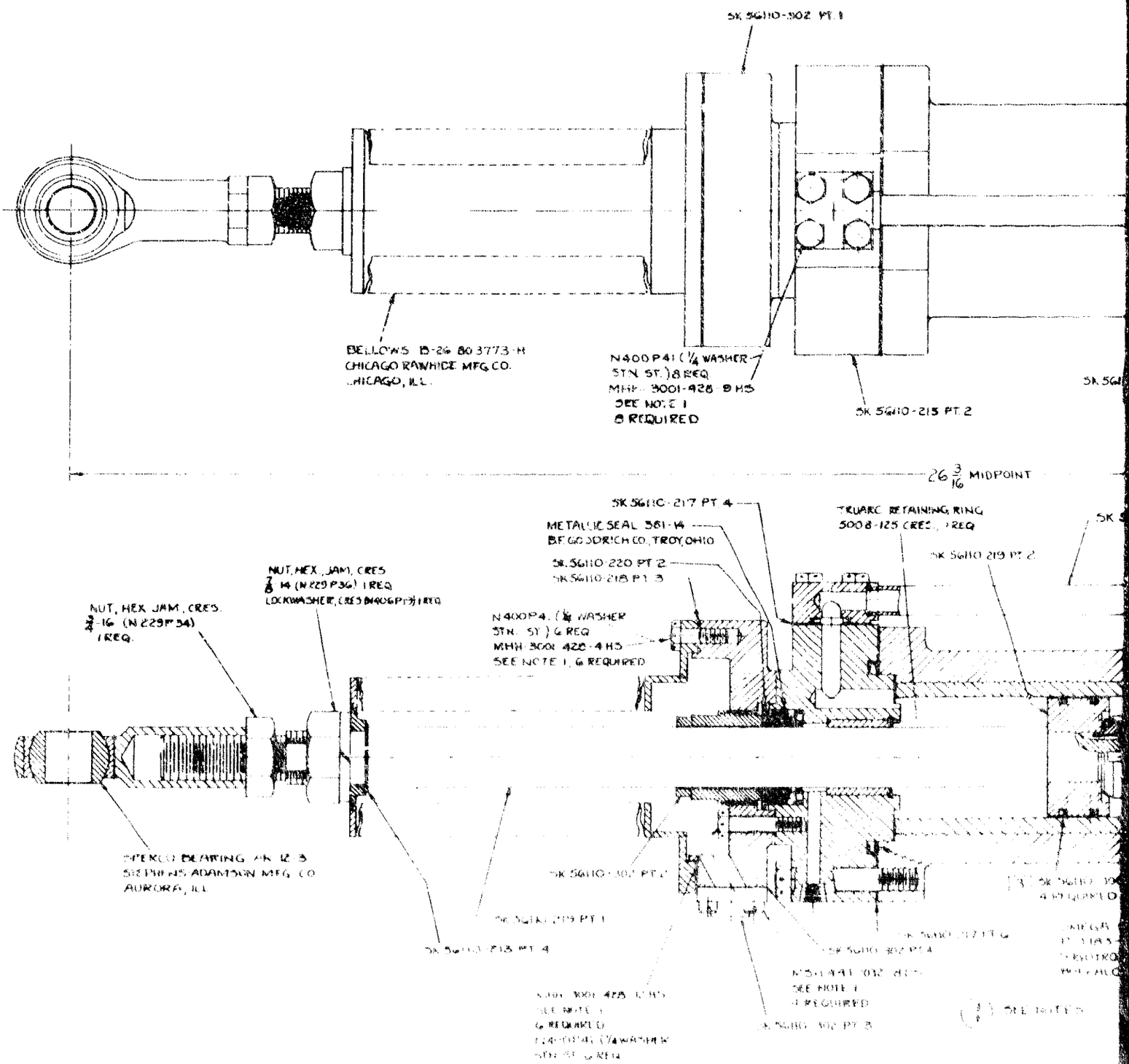

Figure 59 – Assembly Drawing – High Temperature NaK Actuator

NOTES: 1-MERCURY AIR PARTS CO., INC.
CULVER CITY, CAL.

2-STAKE FLAT HEAD SCREWS AT ASSEMBLY

3-SAFETY WIRE DRILLED HEAD SCREWS AT FINAL ASSEMBLY

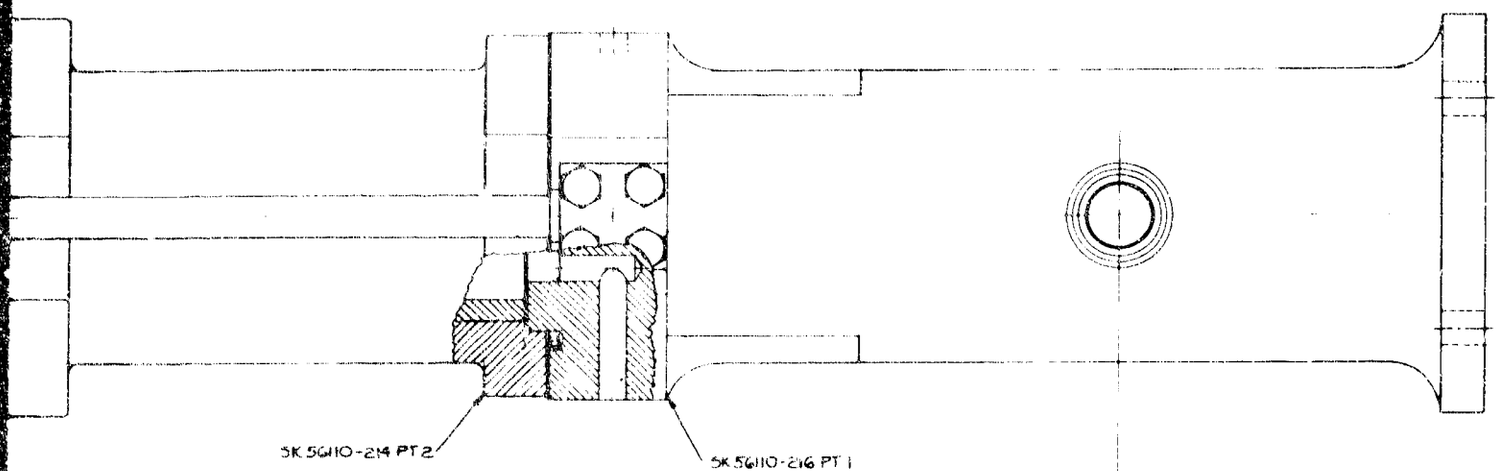

5G110-215 PT 2

$26\frac{3}{16}$ MIDPOINT

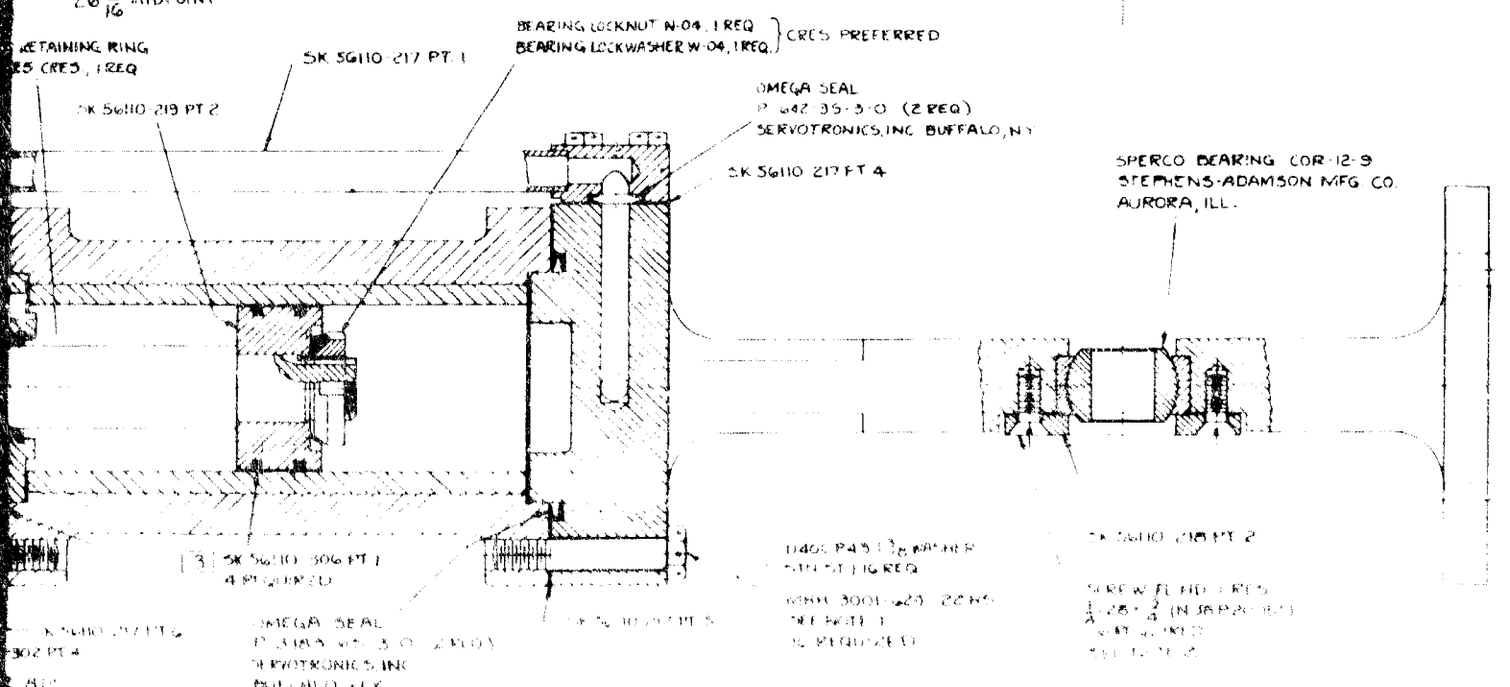

(1) SEE NOTE 3

BLANK PAGE

inhibits the formation of concentrated hydroxides resulting from NaK seepage through the seals. These hydroxides attack flame-plated surfaces severely.

In the current study, this actuator was tested over a temperature range of room temperature to 1000 F with NaK. Necessary re-design and modifications were made and also factored into the design of a second unit. The re-built unit was then used in the experimental model servo-actuating subsystem described in Section III.

Because the actuator was built before a servovalve and pump were available, testing was conducted by mounting the actuator on the load simulator which was then cycled by an hydraulic actuator, as shown in Figure 60. The unit was filled with NaK and both ends were interconnected through a loading valve. By reciprocating the actuator, NaK was forced from one end to the other, and by adjusting the loading valve, high pressures could be generated to test the rod seal and piston rings.

For initial tests, the actuator was installed in an inert atmosphere enclosure but the bellows boot was not in place. The rod seal was adjusted while cycling the actuator at room temperature. Approximately 1700, $\pm$ 2.5 inch cycles were accumulated. Maximum cyclic pressures of 600 psi at the rod seal end and 100 psi at the head end of the actuator were attained.

The difference in pressures is due to a metallic hose assembly on the rod end which provides an accumulator action to compensate for the volume differences between the actuator ends. This allows operation of the actuator with a single line connection between the ends without the complication of check valves and makeup reservoir.

Prior to conducting high-temperature tests, the bellows boot assembly was installed. An additional 1400 cycles at temperatures to 875 F were run before a leak in the rod seal forced termination of the test. This leakage was not due to a seal failure, but resulted from the difference in thermal expansion between the 422 piston rod and the HS-25 sealing member. The seal had been adjusted for zero leakage at room temperature. The coefficient of thermal expansion for 422 is 6.5×10^{-6} in/in/^{o}F, while that of HS-25 is 8.02×10^{-6}. Hence, at 875 F there was a difference of about 0.0012" in the diameters of the rod and seal which relaxed the seal sufficiently to allow leakage.

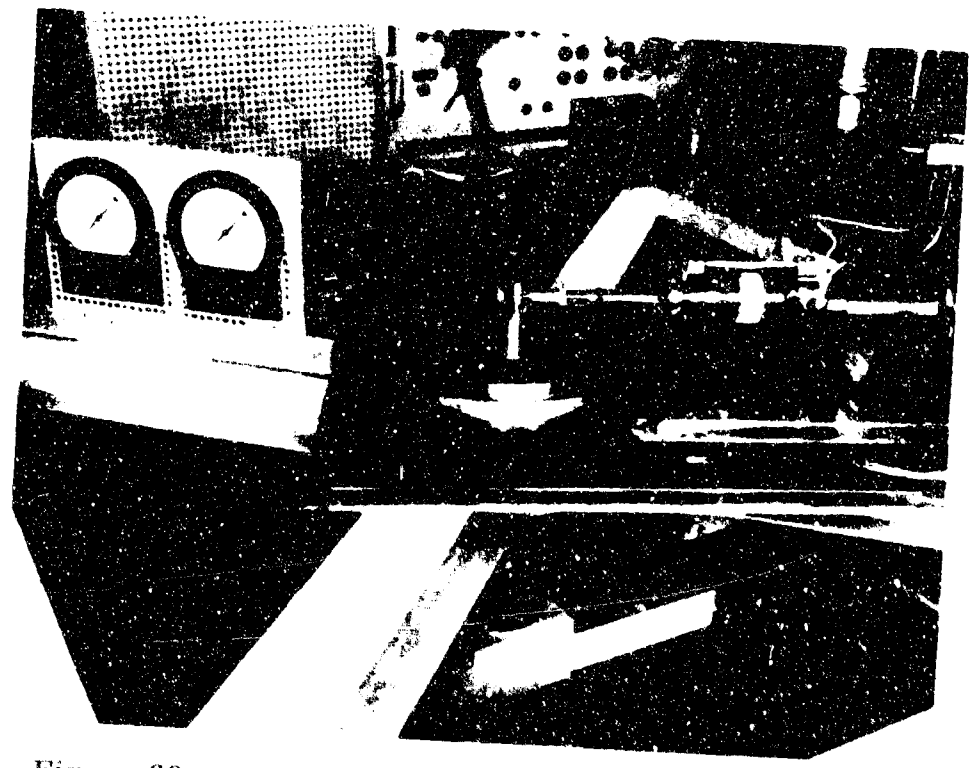

Figure 60 - Cyclic Test Setup - High Temperature NaK Actuator

At the conclusion of the test, it was found that one of the bellows convolutions had completely broken as shown in Figure 61. This boot assembly had undergone about 1600 cycles under conditions far less than its design rated limits of motion or temperature.

After inspection, the bellows vendor reported that failure was definitely due to material overstress and fatigue. Concurrently, a stress analysis made by Battelle Memorial Institute showed that the expected fatigue life for a 14-convolution, Inconel - X bellows at 800 F would be in the vicinity of 2000 cycles of alternating stress. Accordingly, a new 100-convolution bellows was ordered. Calculations indicate that this bellows should have a fatigue life of 500,000 cycles at an operating temperature of 1500 F.

A second high-temperature test was then conducted. Since the protective bellows boot was no longer usable, there was concern for conserving piston rod and seal life as much as possible so as to assure performance of the 1000 F test condition. Consequently, test procedure was changed so that the actuator was operated only at specific temperature points of 300, 500, 750, and 1000 F. A total of 300 cycles were accrued during this test.

Actuator performance was normal for the 300, 500 and 750 F runs. At 1000 F the actuator seized after approximately 30 cycles. Upon disassembly, several areas of distress were observed. The direct cause of failure was pick-up and material transfer between the flame-plated piston rod and the titanium carbide rod bearing. At the same time, the flame-plate was attacked and removed on that portion of the rod which was exposed to both NaK and the atmosphere of the glove box. The condition of the piston rod after test is shown in Figure 62. The rod bearing, showing the deep groove ploughed in the surface is Figure 63.

The titanium carbide cylinder liner was also scored by the sharp corners of the piston ring gaps, as shown in Figure 64.

The appearance of the flame-plated rod and piston, following test, shows that:

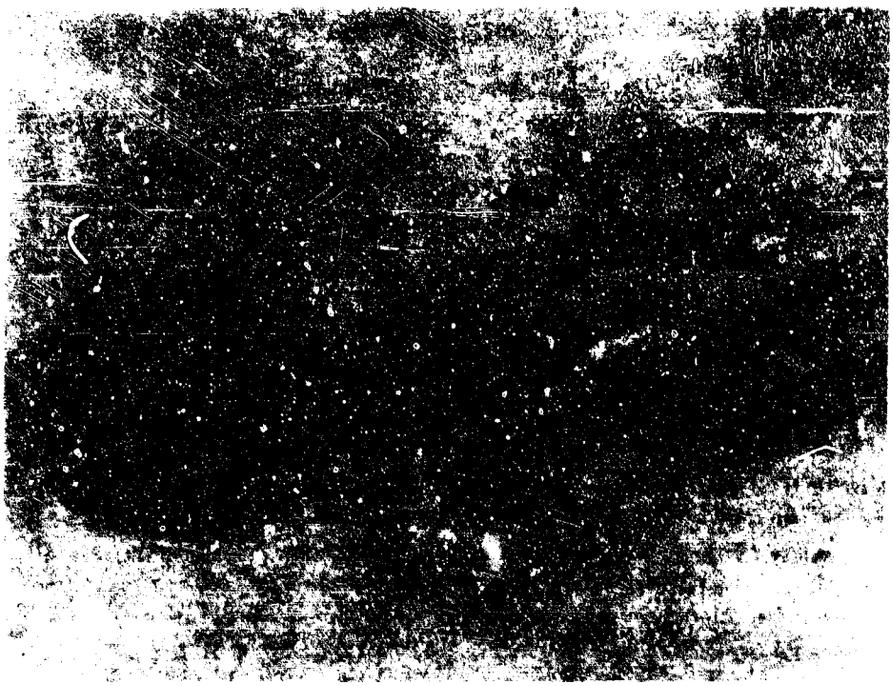

Figure 61 - Welded Bellows Boot Showing Failure of Convolution

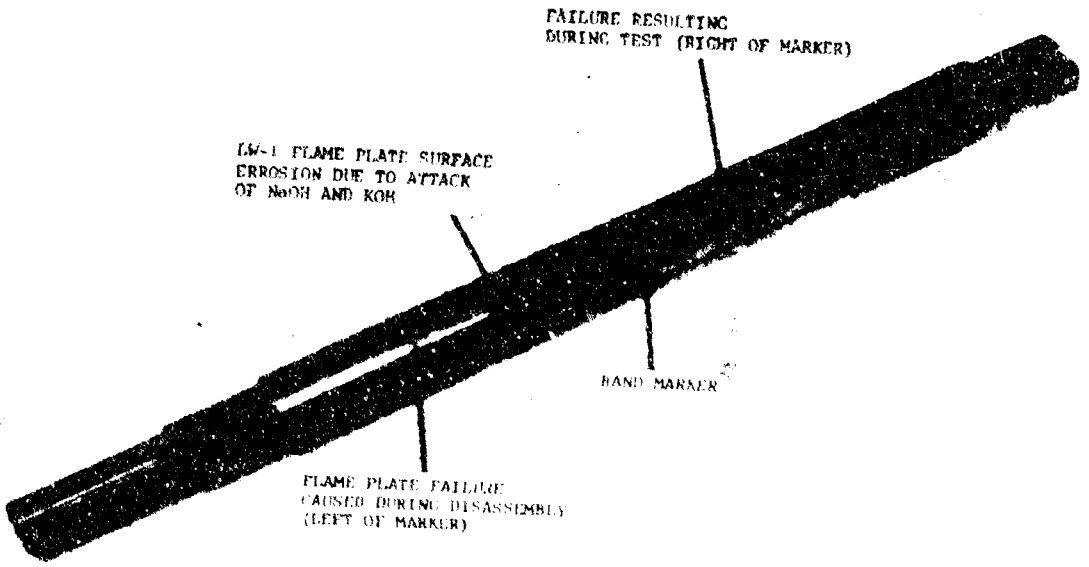

Figure 62 - Actuator Piston Rod After Test

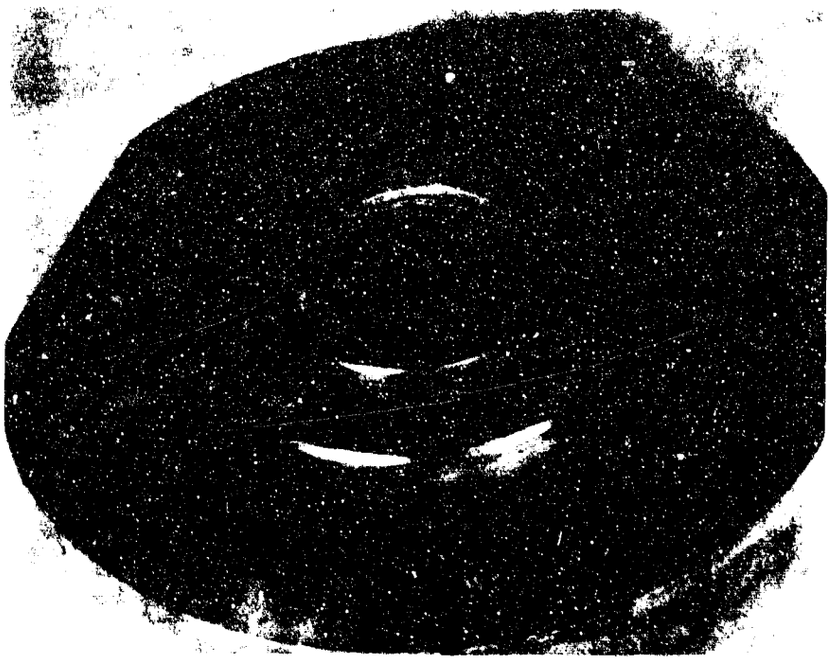

Figure 63 - Actuator Rod Bearing After Test

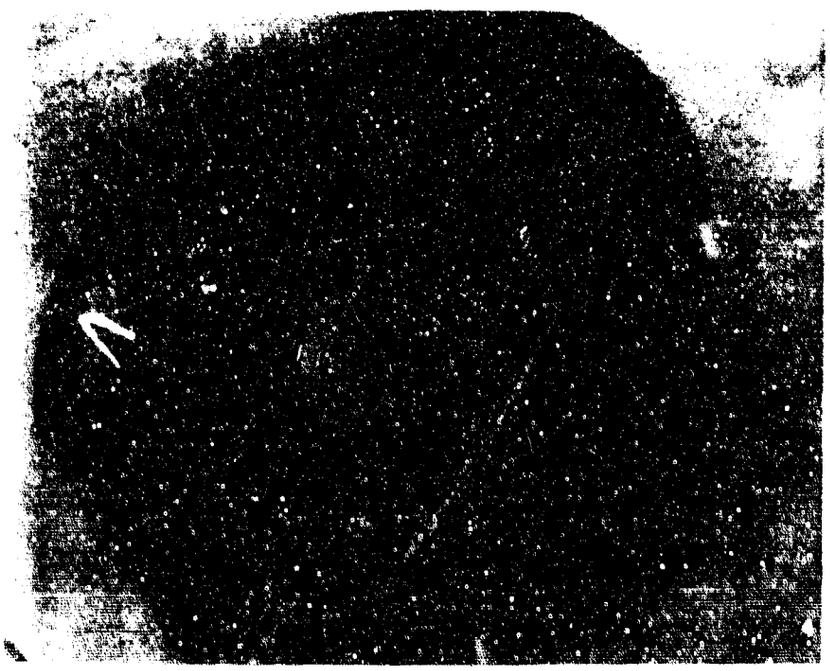

Figure 64 - Actuator Cylinder Liner After Test

1. LW-1 flame plate is severely attacked by hot, concentrated KOH and NaOH, as evidenced by the erosion of the surface which occurred on the exposed part of the actuator piston rod. A protective boot assembly is essential if use of this material is contemplated.

2. Failure of the LW-1 flame plate on the rod and absence of any distress on the piston indicates that cleaning procedures are not the primary cause of such failures.

3. Other evidence indicates excessive porosity and poor adherence of the flame plate on the rod as compared to the coating on the piston.

Figure 65 shows plating porosity on the piston rod. Figure 66 is an illustration of the poor interface bonding between the tungsten carbide flame plate and the 422 base.

Since no better hard surface treatment was available at that time, it was decided to continue use of the tungsten carbide flame spray on the piston and rod but to use the LW-5 grade which is a dense coating. In addition, no further tests would be conducted without installation of the protective bellows boot and inert gas cover.

In view of the excellent results obtained with the HS-25 rod seal, the rod bearing was also changed from K-163B1 titanium carbide to HS-25.

With these modifications, the actuator was re-built, and a duplicate actuator fabricated. An exploded view of the modified actuator, including the 100 convolution bellows boot, is shown in Figure 67. Further evaluation of the actuator was deferred until completion of the experimental subsystem and its operation, which is described in Section III.

The actuator, which was in excellent working order at the completion of the experimental system evaluation tests, was completely disassembled, cleaned and inspected. The results of this inspection were very encouraging.

The new 100 convolution bellows boot replacement operated successfully throughout the test program. The excellent condition of this unit is shown in Figure 68.

The appearance of the LW5 flame plated rod, following the system tests, is shown in Figure 69. Initially, upon removal and cleaning, the rod exhibited no apparent damage and no signs of wear were evident. After several hours of exposure in the air environment following cleaning and the first inspection, however, dimpling of the flame plated surface appeared on the rod at several locations.

It was noted that this condition was found to exist only on that portion of the rod which extended outboard of the wiper seal during operation. As described in Section III, during performance of the experimental subsystem tests, dis-assembly of the bellows boot was required under air environment conditions to tighten the rod seal in order to provide satisfactory sealing under operating conditions above 800 F. Althoughthis seal adjustment was performed at room temperature, the effects of oxidation on the exposed portion of NaK coated rod assembly, even for a short time, appears to have precipitated this surface damage. The actuator piston and remaining portions of the rod assembly which were not exposed to air until the cleaning operation, remained in excellent condition and show no signs of surface deterioration.

The HS-25 rod bearing, following the system tests is shown in Figure 70. This bearing is in excellent condition and shows no evidence of wear. It appears that the material change to HS-25 and other design modifications made to the bearing have eliminated the difficulties experienced in the previous actuator test, shown on Figure 63.

The condition of the K-163B1 actuator cylinder liner, following test is also shown in Figure 71. Here again, it appears that the scoring of the bore experienced during initial testing, Figure 64 was eliminated by replacement of the square cut end type piston rings with ones of the step cut design which also have all sharp corners broken.

The results of the experimental system tests conducted to date have demonstrated a successful actuator design. Improvement of this design, in two areas, is recommended.

1. A more compatible actuator rod and wiper seal material combination should be found to minimize the high rod seal forces that must be applied at room temperature in order to obtain effective sealing at elevated temperatures due to the large thermal expansion coefficient difference that exists between the HS-25 and 422 CRES steel materials.

2. Flame spraying of the actuator rod should be eliminated and other hard surfacing treatments such as boriding be investigated for use as a suitable replacement. Boriding is recommended since this process has produced successful results in both the pump bearing and servovalve sleeve application.

It is therefore recommended that the actuator design be altered to incorporate these modifications, and the unit re-built and assembled for use in the further experimental system static and dynamic testing.

POSITION FEEDBACK TRANSDUCER

The purpose of the transducer is to provide an electrical signal to indicate the exact position of the actuator rod. This signal provides the necessary position feedback information to the servo control system.

The linear position transducer design considered for use in this study is based on the electrical concept of the linear variable differential transformer (LVDT) where a moving slug is used to couple non-linearly wound primary and secondary windings. Thus, as the slug is moved, an electrical output results which is directly proportional to the position of the slug. The operation is made linear by controlling the windings ratio so that the output voltage is directly proportional to the displacement of the movable slug from a reference position. The transducer is of the differential transformer type; its output voltage being the difference between two opposed voltages developed in the secondary windings.

Whenever the LVDT slug is centrally positioned, the voltages in the two halves of the secondary are of equal magnitude, but of opposite phase. This results in a net secondary output voltage of zero. This central position of the slug is called the null point. Any departure of the slug from this null point results in some net output voltage. Because of small out-of-phase components, the AC null voltage does not actually reach zero, but does reach a minimum. A level of 50 mv is not unusual.

When the slug is displaced from the null point, the magnitude of the voltage indicates the amount of the displacement. The phase of the voltage indicates the direction of the slug displacement from the null position. The AC output with amplitude variation and phase change through the null point is changed into a $\pm$ DC signal in a demodulator. An oscillator is used for excitation of the primary winding.

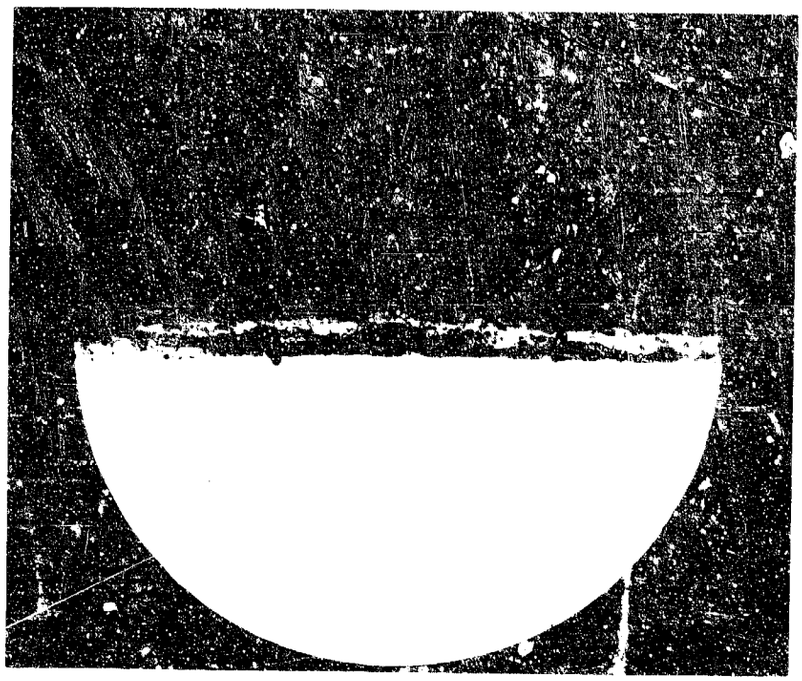

Figure 65 - Piston Rod Showing Porosity of Flame Plating

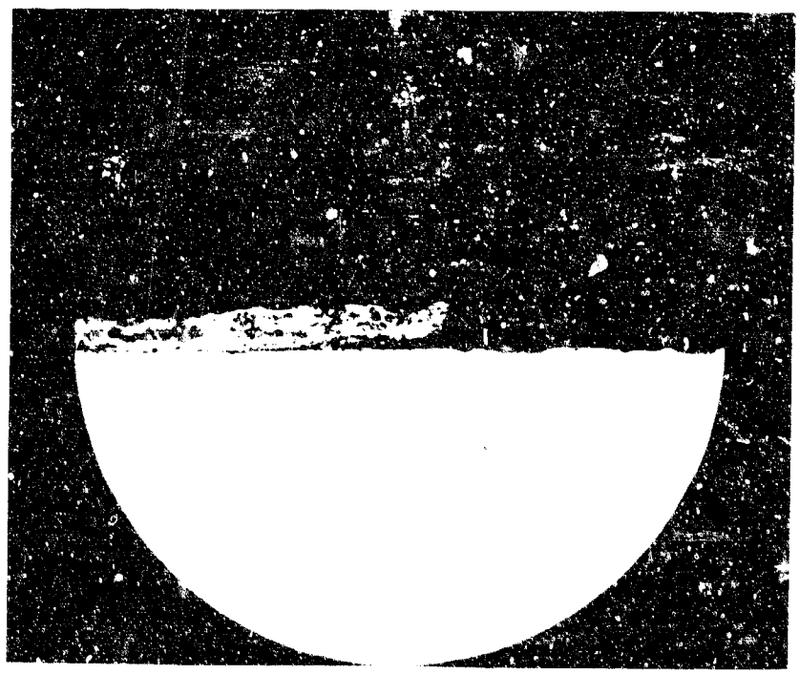

Figure 66 Piston Rod Showing Failure of Interface Bonding

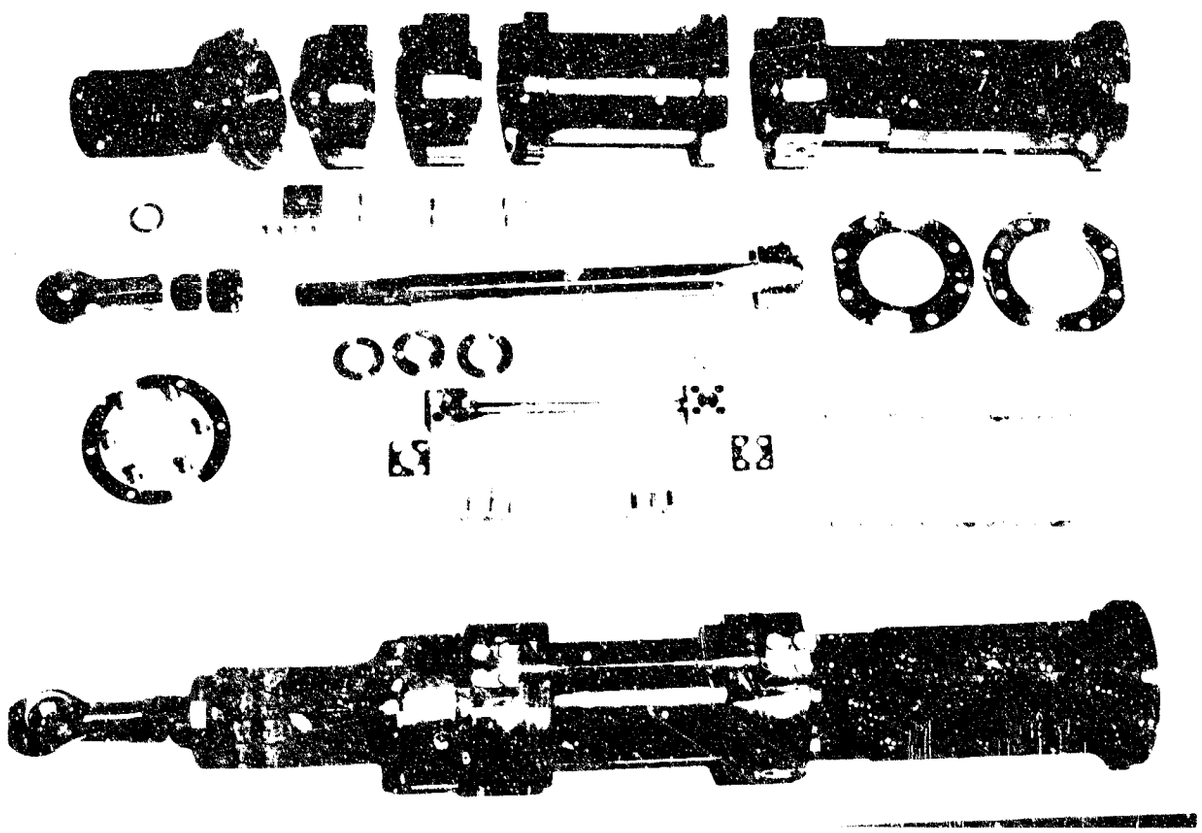

Figure 67 - Modified High Temperature NaK Actuator - Exploded View

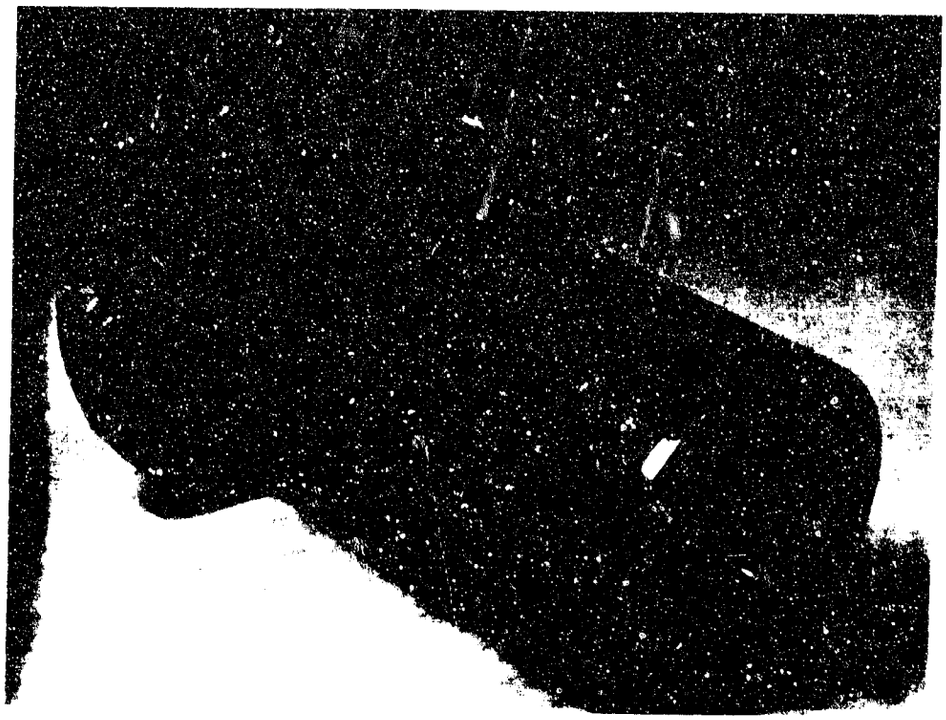

Figure 68 - Condition of Actuator Boot After Test

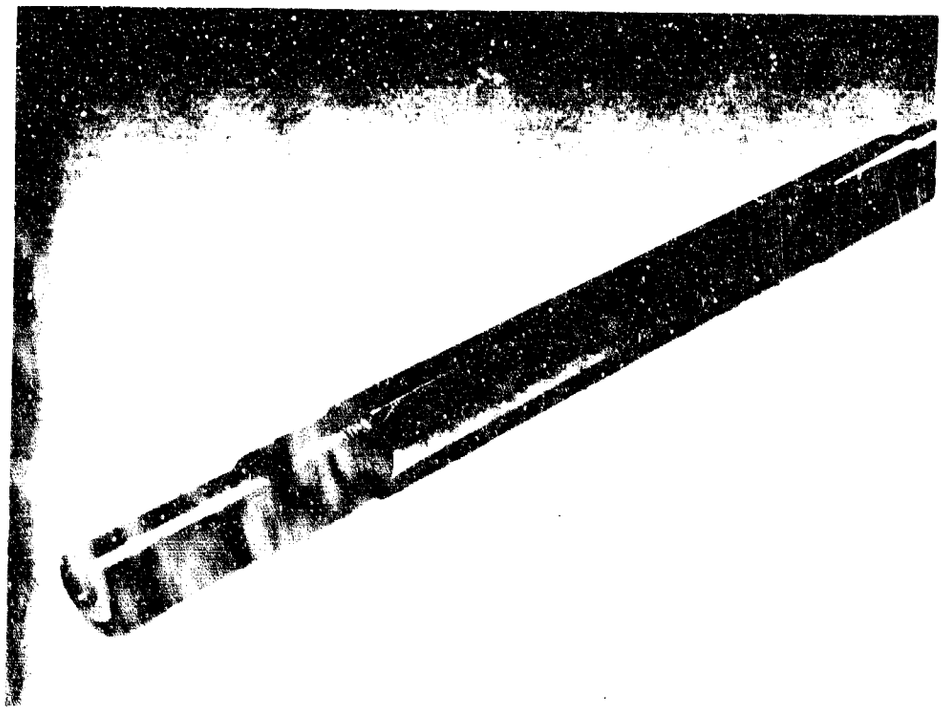

69 Condition of Actuator Rod After Test

Figure 70 - Actuator Rod Bearing Following Test

Figure 71 - Actuator Cylinder Liner After Test

The transducer is mounted on the actuator in the experimental system so that the transducer axis is parallel to the axis of rod movement. A shaft connected to the transformer slug is joined to the rod, so that the rod movement slides the slug through the transducer body.

Procurement of such a position feedback transducer was complicated by the fact that very limited information was available on these devices for high temperature use. Of the various sources contacted, only one offered past experience in the design and construction of transducers for 1200 F service. This situation was confirmed by consultation with qualified agencies and personnel who are involved in the procurement and evaluation of high temperature instrumentation.

It was therefore decided to purchase a transducer from Bendix Research Laboratories who had previously built similar units for the Pluto project. The objective design parameters were as follows:

1.	Mechanical Stroke	$\pm$ 2.5 inches
2.	Electrical Stroke	$\pm$ 2.375 inches
3.	Operating temperature	70 F to 1200 F maximum
4.	Operating environment	Argon and NaK vapor
5.	Thermal cycles (70 F to 1200 F to 70 F)	20 total (time-temperature history to be maintained)
6.	Maximum frequency of operation	25 cps
7.	Life at 1200 F (cumulative)	15 hrs. min. (time-temperature history to be maintained)
8.	Excitation power supply	As per ELIN power oscillator RK-106-53 or equivalent
9.	Gain (output voltage)	0.03 volts/inch/volt input
10.	Gain variation due to temperature	$\pm$ 5 percent maximum
11.	Linearity	0.02 percent
12.	Repeatability	0.02 percent

13.	Resolution	0.02 percent
14.	Noise	100 millivolts maximum

The space envelope for this transducer is outlined in Figure 72.

The transducer as delivered, is shown in Figure 73. It consists of two concentric stainless steel tubes with the primary and secondary windings wound on the inner or bobbin tube. Sliding through the bobbin tube is the slug which is made of magnetic material.

Stainless steel is used for all structural components of the transducer. Non-magnetic components are made of 300 series steels, while type 430 steel is used for components requiring magnetic permeability. Asbestos type insulation is used between the winding layers and the outer winding and transducer housing.

The primary winding is 7.5 inches long, consisting of two layers, totaling 892 turns of stainless steel clad copper wire. Electrical connections to the transducer are made through a special high temperature four pin Cannon connector.

The slug stroke is $\pm$ 2.50 inches from the null position. The design linear operating range of the unit is $\pm$ 2.375 inches.

Development effort in this transducer study was limited to investigation of the winding types and slug designs to obtain the required operating characteristics. Two bobbins with different winding schedules were fabricated and tested. One had a stepped taper winding and the other had a stepped V winding. The stepped taper winding produced the most linear output and was used in the final transducer assembly, Figure 73.

The transducer was subjected to performance checkout tests prior to delivery. These tests consisted of:

1. D.C. resistance of primary and secondary coils.
2. Insulation resistance between primary and secondary coils, primary coil and ground and secondary coil and ground.
3. Null voltage
4. Gain curve, plot of output voltage versus input displacement at room temperature only.

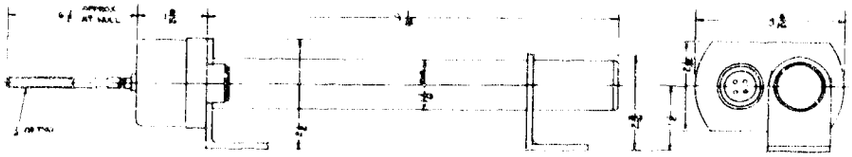

Figure 72 - Space Envelope - High Temperature Position Transducer

Figure 73 - High Temperature Position Transducer

The gain curves for the transducer obtained by the vendor prior to delivery of the unit is given in Figure 74. Similar data obtained from the transducer following its installation in the system prior to initiating the high temperature tests is shown on Figure 75. Variations between the two curves obtained can be attributed to differences in both the method and instrumentation used in obtaining each set of data. It appears from the data proposed by the Vendor (Fig. 74) linearity characteristic of the unit fell short of the design intent. However, further test on the unit when installed in the system demonstrated good linearity (Fig. 75). Because of the nature of difficulties experienced with the torque motor when conducting the experimental system tests, it was not possible to obtain accurate high temperature data from the feedback transducer. However, recorded data was obtained from the transducer throughout the experimental system test, over the complete range of test temperatures. The feedback transducer functioned satisfactorily throughout the entire test program and was in excellent working order at the conclusion of the system evaluation.

The results of the initial experimental system tests definitely indicate need for further high temperature testing on the feedback transducer independently, in order that its characteristics be defined over the 1200 F operating range to determine if all design requirements have been met before any further system testing with this transducer is undertaken.

PRESSURE REGULATION EQUIPMENT

Pressure regulators for 3000 psi, 1200 F service represent a special development, no such equipment being currently available. A survey conducted as part of a previous contract showed at least one manufacturer with a definite interest in undertaking such a development.

Because the current program utilizes a centrifugal pump, pressure regulation equipment was not essential in performing subsystem tests. At the same time, the contract effort did not permit a development program for regulators or relief valves. Consequently, a relatively simple valve, Figure 76, which has given satisfactory service for several years, was incorporated in the test loop.

While more sophisticated designs will be required in flight test applications, and present equipment has satisfied previous test conditions, the initial experimental system tests have demonstrated an immediate need for more effective fluid regulation equipment if good system operation is to be attained. Inherently, the operating characteristics of high pressure centrifugal

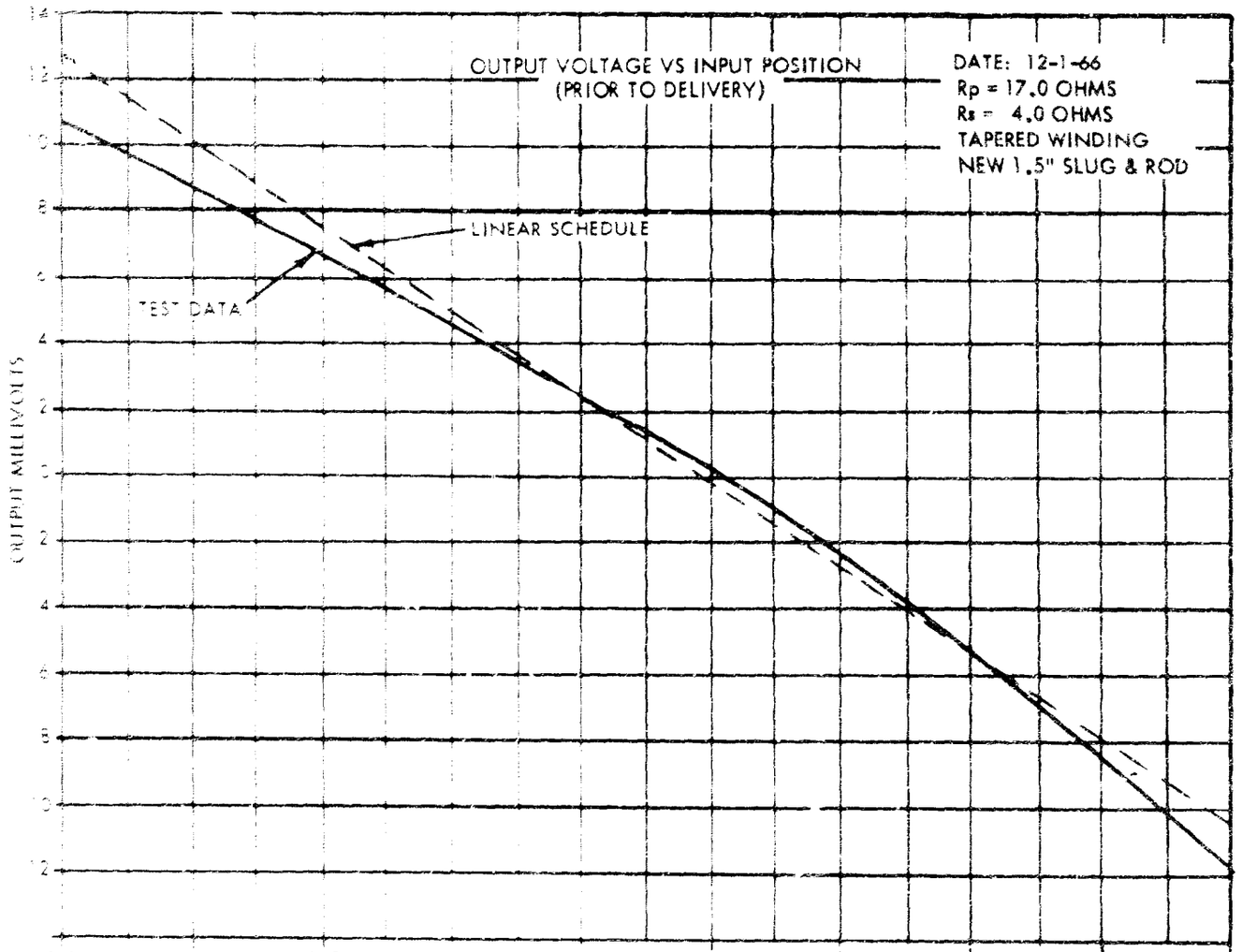

Figure 74 - Transducer Gain Curve as Furnished by Vendor

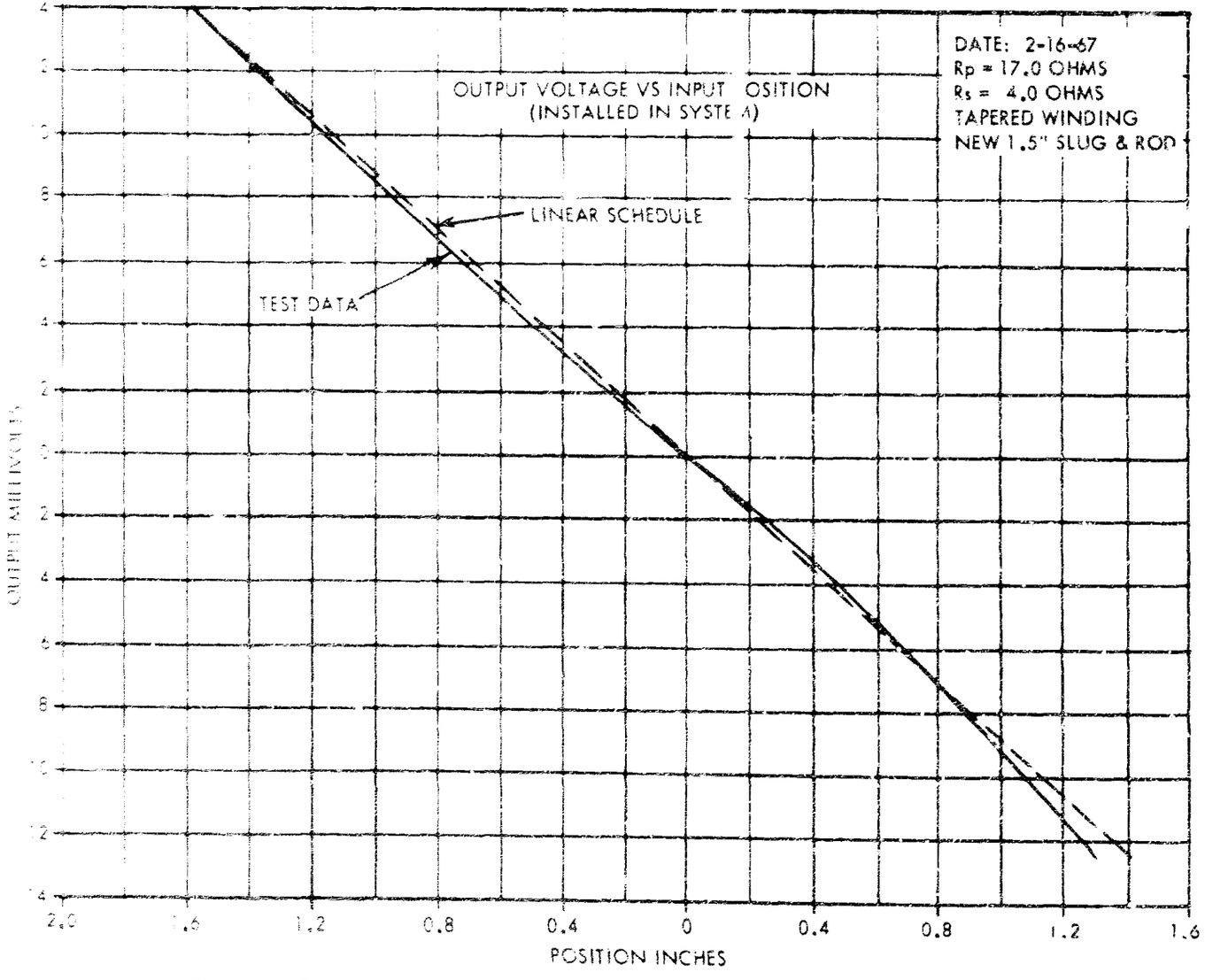

Figure 75 - Transducer Gain Curve Taken After Installation

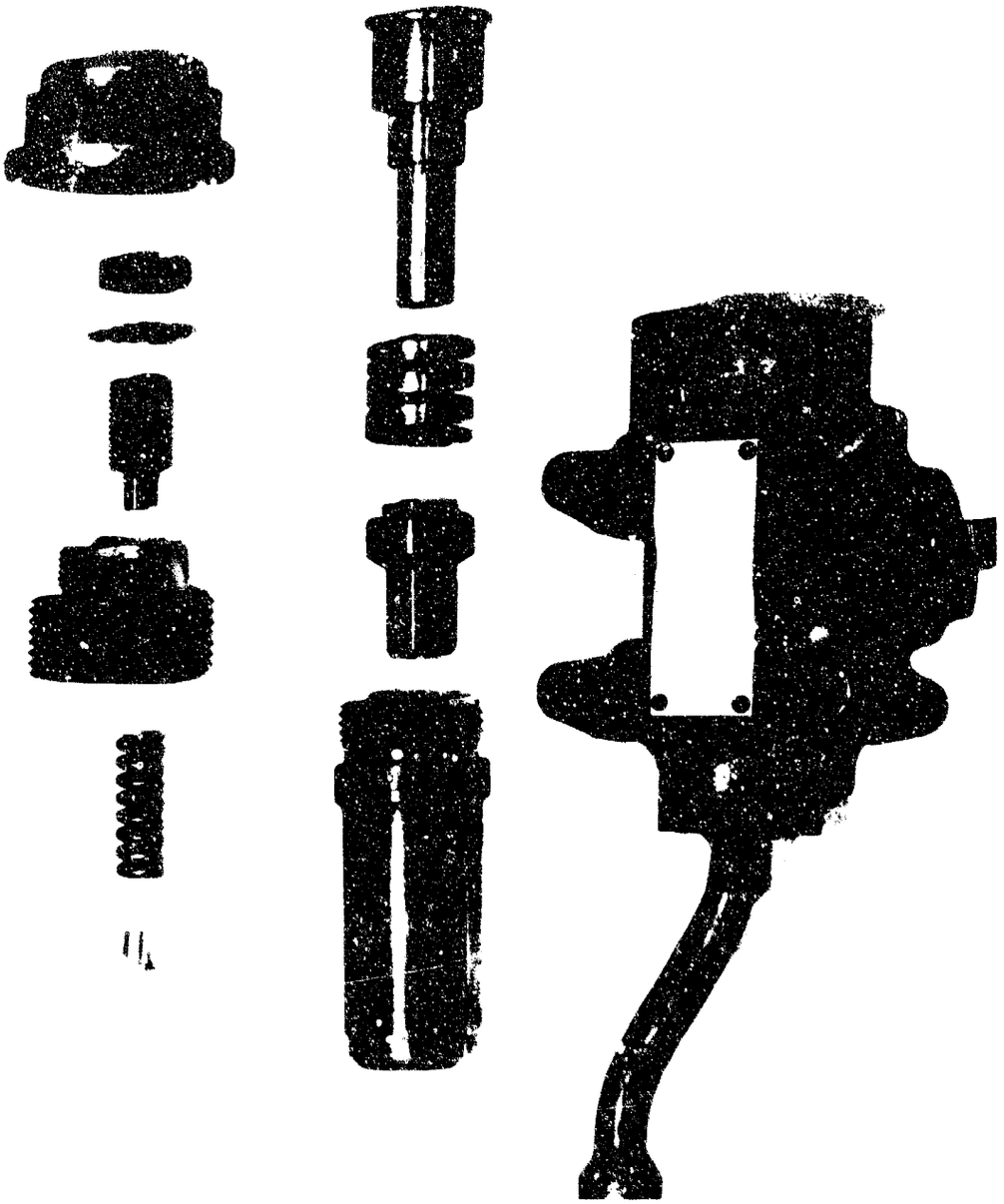

Figure 70 - High Temperature Relief Valve

pumps are not compatible with use of a pressure regulator as a means for fluid control. This control can best be achieved by flow regulation. A combination of both fluid bypassing and throttling would provide the most compatible method of fluid regulation for the system applications considered in this program.

It is therefore recommended that future consideration be given to this problem and that equipment be designed and suitable hardware fabricated for use in the dynamic test evaluation phase of the experimental servoactuating subsystem study.

ACCUMULATORS

A survey of accumulator types has shown that a metallic bellows, providing a positive barrier between fluid and inert pressurizing gas is the most practical design for high-temperature, liquid metal accumulators. At the present time, no such accumulators are available as standard commercial components.

An accumulator designed and built by the General Electric Company for a high-temperature, nuclear radiation environment is illustrated in Figure 77. It has been tested at 2000 psi and 500 F for a total of 305,000 cycles without failure. The design of the bellows is such that liquid or gas pressure alone results in a stacking of the bellows elements so that high differential pressure can be withstood. The design is readily adaptable to liquid metal service by replacing the organic 0 - rings with metallic seals.

A survey has located at least two bellows manufacturers who have built liquid metal accumulators for AEC applications. Sufficient basic design data is available to produce an accumulator when required. The experimental subsystem of Section III does not include an accumulator, since high-frequency dynamic tests are not included in the test schedule. Further study and design refinements will be required to provide units with weight, size and reliability suitable for flight test service.

The need for an accumulator in the experimental model servoactuating subsystem was effectively demonstrated during the initial tests conducted on the system. It is imperative that before a test program to evaluate the dynamic performance of the system can be conducted, a suitable accumulator must be added to the system.

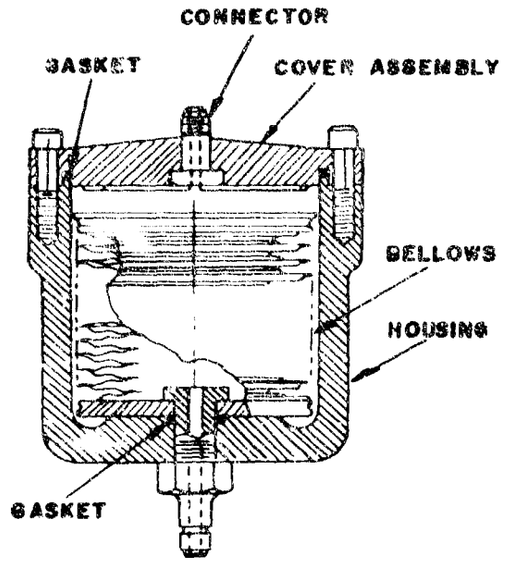

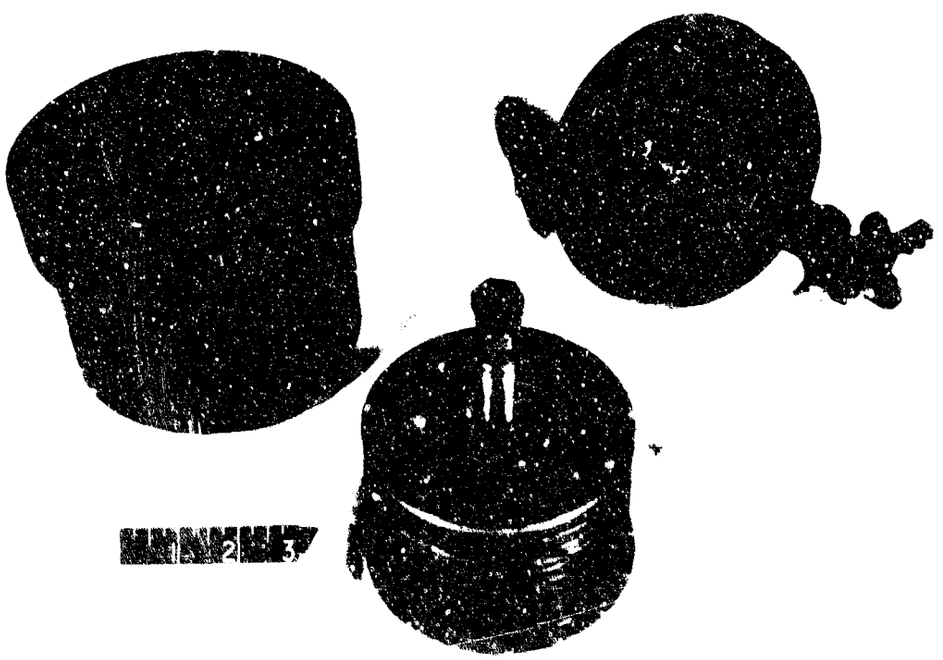

Figure 27. High Temperature Liquid Metal Accumulator

It is therefore recommended that an accumulator be designed similar to that shown in Figure 77 and hardware fabricated for future use in the system test program.

RESERVOIRS

Reservoirs for liquid metal systems may be either directly pressurized by gas or be of the "bootstrap type". In both cases, an inert gas must be used because of the necessity for maintaining an oxygen-free atmosphere. There are several types of stainless steels and heat-resistant wrought alloys which have the proper compatibility with liquid metals for structural purposes.

Because of the priorities on expenditure of effort in this program, no specific designs of reservoirs were carried out. Further study should be devoted to the economics of disposable versus permanent reservoirs. This involves not only consideration of reservoir design to facilitate inspection and cleaning, but also an examination of ground support equipment for reservoir servicing versus periodic replacement.

FILTERS

In the previous liquid metal programs, two sintered stainless steel filters were used in the NaK supply loop, with 200 mesh stainless screens in the pump suction lines.

Results of both vane and centrifugal pump tests gave a strong possibility that this filtration was not adequate. In the case of the vane pump, after several hours of satisfactory operation, the tungsten carbide flame-plate was removed from the shaft sealing member and passed into the pump. This was followed by severe surface damage of bearings, vanes, and cam ring. Similar wear and damage was observed in the journal and thrust bearings of the centrifugal pump.

While fluid contamination was not isolated as the immediate cause of damage, it was felt that provisions should be made to provide better filtration for the various components of the liquid metal subsystem.

As with other system accessories, there are no aircraft type filters available which are rated at 3000 psi and 1200 F. Specifications were drawn up for filter cartridges and submitted to three vendors. Filter housings, where required, were designed and built.

The filter cartridges are shown in Figure 78. Those in the upper left hand corner are 10 micron units and are used in parallel in the pump suction line. The lower cartridges are placed in the high-pressure supply to the servovalve and are also rated at 10 microns.

One of the smaller cartridges shown in the upper right-hand of the photo is installed in the centrifugal pump and filters the flow to the front journal bearing. It has a rating of 5 microns. The other small 5 micron unit is used in the servovalve to filter jet pipe supply flow.

The various filters in the experimental model system functioned effectively, from all outward indications. The successful operation of the pump and the absence of any bearing distress throughout the test programs and the continuous operation of the servovalve without incident, such as plugging of the jet pipe assembly tend to substantiate the effectiveness of the system filters.

Many of these elements have not as yet been removed from the system for inspection because further testing of the pumps is currently planned.

The filters used in this program have been designed to reduce size and weight but further improvements are necessary to develop flyable hardware. Future effort should be directed toward a critical study of filtering concepts and techniques with the object of developing aircraft type filters especially adapted to high temperature and alkali metal systems with maximum efficiency and reliability.

FITTINGS AND CONNECTORS

Experience with chevron-type static seals has shown that satisfactory sealing can be achieved if extreme care is taken to provide absolutely flat sealing surfaces. In several cases, this has required re-lapping of the seal itself as well as lapping of the seating surfaces. Re-design of the seal cross section has extended reusable life of these seals.

During the execution of previous contracts, one type of compression fitting has been used extensively. However, its performance under cyclic conditions of pressure and temperature had not been evaluated. As part of the present study, four fittings were tested. These fittings are the following:

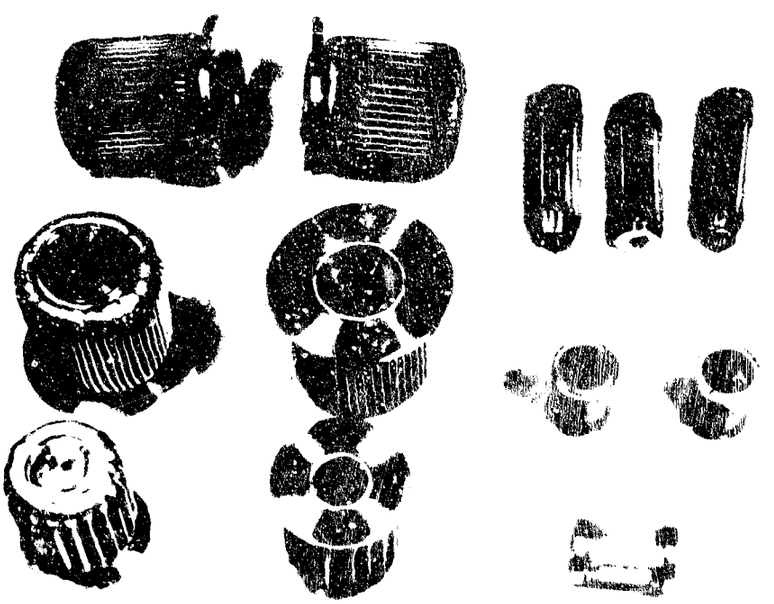

Figure 78 - High Temperature Liquid Metal Filter Cartridges

Name	Manufacturer
Swagelok	Crawford Fitting Co., Cleveland, Ohio
Gyrolok	Hoke, Inc., Cresskill, N. J
Conoseal	Aeroquip Corp., Marman Division, Los Angeles, Calif.
Cajon connector - Omega seal	Cajon Machine Co., Cleveland, Ohio Servotronics, Inc., Buffalo, N. Y.

The first three seals are commercially available items. The fourth seal was fabricated by the General Electric Company from standard parts.

The test sequence was as follows:

1. Fittings heated to 1200 F with NaK pressure of 2500 psi applied.
2. Pressure and temperature held for five minutes, followed by two pressure cycles from 2500 to 0 to 2500 psig.
3. Fitting cooled to 200 F and re-heated to 1200 F with full pressure applied.
4. Pressure and temperature held for five minutes, followed by one temperature cycle from 1200 to 200 to 1200 F.
5. After reducing temperature and pressure, the fittings were disconnected and re-made, followed by repeating the above pressure and temperature cycles.
6. Step 5 was repeated.

The three commercial fittings performed well in this evaluation. The Swagelok and Gyrolok fittings were difficult to seal initially, but once satisfactorily adjusted, they did not leak during the remainder of the test. The Conoseal at no time gave difficulty with regard to leakage but was quite difficult to break once made up. This fitting required a new gasket following

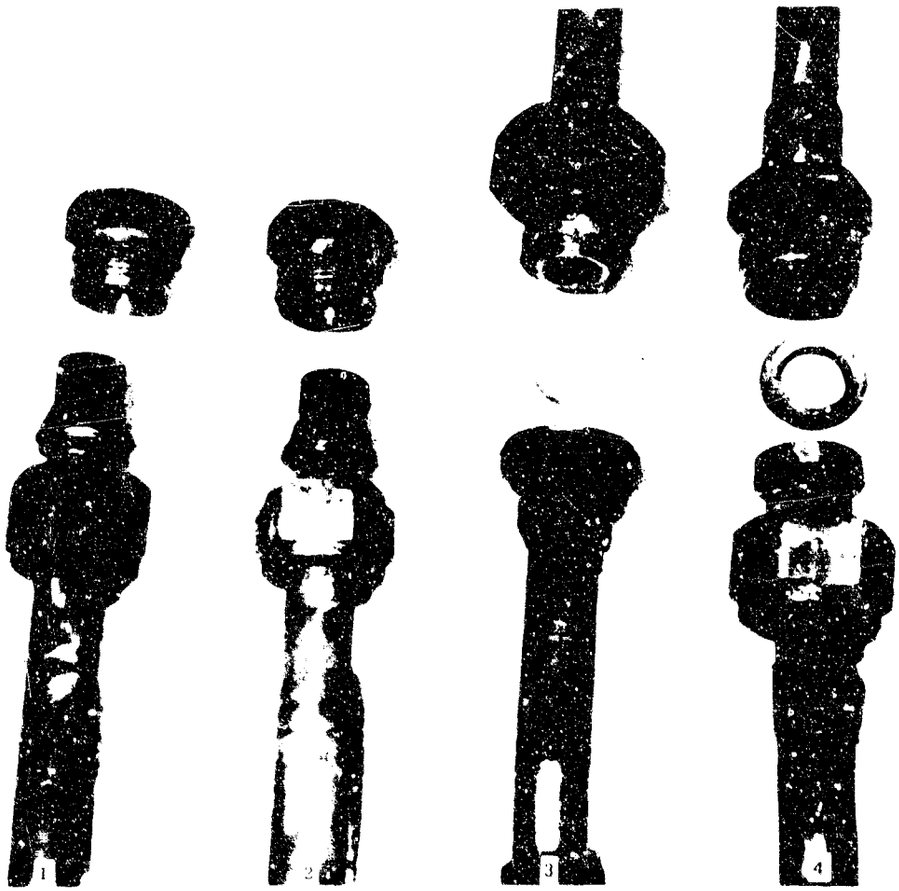

Figure 79 – Tube Fittings After High-Temperature Test

each connection break. The combination of a machined fitting and chevron seal leaked significantly throughout the test. As mentioned previously, this method of sealing can be made effective with considerable attention to flatness, surface finish, and alignment but it is doubtful if these conditions could be met consistently in field service.

The fittings following test are shown in Figure 79. The results of this test program indicated that the Swagelok, Gyrolok and Conoseal fittings are suitable for use in the design of air/nuclear systems and will perform with equal effectiveness. Other types of fittings should be evaluated since the present program did not permit a wide selection of candidate fittings. More extensive tests, particularly the application of bending and torque while at high pressure and elevated temperatures, should be undertaken before the fittings can be given unqualified approval.

MATERIALS

Although no specific material compatibility program was included in the present contract, limited evaluation of candidate materials was continued. Past studies had demonstrated that certain carbides offered promise as materials for liquid metal lubricated bearings and seal faces. These findings were based on the non-galling properties of carbides, their ability to withstand abrasion and their general compatibility with alkali metals.

However, the use of carbides for load carrying members poses several design problems. In addition to the difficulty of fabricating complex parts, it is necessary to provide for thermal compatibility of all the parts while avoiding tensile stresses in the carbide members. Further, some carbides undergo surface deterioration due to the leaching out of the binder material by the liquid metals.

Recently, progress has been made in applying diffusion bonded coatings to steels, high-strength alloys, and the refractory metals. Climax Molybdenum Corp. has successfully nitrided molybdenum. The Research and Development Center of General Electric Company has developed processes for boriding, siliciding and berylliding various metals. In particular, nitriding and boriding produce extremely hard, adherent coatings with good compatibility with the alkali metals.

Because material tests were conducted in conjunction with the design of a servovalve and re-design of the centrifugal pump, attention was concentrated on an evaluation of diffusion bonded coatings on TZM Molybdenum alloy. Two tests were conducted on a binderless carbide.

The material combinations tested are listed in Table II . All tests were planned for 30 minutes duration at 1000 F. Several confirmatory tests of borided TZM were conducted because this was a particularly critical material, being used in both pump and servovalves.

Tests were run with a modified Falex tester, shown in Figure 80. The circular specimens are rotated while the stationary V-blocks are loaded against the cylinder by calibrated weights. The specimens are immersed in the fluid during test. Coefficients of friction are determined by measuring the resisting torque produced by a strain gage-equipped loading ring.

The 779 tungsten carbide vs nitrided molybdenum specimens are shown in Figure 81. It will be noted that the tungsten carbide was actually grooved by the molybdenum. Metallographic examination showed that the nitrided case was apparently unaffected by exposure to high temperature NaK. A microphotograph of the sample is shown in Figure 82. The upper section showed a Knoop hardness ranging from 1730 to 1910. Hardness checks taken below the line of demarcation showed a Knoop hardness of 880 to 900 which is about twice the value to be expected in untreated molybdenum.

The specimen was then fractured and hardness checks taken across the cross-section. It was found that hardness varied normally from a maximum of 65 Rc at the surface to 32 Rc in the interior of the section. The sharply defined, extremely hard layer shown in Figure 82 is the so-called "white nitride" which is normally removed during grinding. It is interesting to note that no discernible demarcation exists between the nitrided surface and substrate, indicating that spalling or separation will not be a problem with this material.

Combinations of TZM Molybdenum versus both nitrided and borided TZM were also to be tested. As a preliminary check, the specimens were installed in the tester and rotated by hand. In both cases, there was immediate pick-up and grooving, indicating that although the chemical composition of the surfaces was altered, compatibility is still generally that of Mo. versus Mo.

Both tests of boron carbide resulted in shattering one of the boron carbide V-blocks as shown in Figures 83 and 84. In consequence, both tests were inconclusive, since the sharp edges of the broken piece cut into the rotating cylinder. It is interesting to note that where the sharp edges did not contact, the finish remained in excellent condition with no wear or marking. Thus, from a compatibility standpoint, the combination is

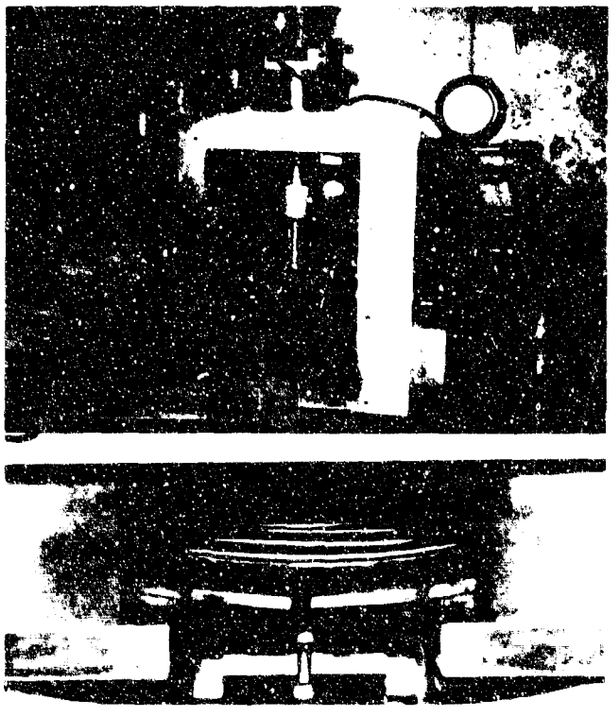

Figure 80 – Material Compatibility and Wear Tester

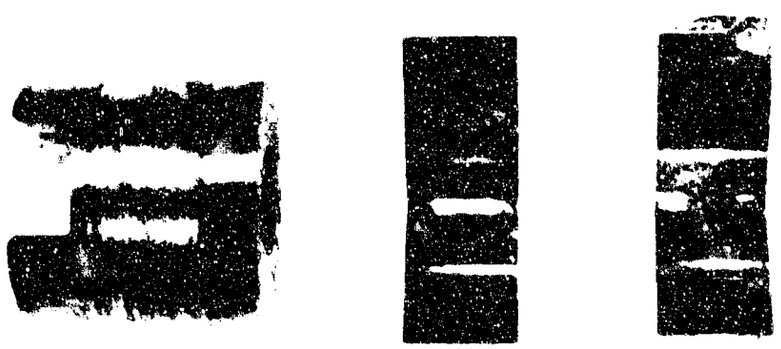

Figure 81 - Tungsten Carbide vs. Nitrided Molybdenum Specimens

Figure 82 - Microphotograph of Nitrided Molybdenum

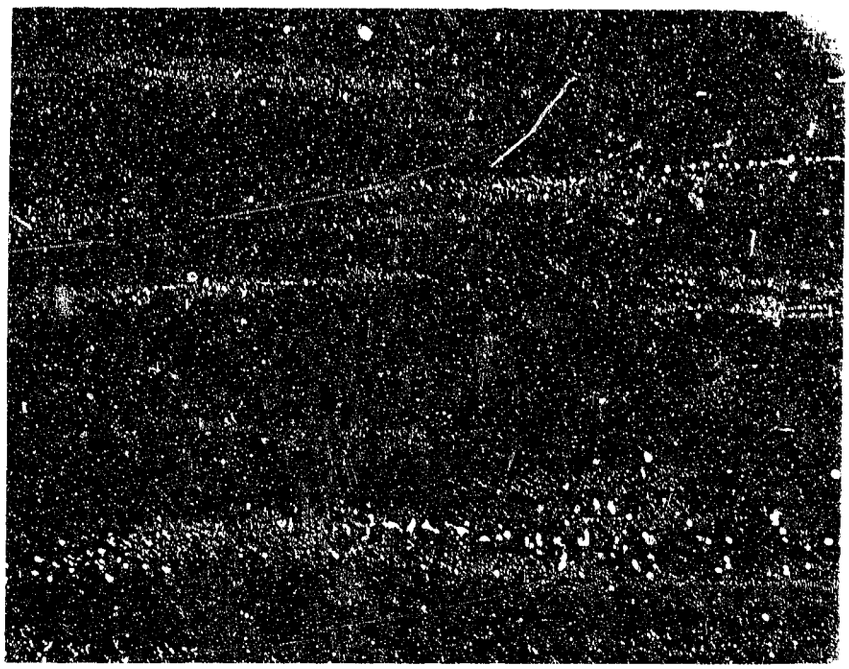

Figure 83 - Boron Carbide vs. Nitrided Molybdenum Specimens

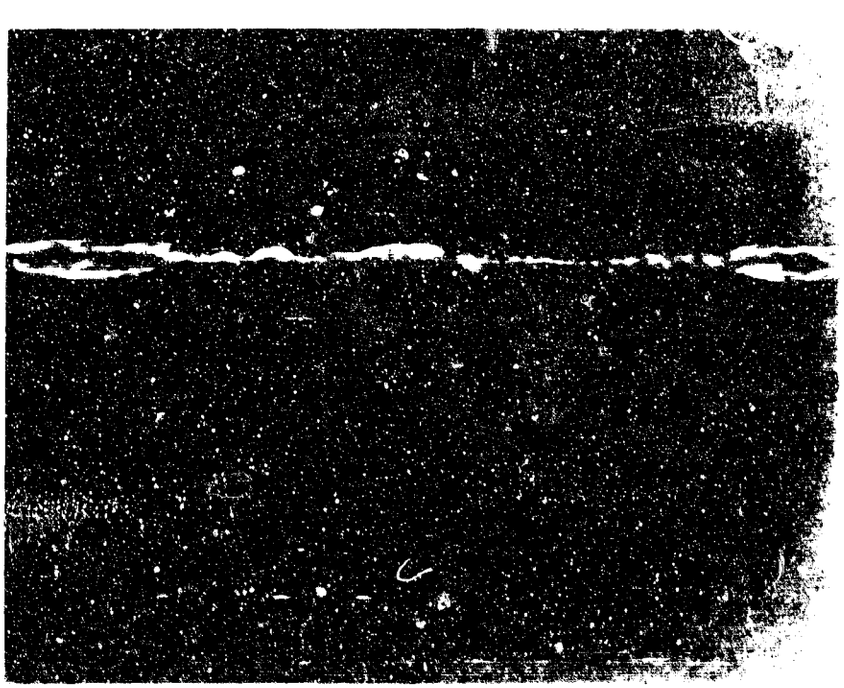

Figure 84 - Boron Carbide vs. Tungsten Carbide Specimens

excellent but, practically, the brittleness of the boron carbide makes its use difficult. Encapsulation tests of boron carbide in NaK at 1000°F for thirty days showed practically no attack.

Bearings have, however, been fabricated from boron carbide, as shown in Figure 85. Since the material has high compressive strength, it should be satisfactory if the bearings are properly supported. Future effort should continue this evaluation, particularly in conjunction with borided molybdenum and 895 tungsten carbide (fine grain, WC 94.0-Co 6.0).

Test results of 883 tungsten carbide versus borided TZM were sufficiently good that this combination was selected for the front bearing of the centrifugal pump and the sleeve of the servovalve. A discussion of the results and photographs of the specimens are included in Section V of this report.

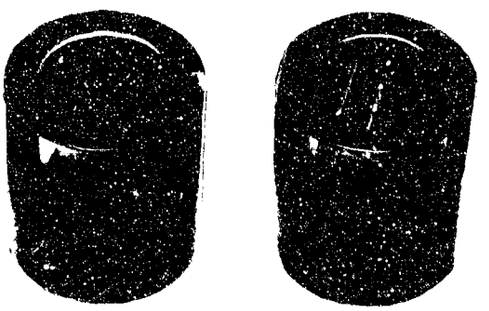

Figure 85 - Boron Carbide Sleeve Bearings

TABLE II

Material Cylinder	Combination V-blocks	Test No.	Fluid	Temp. °F	Testing RPM	Speed ft/min.	Test Time Min.	Specimen Load. lb.	Average Coefficient of Friction
779 Tungsten Carbide	Nitrided TZM Moly	1	NaK-77	1000	1000	147.2	30	24.94	0.277
Nitrided TZM Moly	Boron Carbide	2	NaK-77	1000	1000	147.2	30	24.94	- -
883 Tungsten Carbide	Boron Carbide	3	NaK-77	1000	1000	147.2	25	73.47	- -
Nitrided TZM Moly	TZM Moly	4	None	R.T.	Rotated by hand		-	24.94	- -
Nitrided TZM Moly	Electroless Ni on titanium	5	Oil	R.T.	1000	147.2	15	24.94	- -
883 Tungsten Carbide	Borided TZM Moly	6	Oil	R.T.	1000	147.2	10	24.94	0.139
883 Tungsten Carbide	Borided TZMMoly	7	NaK-77	1000	1000	147.2	30	24.94	0.449
TZM Moly	Electroless Ni on titanium	8	NaK-77	1000	1000	147.2	30	24.94	
883 Tungsten Carbide	Borided TZM Moly	9-10	NaK-77	1000	1000	147.2	60	24.94	0.485
883 Tungsten Carbide	Borided TZM Moly	11	NaK-77	1000	1000	147.2	30	24.94	0.448
883 Tungsten Carbide	Borided TZM Moly	12	NaK-77	1000	1000	147.2	30	24.94	0.451
TZM Moly	Borided TZM Moly	13	None	R.T.	Rotated by Hand		- -	24.94	- -

Section VIII

PUMPS FOR SERVOACTUATING SUBSYSTEMS

The pump study described herein has continued the effort initiated and conducted under previous contracts to:

1. Provide all the essential materials, spare parts and related effort necessary to restore and maintain a liquid metal flow and pressurizing source in good working order to enable high temperature operation and evaluation of a servoactuating subsystem and its related components.

2. Perform related "check-out" evaluation tests of the pumps used as the liquid metal flow pressurizing source.

3. Perform related bearing, seal and material development studies to maintain pump operation and improve unit performance wherever possible.

4. Maintain a classified record of all test data resulting from this study.

The previous studies performed have definitely established the superiority of the centrifugal pump configuration over the positive displacement, balanced vane pump for high pressure-temperature liquid metal service. Therefore, effort in this study was directed to modification of the ten-stage centrifugal pump design as dictated by the results of the performance tests performed under the previous study. In addition, in order to provide some protection to the program, in event of a failure or other irreparable damage to the unit during test, a second pump of identical design was fabricated as part of this program. Since the centrifugal pump was originally a purchased component, a complete set of drawings was not available or obtainable, and the procurement of a second unit no longer possible, a complete re-detailing of the pump design was necessary.

Previous pump tests also clearly established the need for a positive oil seal on the pump speed drive output shaft. It was necessary to re-design the pump drive shaft and shaft housing structure to accommodate a standard high speed carbon face seal.

Features of the re-designed pump shown in Figure 86 include (A) external porting of the NaK leakage past the labyrinth seal, (B) re-design of the pump rotor shaft with a stepped section, machined integral on the shaft to provide positive orientation of the rotating face seal ring and (C) re-adjustment of the labyrinth seal diameter to obtain better thrust load balance at the higher speeds. Re-design (A) eliminated the need for a hollow rotor shaft and allowed more accurate balance of the rotor assembly. Re-design (B) allows removal of the pump shaft seal without complete dis-assembly of the pump and re-design (C) reduced the total seal leakage flow because of the smaller seal diameter.

The detailed modifications of the original pump consisted of (1) re-work of the housing to accommodate the improved fluid porting arrangement, (2) fabrication of a new shaft, labyrinth seal, and support bushing and (3) re-finishing of the diffuser stack tapered surface with tungsten carbide flame spray.

The fabrication of the second centrifugal pump which entails the building of a duplicate unit of the modified design described, was also initiated. Increasing difficulty was experienced in the procurement of the titanium carbide material used in the pump bearings. The specific grades of carbide required for this application are a sole source vendor supplied item and their manufacture was in process of being discontinued. However, a final procurement was made of this material to allow fabrication of the second pump without requiring a material substitution.

Assembly of both centrifugal pumps was undertaken following the completion of the fabrication of all parts. Representative parts for one unit are shown in Figure 87. Each pump rotor sub-assembly was dynamically balanced before the final pump assembly. Figure 88 shows one such shaft-rotor assembly in the process of being balanced.

The completed pumps are shown in Figure 89.

Re-work of the pump speed drive to accommodate an improved high speed positive oil to NaK vapor seal was undertaken simultaneously with the pump fabrication effort. The original speed drive seal consisted of only a labyrinth in which a slight positive gas pressure was introduced in the plenum chamber between the gear drive and the pump to prevent NaK or NaK vapor leakage from entering the gear drive and keep oil or oil vapor away from the NaK pump. The re-designed seal is as shown in Figure 90. The modified shaft and completed seal parts are shown in Figure 91. Final

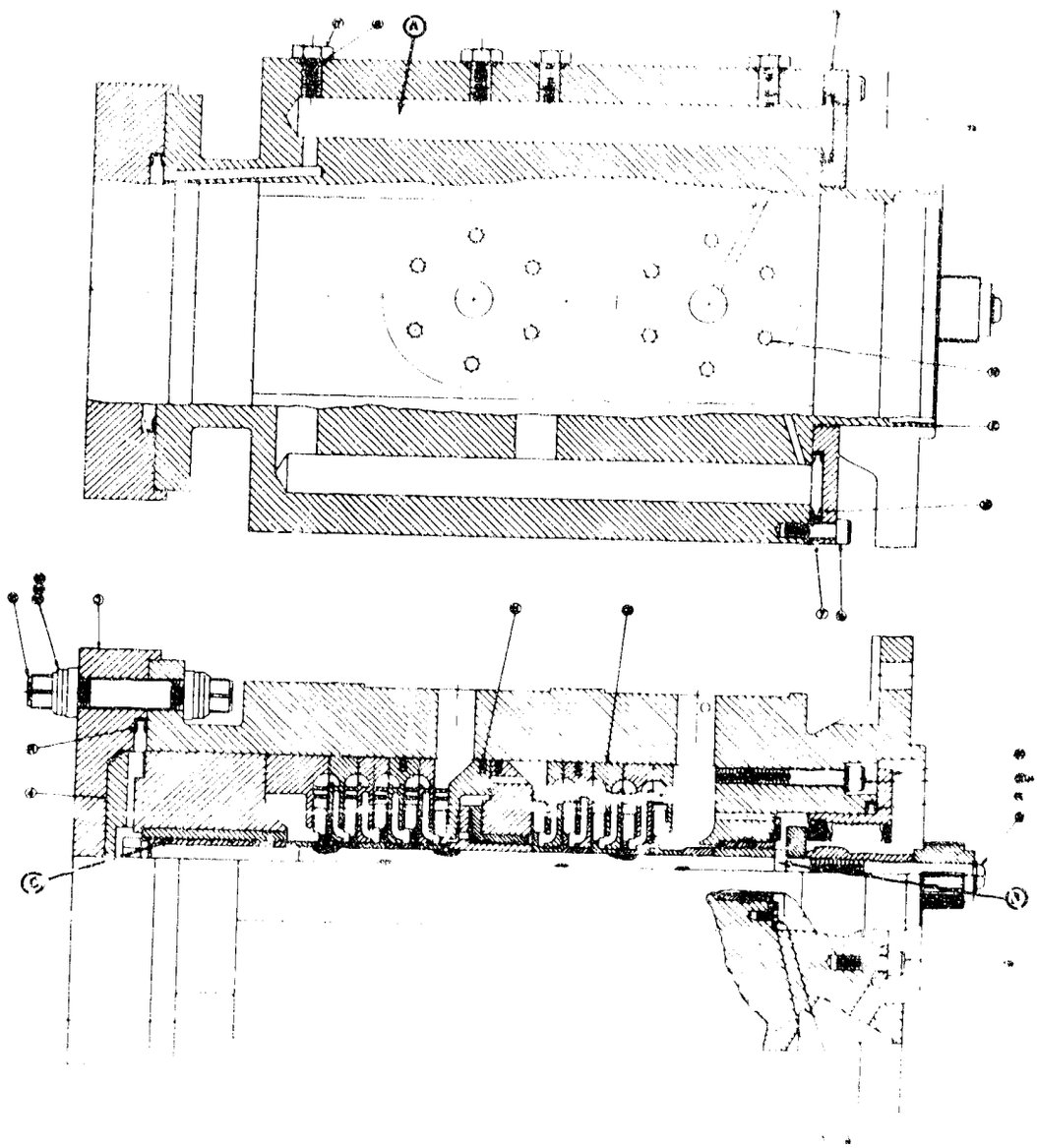

Figure 86 - Assembly Drawing - Modified Ten-stage Centrifugal Pump

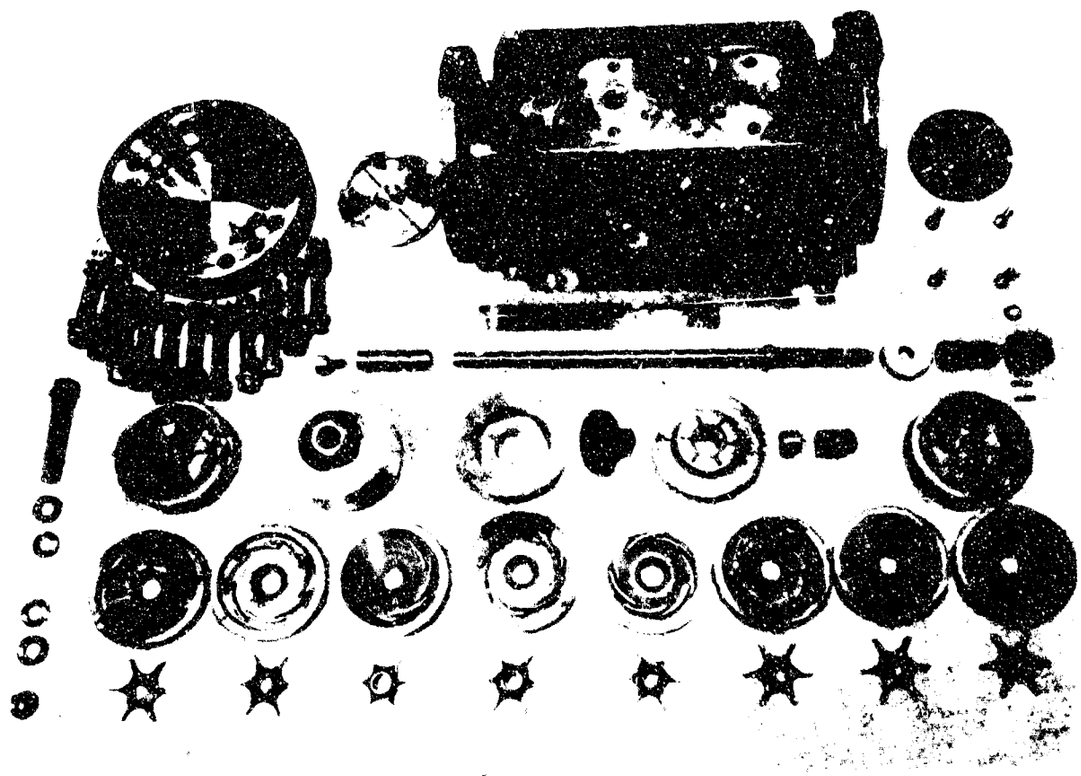

Figure 87 - High Temperature NaK Centrifugal Pump - Exploded View

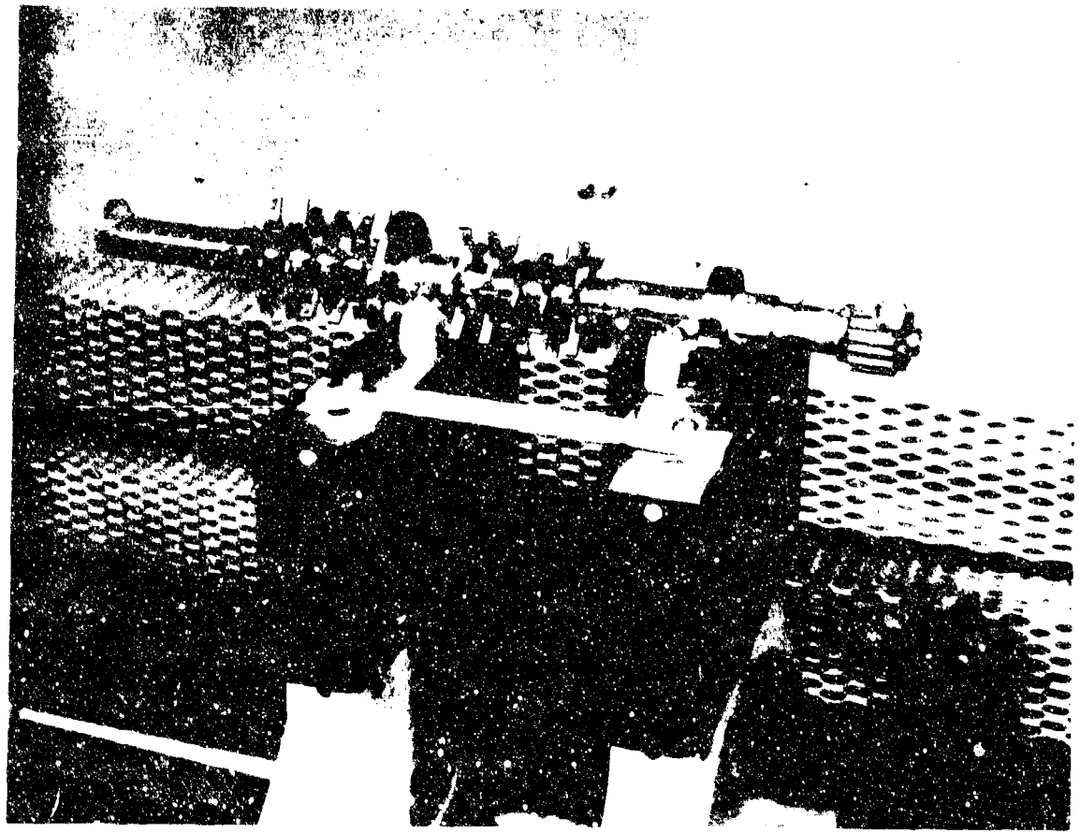

Figure 88 - Balancing of NaK Pump Rotor Assembly

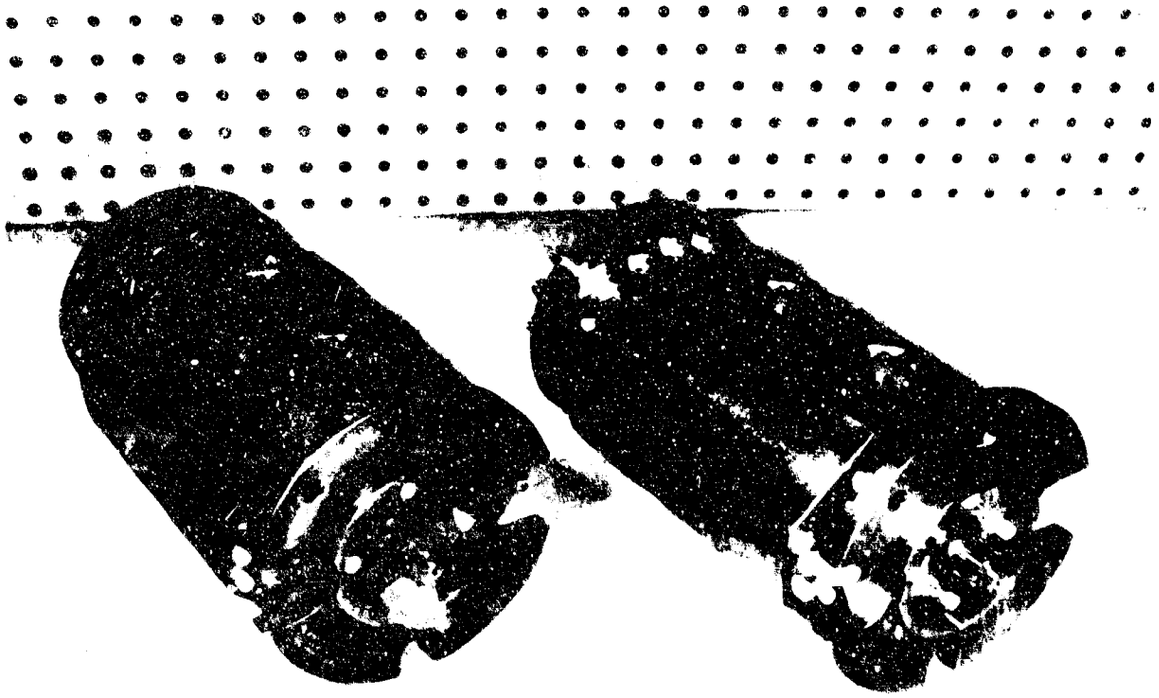

Figure 89 - Completed Ten-stage NaK Centrifugal Pumps

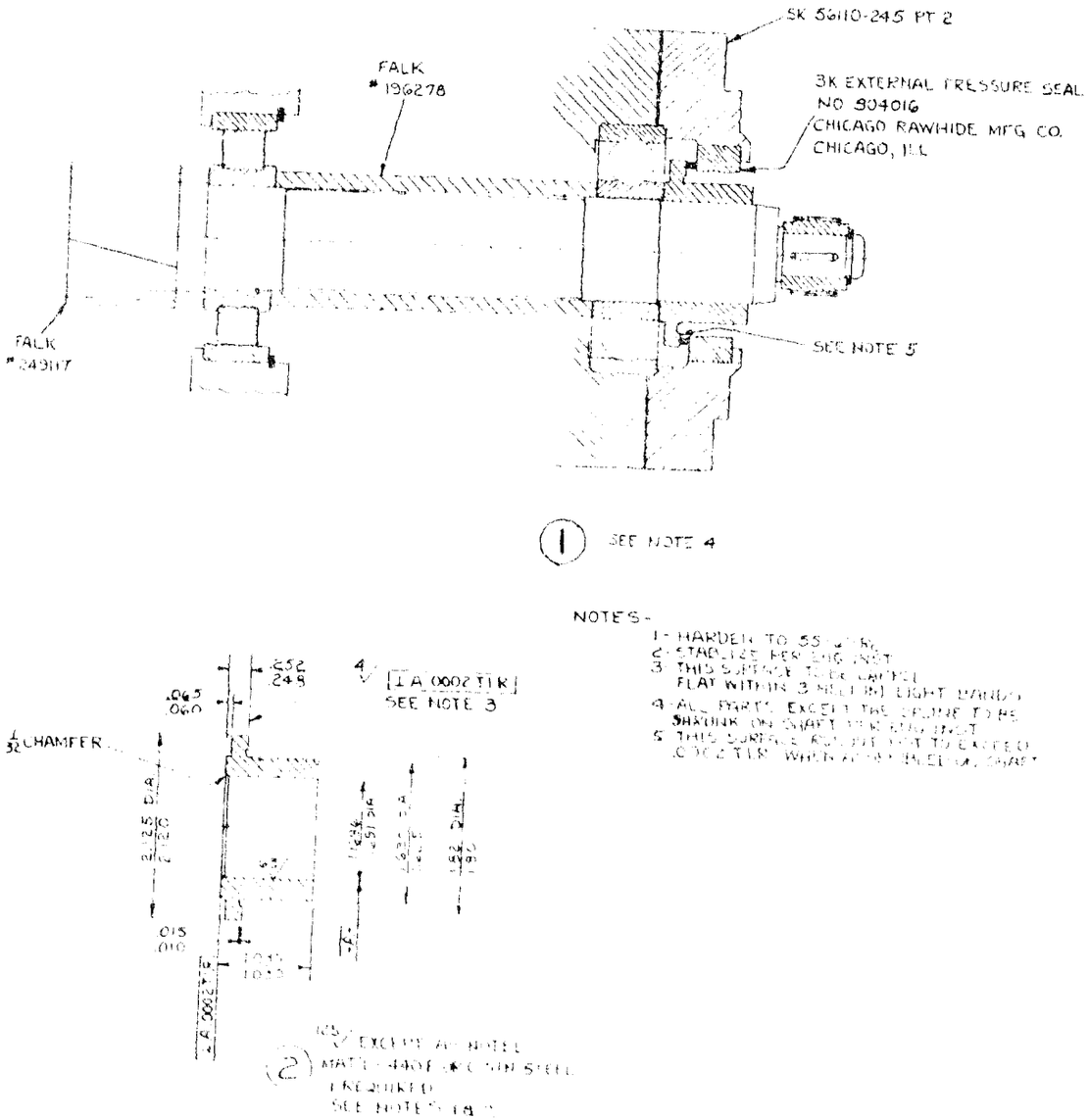

Figure 90 - High-Speed Drive Shaft Oil Seal Re-design

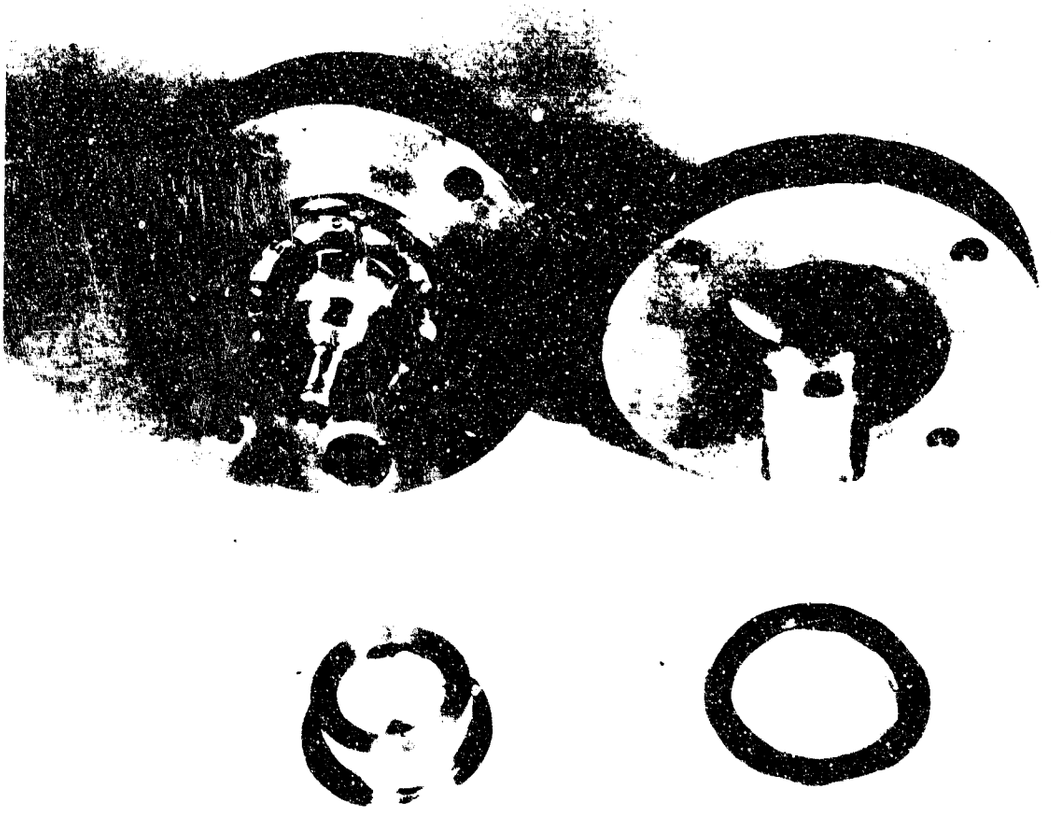

Figure 91 - Modified Drive Shaft and Seal Parts

assembly of the oil shaft seal was made and evaluation tests were conducted. Several operating difficulties were experienced with this seal initially, however, after some re-work and part replacements, satisfactory operation was attained.

Previously, when pump tests were conducted there existed some question as to the accuracy of the method used for evaluating the NaKpump operating efficiency. This was accomplished by calculating the input power to the pump stand hydraulic motor drive from measurement of oil flow and pressure temperature and correcting this power value by the hydraulic motor and the gear drive efficiencies. An average efficiency for the hydraulic motor was used, based upon vendor supplied data. In the case of the gear drive, efficiency measurements were taken under tare or no load conditions over the complete speed range and these values used. Consequently, there existed some question as to the validity of using an average efficiency value for the motor and the tare values for the speed drive. To eliminate further doubt as to the validity of this calculation, a torque sensor was procured and installation made on the low speed side of the pump gear drive system since this was the only available location for the incorporation of this equipment. The torque sensor which was purchased from Lebow Associates, Detroit, Michigan, is shown in Figure 92 and its installation in the pump drive system shown in Figure 93.

Previous pump tests also presented some question as to contamination of the NaK supply. Since several pump failures had been experienced previously, with both the centrifugal and vane pumps and no fluid changes were made during this period, except for the addition of small amounts of make-up fluid, it was decided that this condition be investigated.

Prior to conducting each pump test, routine procedure includes the cold trapping of the NaK supply for removal of oxides and fluid purification. This operation, however, would have little effect upon inert material, such as carbide bearing debris, which may have been introduced into the system during pumping failure. It was therefore decided that some method be devised whereby a particle size analysis of liquid samples could be performed which would conform closely to SAE ARP-598 specification. Representatives of the Millipore Corp., Bedford, Mass., were contacted and this problem reviewed.

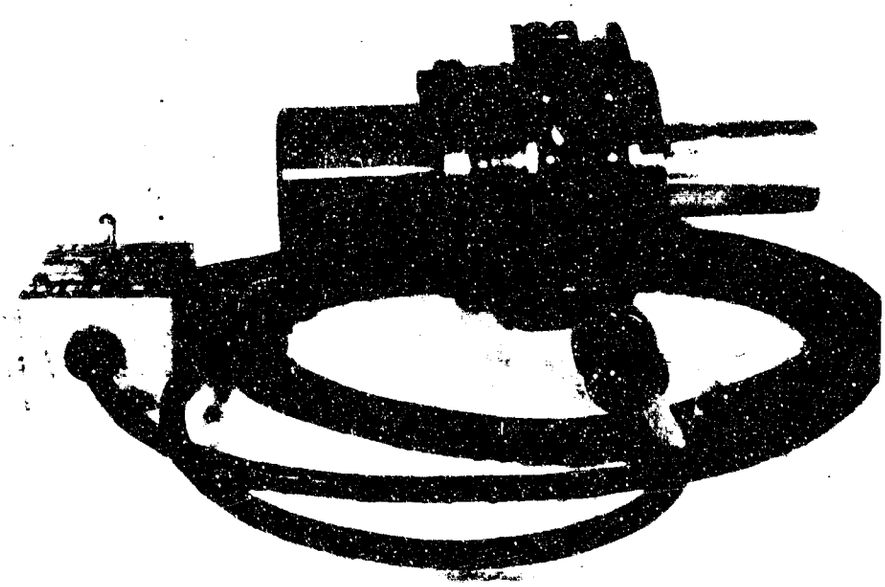

Figure 92 - Torque Sensor for NaK Pump Test Facilitiy

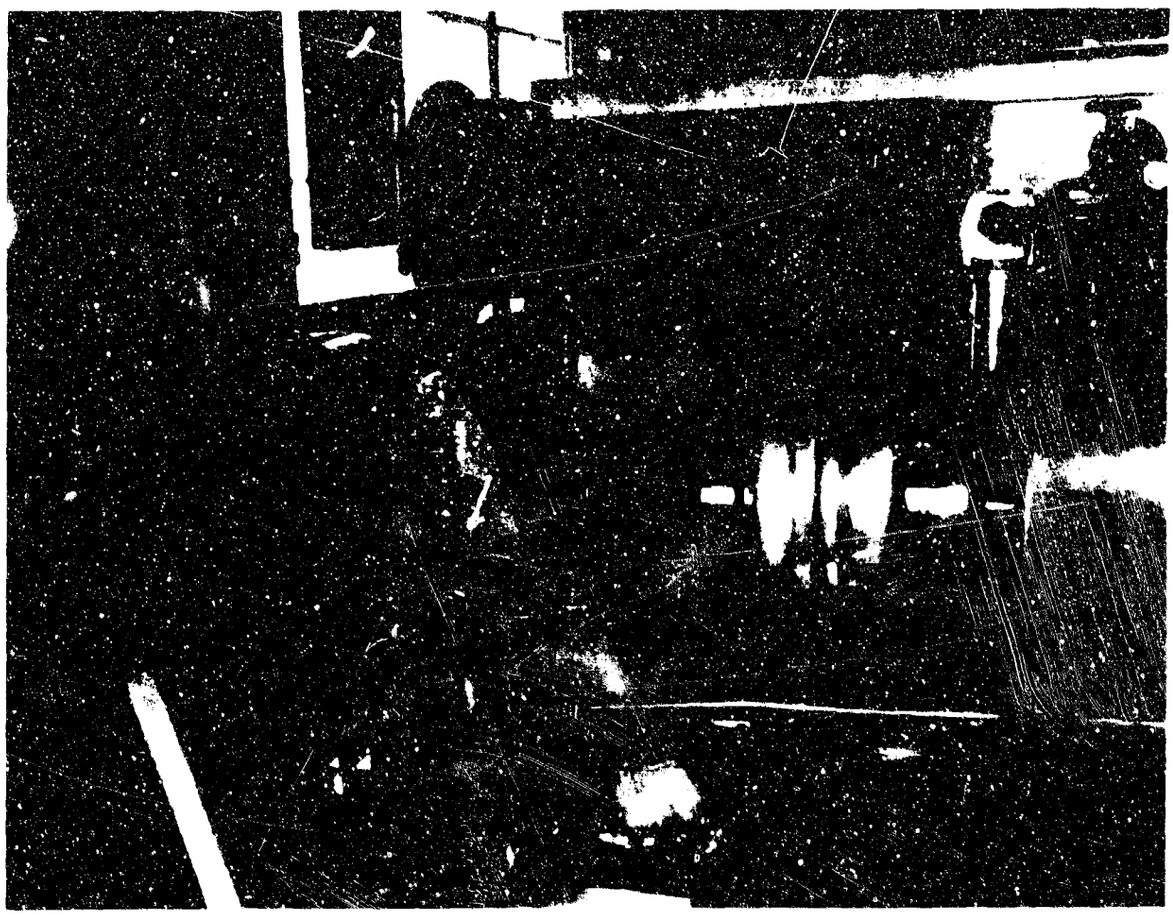

Figure 93 - Torque Sensor Installation in High-Speed Pump Drive

It was determined that samples of NaK in the test system be removed in containers of known cleanliness and reacted with butyl alcohol of known purity. This was performed and a contaminant evaluation was made in accordance with SAE ARP-598 at the Millipore Corp., Bedford, Mass. Three other hydraulic fluid specimens taken from existing aircraft applications were also evaluated in this investigation as a matter of comparison. The findings of this study are given in Table III.

In general, the results of this sampling test indicated that the NaK fluid being used in the centrifugal pump test system was much cleaner than the oil and mineral base hydraulic fluids taken from conventional systems.

These results also show that the system contaminant level in the small particle size markedly increased following a cold trapping operation. This indicated that there exists a high level of small particle contamination within the system that becomes dislodged from the system and is re-introduced into the fluid at the elevated temperatures. It further exhibits the need for small particle size mechanical filtration equipment in the liquid metal system. As a result of this study, effort was initiated to provide such equipment. However, because of the long procurement cycle for these filtering elements, the pump test program could not be delayed and the test program was continued without such filters installed.

The first of the series of pump tests conducted in this study was initiated on 7 July 1965. Prior to this, check-out tests of a modified pump NaK manifold, including fluid circulation through the centrifugal pump to temperature of 400^{o}F, were conducted. A NaK leak developed at the pump shaft seal during these static tests, however, and it was decided to continue testing since the leak rate was small and under control. Except for the seal leak, pump operation was normal and in accord with predicted performance. Values of operating speeds, pressures and flow rates obtained during this test exceeded those previously attained in the liquid metal program. The test was terminated after 2 hours and 42 minutes of operation when the seal leak could no longer be controlled, and an increase in pump operating torque developed. The effects of the pump shaft seal leak is shown in Figure 94. The pump was removed from the test installation and an inspection made. The unit was found to be in excellent condition except for the shaft seal. The seal was removed from the pump and refinished. Static sealing of the pump was once again established following re-installation of this re-worked shaft seal.

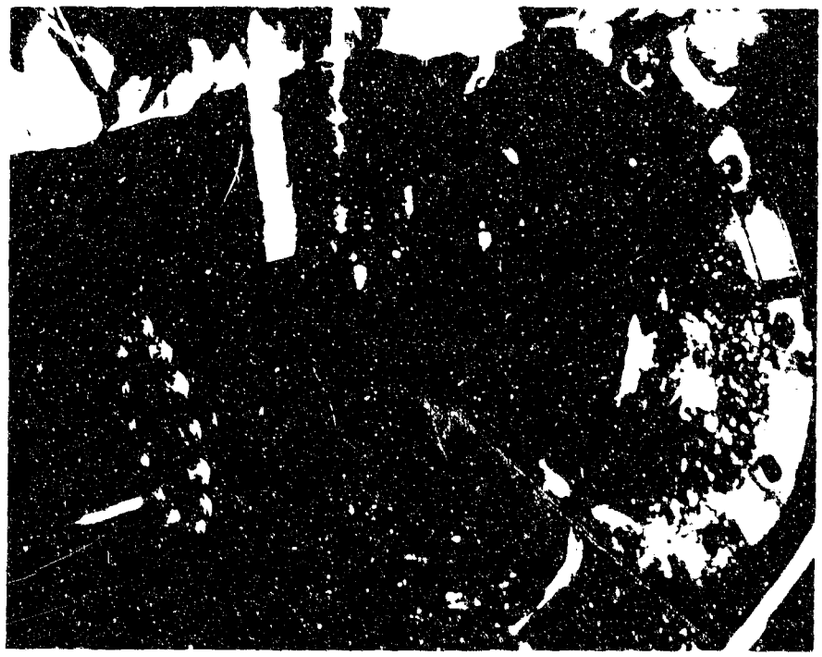

Figure 94 - NaK Pump Showing Effect of Shaft Seal Leak

TABLE III

Particle size analysis of liquid samples per S. A. E. ARP-598

Procedure: Liquid samples were filtered through MF membranes, and the remaining particulate contaminants were then microscopically counted and sized as per ARP-598. Results are given as corrected figures after subtracting control filter figures

Sample Identification:

No. 1	1B 5606 Hyd. oil
No. 2	2B Lub. oil 7277
No. 3	3B 5606 Hyd. oil
No. 4	Butyl alcohol - 2.3 gms NaK taken on 5/12/65
No. 5	Butyl alcohol - 2 gms NaK taken on 5/5/65

Results:

	10-25μ	25-50μ	50-100μ	<100μ
No. 1	8,400	2,900	650	275
No. 2	12,970	3,120	400	230
No. 3	9,200	3,100	550	180

	5-15μ	15-25μ	25-50μ	50-100μ	<100μ	Fibers
No. 4	18,950	1,590	145	35	30	12
No. 5	3,585	515	155	55	30	16

Further investigation of the high speed drive revealed that the oil seal had also been damaged which very probably caused the increased torque that was evident during the last few minutes of test operation. As a result, the speed drive was disassembled and the seal repaired.

Pump tests were re-initiated on 21 September 1965. During the test, pump speeds were in excess of 22000 rpm and fluid temperatures above 600°F. Flow obtained exceeded the nominal pump rating.

After approximately 3 1/4 hours of operation, variation in pump speed and torque readings were observed. It was decided to terminate testing at this point to determine the cause of these effects. No shaft seal leakage was observed throughout the entire test. After inspection and review of the pump test results, it was decided to resume testing. Operating speeds attained during this test exceeded 30,000 rpm and output pressures of over 2200 psi were experienced. Flow again exceeded the nominal pump rating. Approximately one hour of operation at speeds above 20,000 rpm and temperatures in excess of 750°F was accrued before a pump seizure occurred.

Subsequent inspection of the pump parts showed that the front carbide bearing had shattered (Figure 95), possibly the result of the carbide sleeve rotating on the molybdenum shaft, causing material pick-up which produced tensile stress in the carbide, thus cracking the sleeve.

It was also noted that the thrust bearing surface toward the drive shaft end of the pump had sustained considerable wear (Figure 96). This was apparently caused by an over-correction of the area adjustment made in the pump shaft labyrinth seal.

No other difficulties or problem areas were found during the pump inspection following test, (Figure 97.) The pump shaft seal shown in Figure 98 was found to be in excellent condition and exhibited no appreciable sign of wear.

Since the front bearing design had been recognized to be marginal, its failure during test was not entirely unexpected. It was therefore, planned to improve both the front and thrust bearing designs, as well as re-adjust the labyrinth seal bearing area to reduce the forward thrust loading effect at high speeds. It was also decided to fabricate a new pump shaft since some question existed regarding its alignment and balance following the front bearing failure. Upon completion of these design modifications, rework of the pump was initiated.

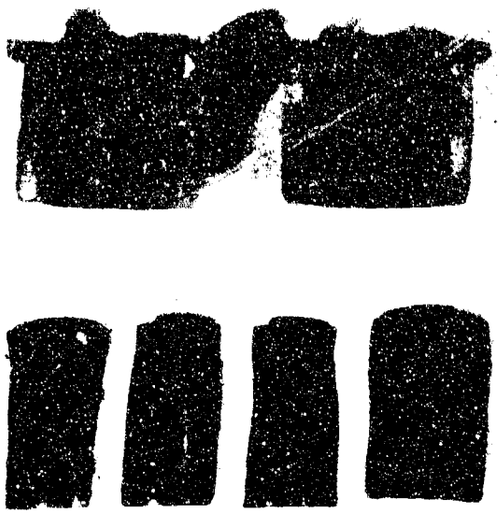

Figure 95 - NaK Pump Front Bearing Following Test

Figure 96 - NaK Pump Thrust Bearing Following Test

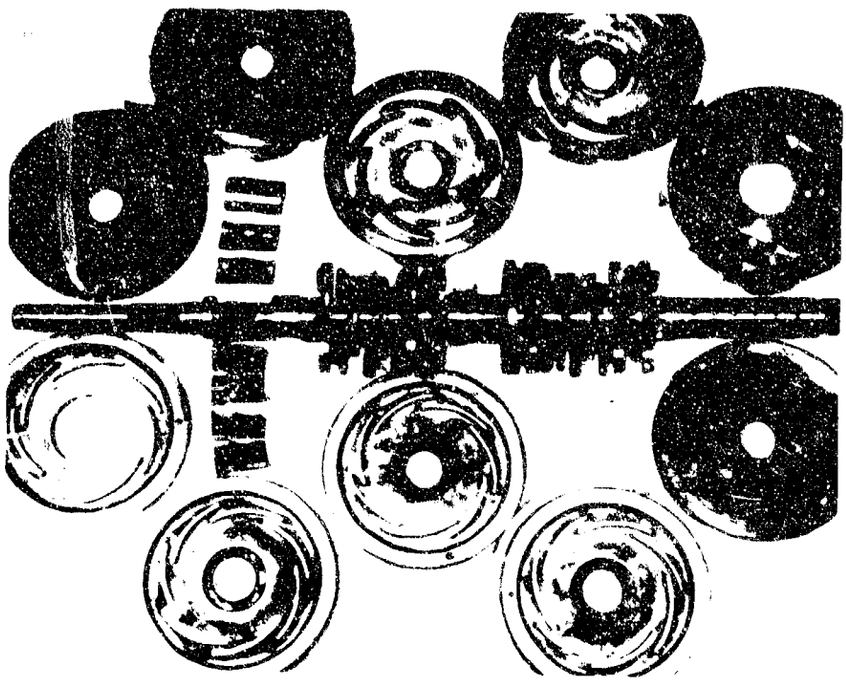

Figure 97 - NaK Pump Parts Following Test

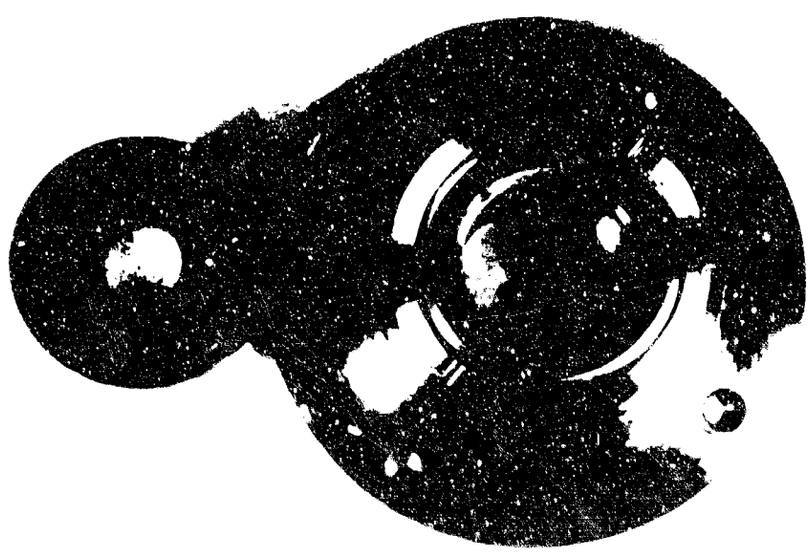

Figure 98 - NaK Pump Shaft Seal Following Test

During the course of rebuilding the pump, procurement of the titanium carbide materials used in the bearing design again posed a problem. This time however, this material could no longer be procured; consequently, an alternate material had to be secured. Consideration was given to the tungsten carbide (grade 883) - borided TZM Molybdenum combination, being evaluated for use in the design of the servovalves, (references pages 147 through 148). The results of this material evaluation were so encouraging that it was decided to use this combination on the pump bearing designs if at all possible.

The re-design of the front bearing included the incorporation of static pressure pads located 120 degrees apart. This not only provides increased bearing stiffness, but furnishes hydrostatic lubrication which based upon past experience appears superior to hydrodynamic lubrication for liquid metal bearings.

A compromise was necessary in the thrust bearing re-design in an effort to keep bearing flow losses at a reasonable level. The rear thrust plate was designed as a Rayleigh step-type hydrostatic bearing.

The front bearing face also contains stepped pads, but without peripheral sealing. Therefore, the front face of the thrust bearing is not a true hydrostatic bearing, but its load carrying capacity has been increased over the original flat pad design. A differential area has also been added to the pump shaft so that the thrust forces are balanced at 1000 psi output pressure, and increase toward the rear thrust face as the output pressure rises above that value. The area is proportioned so that at maximum pressure, the bearing unit loading is approximately 50 per cent of theoretical capacity. Below 1000 psi, the thrust is in the forward direction but its maximum load is within the capability of the stepped pad design.

Another modification incorporated in the pump design was a two micron internal filter in the fluid line supplying the front journal bearing of the pump.

Some difficulty was experienced in generating the extremely shallow steps in the thrust bearing. The electrical discharge method of machining, first attempted, did not prove successful because of the inability to control pocket depth accurately. It was found that this operation could be satisfactorily performed by chemical milling. The thrust bearing, as modified, is shown in Figure 99.

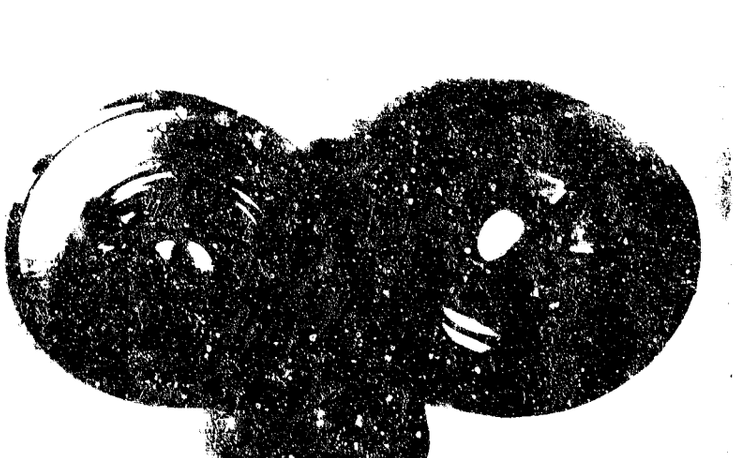

Figure 29 - Modified NaK Pump Thrust Bearing

The various pump parts as fabricated of borided TZM molybdenum are shown in Figures 100 and 101.

The final assembly of this test pump was completed on 29 April 1966.

Operation of the pump was postponed until tests of the servoactuating subsystem were initiated on 2 March, 1967. At this time the pump was used to supply flow and pressure for testing. It was fun for approximately 9 hours at high pressure and to temperatures approaching 1000 F. Operation was normal in every respect with the exception of slight leakage from the shaft seal. This, however, was not sufficient to require disassembly or shortening of the overall test time.

The total operating time accumulated to date on the test pump has been 50.75 hours. Of this, 32.5 hours of operation have been in excess of 500 F, 13.25 hours above 700 F, 5 hours above 900 F, and 1 hour in excess of 1000 F.

Upon completion of tests the pump was dismounted and the shaft seal removed for inspection. No further disassembly was done since pump operation had been satisfactory. The pump will be re-tested at higher speeds and pressures to assess the re-designed journal and thrust bearings.

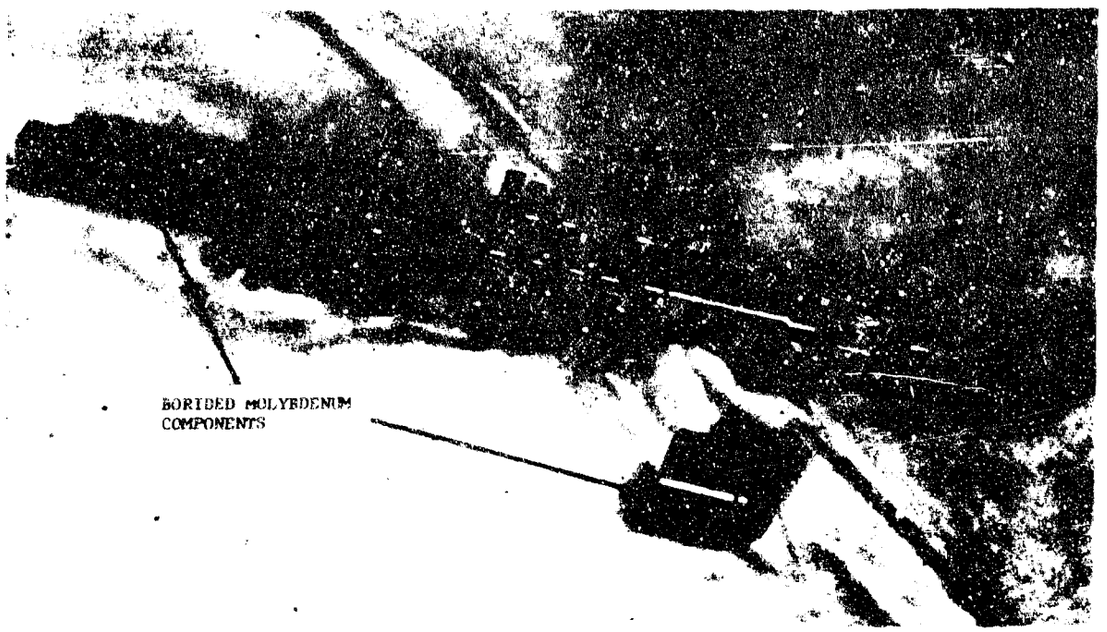

Figure 100 - Pump Rotor Assembly with Borided Molybdenum Parts

Figure 101 - Borided Mo Front Bearing Bushings for NaK Pump

Section IX

CONCLUSIONS AND RECOMMENDATIONS

The primary objective of the program described in this report was the test evaluation of an experimental model servoactuating subsystem. Contributory phases were in the areas of electro-hydraulic servovalves, high temperature, high-pressure pumps, and related subsystem components. The overall program also contained an application study aimed at future potential uses of liquid metal in flight control systems, a preliminary investigation of an air/nuclear actuating system, and the establishment of design criteria for a possible application of liquid metals in the elevon control system of the XB-70 vehicle.

Current application surveys have shown that there is a wide and growing interest in the development of high-temperature liquid metal hydraulic systems as representing the only effective method for meeting specific projected flight control system actuation requirements. During the course of the program contacts were made with potential users and a liquid metals progress brochure was prepared and distributed. General dissemination of information was effected by presentations to Air Force personnel and engineering societies, and publication in a national technical magazine.

This type of effort affords a desirable method for attaining the ultimate goals of a long-range study by providing current information essential to the establishment and maintenance of program direction. At the same time, it provides an unusual opportunity for the exchange of information between related investigative programs. It is, therefore, recommended that application surveys of this type be included as a basic part of any future investigations.

Test evaluation of the experimental model servoactuating subsystem was affected by torque motor failure, as described in Section III. Nevertheless, sufficient operating time was accumulated to definitely establish the feasibility of liquid metal actuation at high temperatures. As discussed in detail elsewhere, all other components functioned satisfactorily and showed no evidence of damage or excessive wear. It is recommended that the torque motor be re-designed, an accumulator added to the system, and complete static and dynamic tests conducted as an essential phase of any future program.

Servovalve operation was greatly hampered by leakage and instability of the torque motor. The general design of the jet pipe-spool combination and the principle of hydraulic interstage feedback were proven by extensive testing with MIL-H-5606A fluid at pressures to 3000 psi. This was accomplished with a test fixture which positioned the jet pipe mechanically. It was thus established that instability existed in the torque motor rather than the second-stage valve.

Before the completion of the program, preliminary re-design of the torque motor was undertaken and stiffening of the jet pipe spring gradient showed that stable operation could be achieved under test conditions.

Electro-mechanical torque motors still present serious problems when considered for sustained, reliable operation at temperatures of 1000F and above. On the other hand, flueric devices are rapidly being developed and show considerable promise for high-temperature applications. Concurrent with the present program preliminary investigation of an all-flueric, combined transducer and pilot stage was conducted. Results, while rudimentary, indicate that this is a feasible approach which could greatly decrease complexity and increase reliability of servovalve actuation. The application of this concept, while specifically directed to high-temperature, liquid metal servovalves at present, can be extended to actuation of servovalves in conventional oil hydraulic systems.

Future effort should, therefore, include both modification and repair of the present torque motor to permit completion of subsystem tests, and an investigationof flueric devices as applied to servovalve actuation and load position indication.

Of the various related system components, the most critical is the linear actuator. During the current program the actuator was re-designed by procurement of a 100-convolution bellows boot and material substitution in the rod bearing. Examination of the actuator after NaK tests showed excellent condition of most parts. The flame-plated piston rod, however, was affected by the concentrated hydroxides generated by NaK leakage past the rod seal. Sealing efficiency was less than optimum, due to differences in thermal expansion between the rod seal and piston rod.

It is recommended that future effort be directed toward elimination of flame-plating and the use of thermally compatible structural materials.

Investigation of hard-surfacing, such as boriding, on high-temperature alloys should be conducted. This would eliminate the use of any carbides and tend to produce a more reliable design.

While the high-temperature position transducer functioned satisfactorily, its gain characteristics at high temperature have not been established. At the same time, the useful life of such devices at temperatures of 1000 F or higher is limited.

Future effort should be directed toward a study of hydraulic position transducers in conjunction with flueric servovalve actuation. This not only reduces the complexity of the system but eliminates a portion of the electrical circuitry now necessary in conventional hydraulic systems.

The present program has not devoted specific effort toward the development of pressure regulation devices. Centrifugal pumps require flow control rather than pressure control. It is recommended that any future effort include a study of flow control devices for pump regulation with particular emphasis on the application of flueric principles.

The accumulator described in Section VII has had limited testing under another program. Test evaluation of the servoactuating subsystem has shown that an accumulator will be necessary for dynamic tests. Sufficient design data is presently available to fabricate such an accumulator. It should be made available as a system component in future programs.

Before the initiation of servoactuating subsystem tests, the centrifugal pump was modified by installation of a hybrid journal bearing and a Rayleigh step-type thrust bearing. Because of torque motor instability, maximum pump output pressure during tests was limited to 1000 psi.

The pump was operated for approximately 10 hours at temperatures to about 930 F with no difficulties except minor leakage of the rotating shaft seal. Nevertheless, it is felt that this operation was not sufficiently rigorous to evaluate the re-designed bearings fully.

As part of any future program, the pump should be subjected to tests at rated speed, pressure, and flow or as close to rated conditions as the present pump supply loop will permit. The results of these tests would influence the retro-fitting of the back-up pump which still retains the original bearing designs. At the same time, it would be advisable to consider a new pump design, such as a four-stage unit, to reduce complexity, size and weight, and increase overall reliability of the flow and pressure source.

Finally, it is important, if not essential, that flight testing of a liquid metal servoactuating subsystem be conducted at an early date. Past experience and present studies indicate that such a system should be an integrated package rather than a centrally located pump with vulnerable hydraulic lines. The integrated package would have only electrical connections which could easily be made redundant.

While there are presently no vehicles whose temperature requirements are in the 1000-1200 F regime, the most important factor is the actual flight performance of an operating liquid metal system even at reduced temperatures.

It is, therefore, strongly recommended that a program be initiated with the goal of designing, building, and flight testing an integrated, liquid metal flight control actuating subsystem. The package would be specifically designed to fit into a currently available test vehicle.

Appendix A
PROPERTIES OF LIQUID METALS

Components of alloy	NaK-77	NaKCs
	potassium (77.2%) sodium (22.8%)	cesium (72.6%) potassium (24.1%) sodium (3.1%)
Type of alloy	eutectic	eutectic
Melting point (atmospheric pressure)	9.95 F	-104.8F
Boiling point (atmospheric pressure)	1446F	1330F
Specific gravity	0.871 (68F) (see Note 1A) 0.693 (1200F)	1.467 (77F) 1.207 (1230F)
Absolute viscosity, centipoises	0.62 (100F) 0.14 (1200F)	0.95 (135F) 0.19 (1302F)
Thermal conductivity, watts/cm^2-^oC/cm	0.238 (300F) 0.255 (1300F)	
Electrical resistivity, microhm-cm	41.6 (300F) 89.3 (1300F)	76 (300F) 139.7 (1300F)
Average heat capacity (78.3% K weight) temperature range of 32-1292C, cal/gm/^oC	0.2163	
Vapor pressure, mm Hg	1.81×10^{-3} (441F) 431.85 (1341F)	757 (1319F)
Adiabatic bulk modulus, psi	463,000 (212F) (see Note 1B) 318,000 (1000F)	

Note 1A. The specific gravity figures are calculated from the equation:

$$V = M_k V_k + M_{na} V_{na}$$

where V = specific volume (reciprocal of density) of alloy
V_k = specific volume of potassium
V_{na} = specific volume of sodium
M_k = mole fraction of potassium
M_{na} = mole fraction of sodium

For NaK-77 $M_k = 0.6657$ and $M_{na} = 0.3343$.

Note 1B. Source of data:
Abowitz and Gordon, Journ. Chem. Phys., Vol. 37, No. 1, July 1, 1962.

Appendix B

REFERENCES

1 Blackmer, R. H., Research on Liquid Metals as Power Transmission Fluids, WADC Technical Report 57-294, Part I, General Electric Company, Schenectady, N. Y., May 1957

2 Kumpitsch, R. C., Research on Liquid Metals as Power Transmission Fluids, WADC Technical Report 57-294, Part II, General Electric Company, Schenectady, N. Y., February 1959

3 Kumpitsch, R. C., and Granan, J. R., Research on Liquid Metals as Power Transmission Fluids, WADC Technical Report 57-294, Part III, General Electric Company, Schenectady, N. Y., August 1962

4 Kumpitsch, R. C., Granan, J. R., and Kroon, P. J., Study of a Liquid Metal, NaK-77, for Application in Flight Control Systems, Vols. I and II, Technical Documentary Report ASD-TDR-597, Vols. I and II, General Electric Company, Schenectady, N. Y., March 1963 (Vol. II classified)

5 Kumpitsch, R. C., Granan, J. R., and Kroon, P. J., Study of a Liquid Metal, NaK-77, for Application in Flight Control Systems, Vols. III and IV, Technical Documentary Report ASD-TDR-62-597, Vols. III and IV, General Electric Company, Schenectady, N.Y., September 1964, Vol. IV Classified)

6 Kumpitsch, R.C., Granan, J.R., and Kroon, P.J., Research and Experimental Investigation of Liquid Metal, NaK-77, for Application in Flight Control Systems, Vols. I and II, Technical Report AFFDL-TR-64-183, Vols. I and II, General Electric Company, Schenectady, N. Y. June, 1965 (Vol. II classified)

7 Tepper, F., King, J., and Greer, J., Multi-component Alkali Metal Alloys, Technical Report AFAPL-TR-65-73, MSA Research Corp., Callery, Penna. July, 1965

8 Elliott, D. F., et al, Some Preliminary Tests on Bearing Materials to Operate under Liquid Sodium, AERE-R/R-1891, Great Britain Atomic Energy Research Establishment, Harwell, Berks, England, 23 April 1956 (Decl. 17 September, 1957)

9 Hall, J., and Spies, R., Research in the Field of Liquid Metal-Lubricated Bearings, Part I, Technical Documentary Report RTD-TDR-63-4289, Part I, Rocketdyne Division of North American Aviation, Inc., Canoga Park, Cal., 1 March, 1964

10 Lyon, R.N., Liquid Metals Handbook, 2nd Edition, NAVEXOS P-733 (rev) Atomic Energy Commission and Department of the Navy, June, 1952

11 Jackson, C. B., Editor-in-chief, Liquid Metals Handbook - Sodium-NaK Supplement, TID-5277, Atomic Energy Commission and Department of the Navy, 1 July, 1955

12 Liquid Metals Technology, Part I, Chemical Engineering Progress Symposium No. 20, Vol. 53, American Institute of Chemical Engineers, 1957.

13 Vail, D. B., Compatibility of Materials in Liquid Metal, Report KAPL-589, Knolls Atomic Power Laboratory, Schenectady, N. Y. August 1951

14 Vail, D. B., Compatibility of Materials in Liquid Metal, Second Report, KAPL-1021, Knolls Atomic Power Laboratory, Schenectady, N. Y. January, 1954

15 Wilkinson, W. D. and Murphy, W. F., Nuclear Reactor Metallurgy, D. Van Nostrand Company, New York, N. Y., 1958

16 Liquid Metals for Flight Control Systems, General Electric Company, Johnson City, N. Y., October 1966

Appendix C

LIQUID METALS SERVO-ACTUATOR ANALYSIS

SERVO-ACTUATOR DESCRIPTION

Analysis is made of a liquid metals servo-actuator designed for 1400 F operation. The servo-actuator consists of a two stage servovalve and linear actuator. The servovalve utilizes a jet-pipe first stage and a spool-type second stage. A high-temperature electromagnetic torque motor positions the jet pipe in proportion to electrical command signal. The jet pipe receiver ports are located in the spool valve so that unity hydraulic position feedback from second to first stage is provided.

SYSTEM EQUATIONS

Torque Motor Analysis

The torque motor electrical characteristic relating input voltage to the coil current is described by the equation:

$$E = L \frac{di}{dt} + Ri + K_E \frac{d\theta}{dt} \qquad (1)$$

where
- E = voltage input - volts
- L = coil inductance - henries
- R = coil resistance - ohms
- i = differential current - amperes
- θ = armature rotation - radians
- K_E = back EMF gain - volts-sec-rad^{-1}

The magnetic torque acting on the armature is proportional to the differential current input to the coils. Mathematically, this relationship is simply defined as:

$$T_M = K_M i \qquad (2)$$

where
- T_M = magnetic torque - in-lb.
- $K_M = \frac{dT}{di}$ = magnetic torque gradient - in-lb-amp^{-1}

The summation of torques on the armature defines the torque motor armature motion resulting from the applied magnetic force. The torque acting on the

armature provides the torque components, including that to accelerate the armature and jet pipe assembly inertia and to overcome armature assembly, damping, flexure tube spring gradient, and jet pipe flow reaction. This relationship is shown in the following torque-motion equation.

$$T_M = J_F \frac{d^2\theta}{dt^2} + D_F \frac{d\theta}{dt} + (K_F + K_J)\ \theta \qquad (3)$$

where J_F = armature-jet pipe inertia - in-lb-sec^2
D_F = armature-jet pipe damping - in-lb-sec
K_F = magnetic-flexure tube net spring rate - in-lb-rad^{-1}
K_J = jet pipe spring and flow reaction gradient - in-lb-rad^{-1}

Jet-Pipe First Stage Analysis

The armature angular motion is transformed into jet displacement by the relationship

$$x = r_J\ \theta \qquad (4)$$

where x = jet displacement - inch
r_J = radius of rotation of jet - inch

The jet velocity head is recovered in receiving ports located in the second stage spool. Position feedback is, thus, provided hydraulically between the jet-pipe first stage and the second stage spool. The significant input motion controlling the receiving port pressures is the relative displacement between the jet and spool. This position relationship is defined as

$$z = x - v \qquad (5)$$

where z = relative jet-spool motion - inch
v = spool displacement - inch

The velocity head available in the jet is converted into static pressure in the receiving ports. The differential pressure developed in the receiving ports is a function of the relative position of the jet and the receiving ports. It is also dependent upon the flow from the receiving ports.

The position-pressure characteristic is influenced by the jet and receiver block geometry. The actual characteristic can best be determined empirically. Mathematically, the relationship for the simple case of blocked spool

defining a change in recovered pressure is

$$dP_R = K_x\, dz \tag{6}$$

where P_R = receiver port pressure - $lb\text{-}in^{-2}$

$K_x = \frac{\partial P_c}{\partial z}$ = position-pressure gain - $lb\text{-}in^{-3}$

For the case where there is flow from the receiver, the pressure difference is described by the equation

$$dP_c = K_x\, dz - K_q\, dQ_c \tag{6a}$$

where $K_q = \frac{\partial P_R}{\partial Q_c}$ = flow-pressure gain - $lb\text{-}sec\text{-}in^{-5}$

Q_c = flow to spool control volume - $in^3\text{-}sec^{-1}$

P_c = spool control pressure - $lb\text{-}in^{-2}$

A portion of the jet-pipe flow enters the receiving port to provide the velocity, compressibility and leakage flow components to the control volumes at the ends of the spool valve. The differential equation defining this relationship is

$$Q_c = A_c \frac{dv}{dt} + \frac{V_c}{B} \frac{dP_c}{dt} + C_c P_c \tag{7}$$

where A_c = spool valve piston area - in^2

V_c = entrained spool control volume - in^3

B = fluid bulk modulus - $lb\text{-}in^{-2}$

C_c = spool control volume leakage coefficient - $in^5\text{-}lb^{-1}\text{-}sec^{-1}$

Second Stage Spool Valve Analysis

The pressure recovered from the jet velocity in the receiving ports and acting on the spool piston areas develops the force required to accelerate the spool mass, to overcome the viscous damping of the spool and to equalize the valve flow reaction. The differential equation defining the spool force-motion relationship is

$$A_c (P_{c_1} - P_{c_2}) \quad M_v \frac{d^2 v}{dt^2} + D_v \frac{dv}{dt} + K_R Q_v \tag{8}$$

where M_v = spool mass - lb-sec^2-in^{-1}

D_v = spool viscous damping - lb-sec-in^{-1}

K_R = valve flow-force gain - lb-sec-in^{-3}

Q_v = spool port flow - in^3-sec^{-1}

The basic orifice equation defines the output flow from the spool valve ports. This equation is

$$Q_v = C_o W v \sqrt{\frac{2g (P_s - P_o)}{\rho}} \tag{9}$$

where C_o = orifice discharge coefficient

W = port width - inch

P_s = supply pressure - lb-in^{-2}

P_o = servo pressure - lb-in^{-2}

ρ = fluid density - lb-in^{-3}

g = gravitational acceleration - in-sec^{-2}

The servovalve output flow is a variable function of spool displacement and servo pressure assuming constant supply pressure and port geometry. Differentiation of the basic orifice equation, thus, describes the essential relationship for change in flow.

$$dQ_v = \frac{\partial Q_v}{\partial v} dv + \frac{\partial Q_v}{\partial P_o} dP_o = K_v dv - K_p dP_o \tag{10}$$

The spool valve displacement-flow gain is thus defined analytically as

$$K_v = \frac{\partial Q_v}{\partial v} = C_o W \sqrt{\frac{2g (P_s - P_o)_o}{\rho}} \quad \text{in}^2\text{-sec}^{-1} \tag{10a}$$

and the pressure-flow gain is

$$-K_p = -\frac{\partial Q_v}{\partial P_o} = C_o W v_o \sqrt{\frac{g}{2\rho (P_s - P_o)_o}} \quad \text{in}^5\text{-lb}^{-1}\text{-sec}^{-1} \tag{10b}$$

These gains may also be determined experimentally.

Actuator and Load Analysis

The servovalve flow output to the actuator is separated into three primary flow components. They are the velocity, compressibility and leakage flows. This conventional hydraulic actuator flow relationship is given by the following equation.

$$Q_v = A_a \frac{dy}{dt} + \frac{V_a}{B} \frac{dP_o}{dt} + C_L P_o \qquad (11)$$

where
A_a = actuator piston area - in^2
y = actuator piston displacement - in
V_a = actuator entrained volume - in^3
C_L = actuator leakage coefficient - in^5-lb^{-1}-sec^{-1}

The servovalve differential pressure output acting on the actuator piston area provides the force to accelerate the load mass and to overcome viscous damping and load spring stiffness.

The classic differential equation used to describe the actuator force-motion relationship is

$$A_a(P_{o_1} - P_{o_2}) = ML \frac{d^2y}{dt^2} + D_L \frac{dy}{dt} + K_L y \qquad (12)$$

where
M_L = actuator mass load - lb-sec^2-in^{-1}
D_L = actuator viscous damping - lb-sec-in^{-1}
K_L = load spring rate - lb-in^{-1}

Linearized Equations

The foregoing system basic equations are linearized and put into differential operator form. The resultant equations utilized to describe small incremental system changes around given initial conditions are summarized as follows:

Torque Motor Relationships

Differential Current:

$$\Delta E = LS\Delta i + R\Delta i + K_E S\Delta\theta \qquad (13)$$

Magnetic Torque:

$$\Delta T_M = K_M \Delta i \tag{14}$$

Armature-Jet Pipe Torques:

$$\Delta T_M = J_F S^2 \Delta\theta + D_F S\Delta\theta + (K_F + K_J)\Delta\theta \tag{15}$$

Jet Pipe First Stage Equations

Jet Pipe Displacement:

$$\Delta x = r_J \Delta\theta \tag{16}$$

Jet Pipe-Spool Relative Motion:

$$\Delta z = \Delta x - \Delta v \tag{17}$$

Spool Control Differential Pressure:

$$\Delta P_c = K_x \Delta z - K_q \Delta Q_c \tag{18}$$

Flow From Receiver to Control Volume:

$$\Delta Q_c = A_c S\Delta V + \frac{V_c}{B} S\Delta P_c + C_c \Delta P_c \tag{19}$$

Second Stage Spool Valve Equations

Spool Forces - Displacement:

$$2A_c \Delta P_c = M_v S^2 \Delta V + D_v S\Delta V + K_R \Delta Q_v \tag{20}$$

Servovalve Second Stage Flow:

$$\Delta Q_v = K_v \Delta V - K_P \Delta P_o \tag{21}$$

Actuator and Load Relationships

Actuator Flows:

$$\Delta Q_v = A_a S\Delta y + \frac{V_a}{B} S\Delta P_o + C_I \Delta P_o \tag{22}$$

Actuator Force - Displacement:

$$\Delta 2A_a \; P_o = M_L S^2 \Delta y + D_L S \Delta y + K_L \Delta y \qquad (23)$$

BLOCK DIAGRAM REPRESENTATION

The basic block diagram representation of the linearized equations for the servovalve-actuator position control system is shown in Figure C-1. The control loop is closed as shown with a linear displacement transducer with gain K_y. A servo amplifier with gain K_A is utilized to sum the command and position feedback voltages.

A mathematical model of servovalve-actuator derived from the basic block diagram is represented in Figure C-2. Valve reaction force feedback has been neglected to simplify the initial frequency response analysis.

INITIAL VALUES OF DESIGN PARAMETERS

Torque Motor

A high temperature torque motor is to be provided by the Bendix Corporation Research Laboratories. Data for this torque motor is provided as follows:

L	=	0.04 henries/coil
R	=	8 ohms/coil
K_M	=	1.25 in. lb-amp^{-1}
I(max)	=	1 amp
K_E	=	not specified (neglected in analysis)
K_F	=	40 in-lb-rad^{-1}

Jet Pipe Valve

Pertinent data for the jet pipe valve obtained from preliminary design calculations and experimental tests are summarized below. Data supplied pertains to a nozzle diameter of 0.020 inch and receiver port diameter of 0.030 inch.

Q (max)	=	2.3 in^3-sec^{-1} (at P_s = 3000 psi)
K_J	=	125 in-lb-rad^{-1}
J_F	=	1.3×10^{-5} in-lb-sec^2
D_F	=	0.01 in-lb-sec (assumed)

r_J = 1.5 inch

$x(max)$ = ± 0.015 inch

K_x = 2.7×10^5 lb-in^{-3} (test data)

K_q = 760 lb-sec-in^{-5} (test data)

Spool Valve

The spool valve design is based on a maximum flow requirement of 7 gpm at 3000 psi. Design data for the spool valve are as follows:

A_c = 0.25 in^2

V_c = 7.5×10^{-3} in^3

$V'(max)$ = ± 0.015 inch

C_c = 10^{-4} in^5-lb^{-1}-sec^{-1}

M_v = 10^{-3} lb-sec^2-in^{-1}

D_V = 0.1 lb-sec-in^{-1}

K_R = not specified (neglected in analysis)

$Q_V(max)$ = 27 in^3-sec^{-1}

K_v = 3000 in^2-sec^{-1} (at $P_S - P_O$ = 1500 psi)

K_P = 9.55×10^{-4} in^5-lb^{-1}-sec^{-1} (at v = 0.001")

Actuator and Load

The actuator-load requirements are specified by system design. An actuator designed on a preceding contract effort is to be used. The significant data is presented.

Y (max) = ± 2.25 inch

A_a = 2.75 in^2

V_o = 6.2 in^3

C_L = 10^{-3} in^5-lb^{-1}-sec^{-1}

M_L = 3.75 lb-sec^2-in^{-1} (45 slugs)

D_L = 10 lb-sec-in^{-1} (assumed)

K_L = 1300 lb-in^{-1}

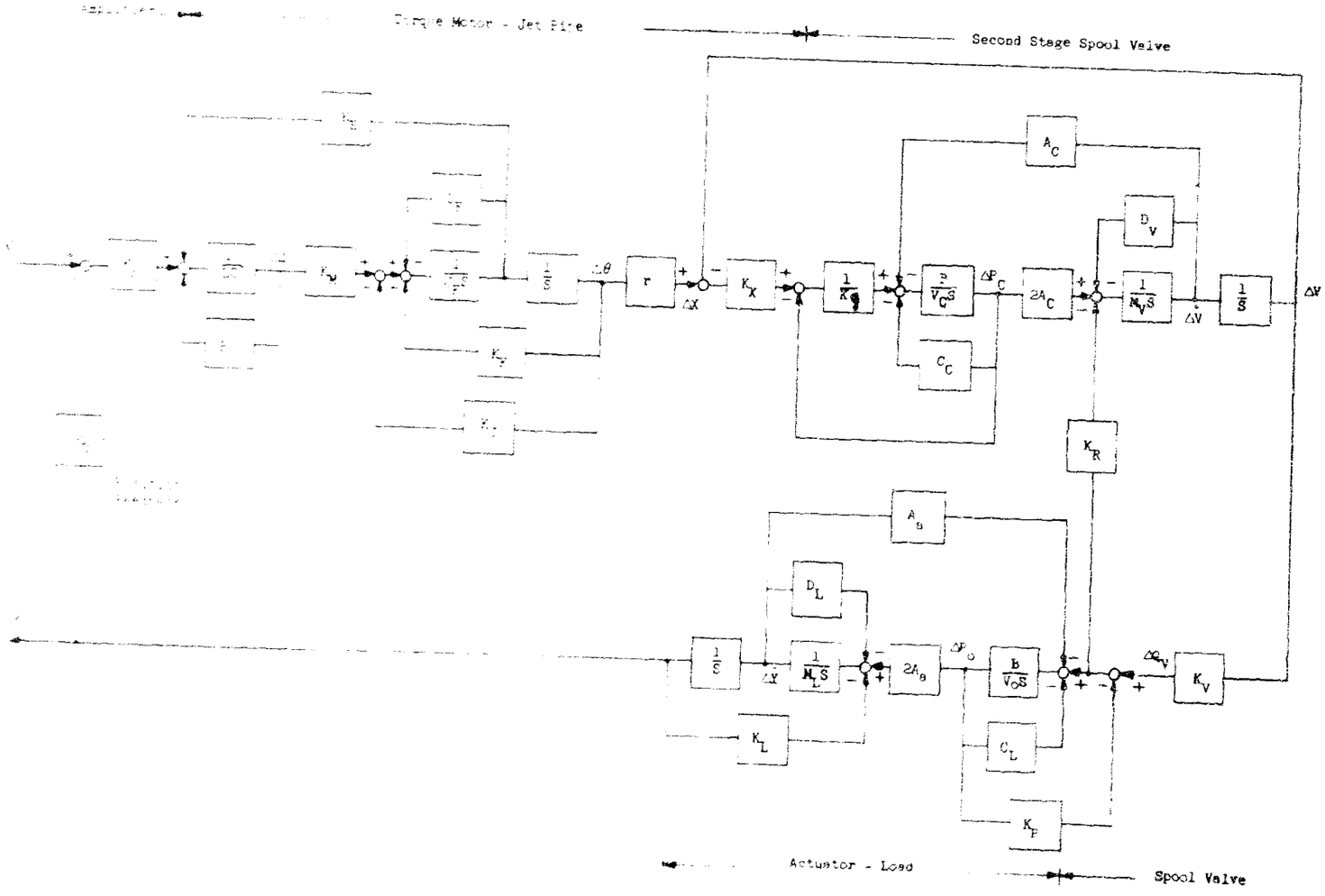

Figure C-1 - Liquid Metal Servovalve - Actuator Block Diagram

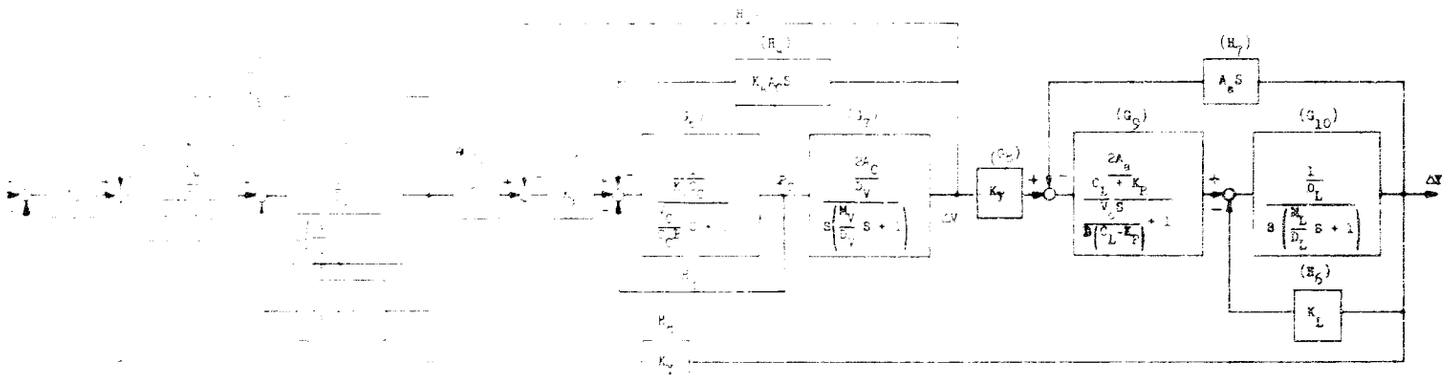

Figure C-2 - Liquid Metal Servovalve - Actuator Block Diagram

Feedback Transducer

A high temperature position transducer is to be supplied by Bendix. The transducer gain specified is:

$$K_y = 0.42 \text{ volt-in}^{-1}$$

Fluid

NaK-77 at 1400 F is the system fluid. Its significant properties and conditions are:

$$B = 7.5 \times 10^5 \text{ lb-in}^{-2}$$
$$\rho = 6.77 \times 10^{-5} \text{ lb-sec}^2\text{-in}^{-4}$$
$$P_S = 3000 \text{ lb-in}^{-2}$$
$$P_D = 100 \text{ lb-in}^{-2}$$

Numerical Calculation of Servo Transfer Functions

The foregoing data is substituted to calculate the gains and transfer functions shown in Figure C-2. The results are given below.

$$G_2 = \frac{\frac{K_M}{R}}{\frac{L}{R}S + 1} = \frac{0.156}{\frac{S}{200} + 1} \quad \text{in-lb-volt}^{-1}$$

$$G_3 = \frac{\frac{1}{D_F}}{S\left(\frac{J_F}{D_F}S + 1\right)} = \frac{100}{S\left(\frac{S}{770} + 1\right)} \quad \text{rad-in}^{-1}\text{-lb}^{-1}$$

$$H_1 = K_F + K_J = 165 \text{ in-lb-rad}^{-1}$$

H_2 (neglected)

G_4 = 1.5 inch

$G_5 = K_x = 2.7 \times 10^5 \text{ lb-in}^{-3}$

$$G_6 = \frac{\frac{1}{K_q C_c}}{\frac{V_c}{C_c B} S + 1} = \frac{13.2}{\frac{S}{10} + 1}$$

$$M_3 = 1$$

$$G_7 = \frac{\frac{2A_c}{D_v}}{S\left(\frac{M_v}{D_v} S + 1\right)} = \frac{5}{S\left(\frac{S}{100} + 1\right)} \quad in^3\text{-}lb^{-1}$$

$$H_4 = K_9 A_c S = 190\,S \quad lb\text{-}in^{-3}$$

$$H_5 = 1$$

$$G_8 = K_v = 3000\ in^2\text{-}sec^{-1}$$

$$G_9 = \frac{\frac{2A_a}{C_L + K_P}}{\frac{V_o}{B(C_L+K_P)} S + 1} = \frac{5220}{\frac{S}{127.5} + 1} \quad lb\text{-}sec\text{-}in^{-3}$$

$$G_{10} = \frac{\frac{1}{D_L}}{S\left(\frac{M_L}{D_L} S + 1\right)} = \frac{.1}{S\left(\frac{S}{2.67} + 1\right)} \quad in\text{-}lb^{-1}$$

$$H_6 = K_L = 100\ lb\text{-}in^{-1}$$

$$H_7 = A_a S = 2.75\,S\ in^2\text{-}sec^{-1}$$

$$H_8 = K_y = 0.42\ volts\ in^{-1}$$

$$G_1 = K_A = 154 \text{ (for } \omega_c = 100 \text{ rad/sec)}$$

Frequency Response Analysis

Frequency response analysis of the internal loops shown in Figure C-2 indicates that some of the internal loops can be neglected to simplify the servovalve transfer function. The transfer function can thus be approximated as follows:

$$\frac{\Delta Q}{\Delta E}(S) = \frac{\dfrac{r K_M K_v}{R (K_F + K_S)}}{\left(\dfrac{L}{R} S + 1\right)\left(\dfrac{K_q A_c}{K_x} S + 1\right)} \quad in^3\text{-}sec^{-1}\text{-}volt^{-1}$$

$$= \frac{4.25}{\left(\dfrac{S}{200} + 1\right)\left(\dfrac{S}{1420} + 1\right)} \quad in^3\text{-}sec^{-1}\text{-}volt^{-1}$$

The actuator transfer function is simply approximated as:

$$\frac{\Delta Y}{\Delta Q}(S) = \frac{1}{A_a S} = \frac{.363}{S} \quad in^{-2}\text{-}sec$$

The open loop frequency response of the servoactuator including the amplifier is shown in Figure C-3. The 135 degree phase shift occurs at about 130 radians per second. Thus the system can be closed stably at 130 rad/sec or less. Assuming a loop crossover at 100 rad/sec is conservative, a loop gain of 100 is required. Thus

$$\frac{K_A K_{s.v.} K_y}{A_a} = 100$$

or the amplifier gain required is:

$$K_A = \frac{20 A_a}{K_{s.v.} K_y} = \frac{100 \times 2.75}{4.25 \times .42} = 154$$

The servoactuator closed loop frequency response predicted is shown on the Bode diagram in Figure C-4. It shows that the predominant break frequencies contributing to phase shift at crossover are those due to the torque motor coil electrical time constant and jet-pipe position input to spool position response. The actuator transfer function from servovalve output flow to position output in exact form is:

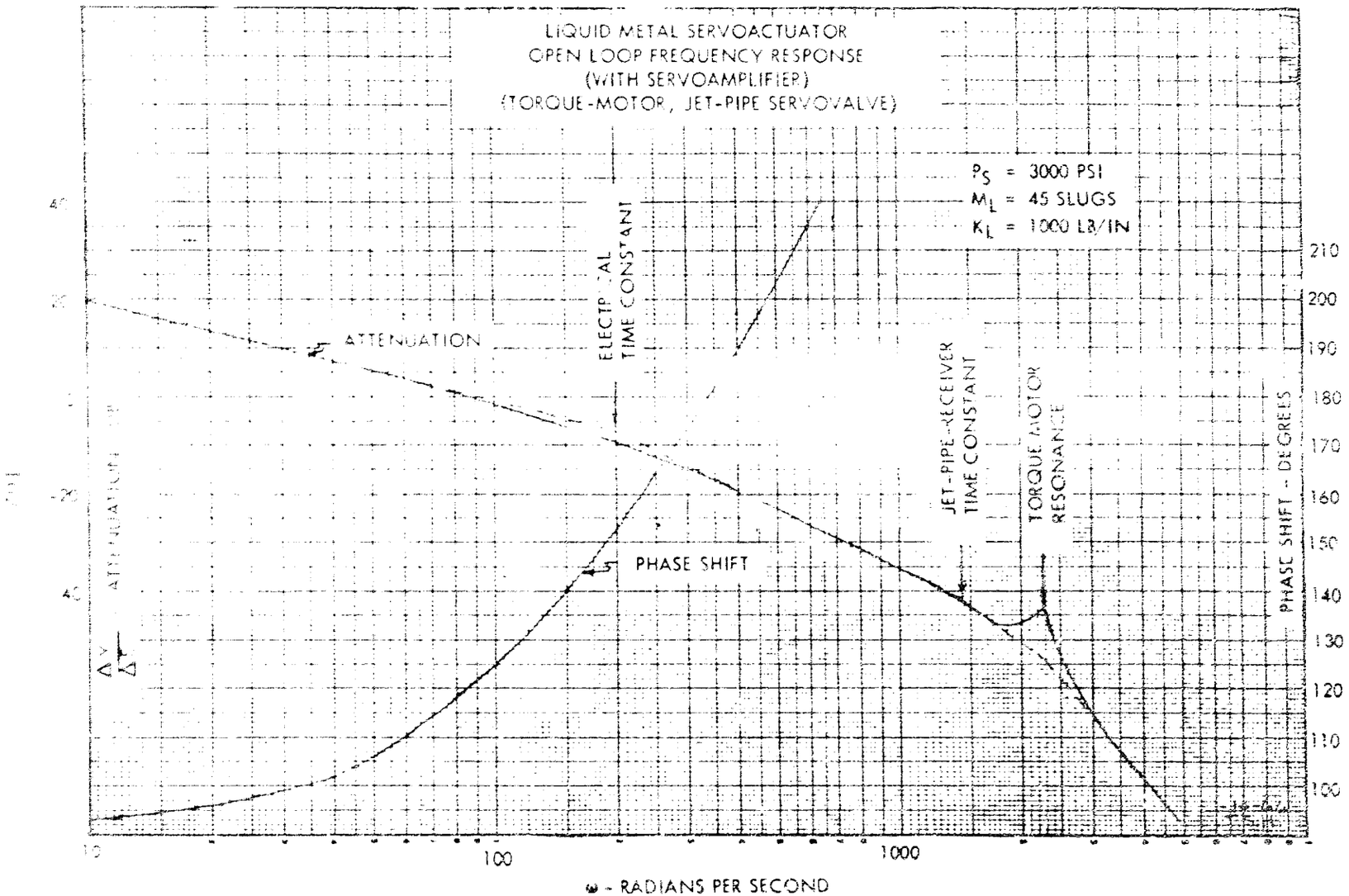

Figure C-3 - Liquid Metal Servoactuator Open Loop Frequency Response With Servoamplifier (Torque-Motor, Jet-Pipe Servovalve)

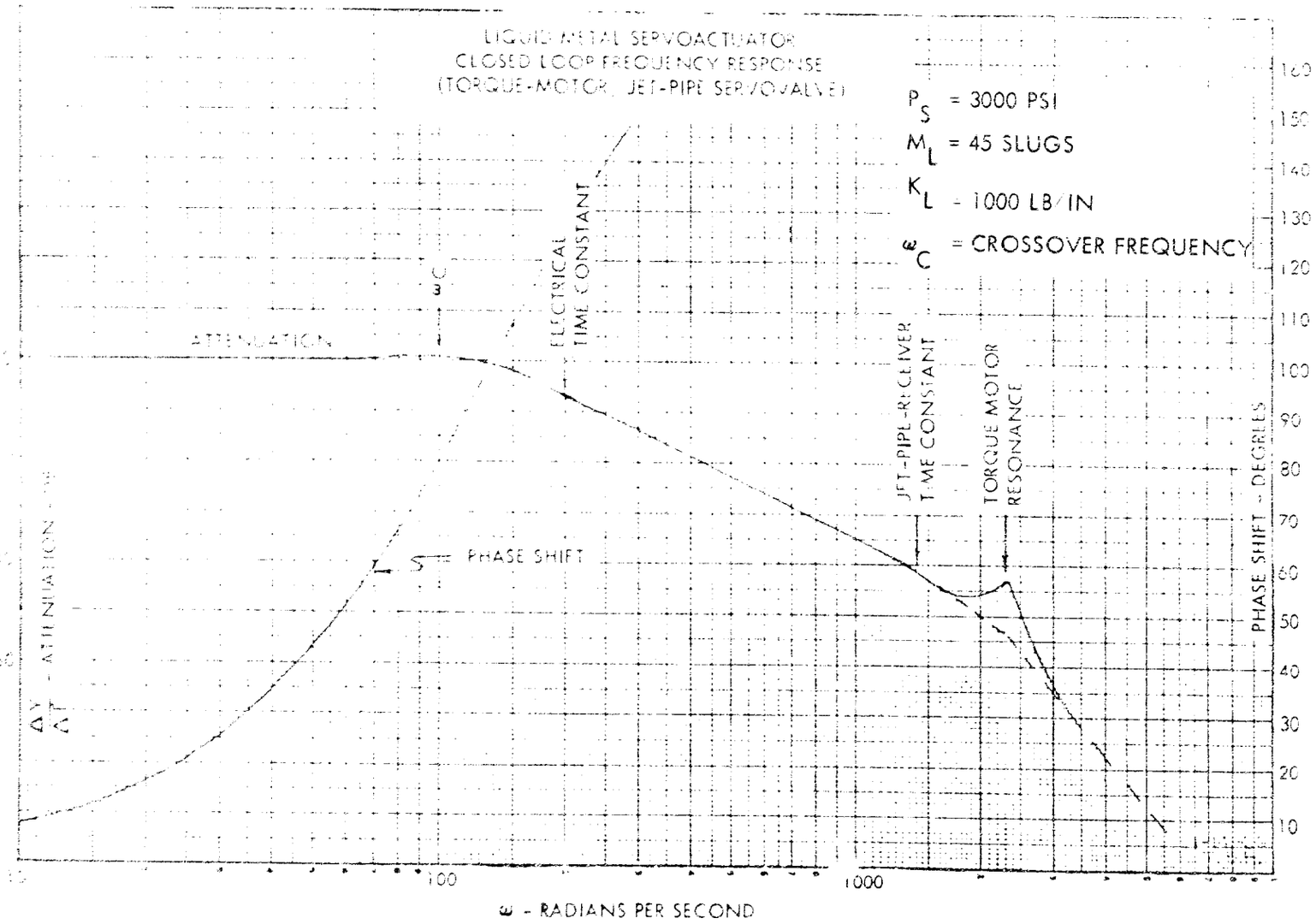

Figure C-4 - Liquid Metal Servoactuator Closed Loop Frequency Response (Torque-Motor, Jet-Pipe Servovalve)

$$\frac{\Delta Y}{\Delta Q}(S) = \frac{\dfrac{1}{A_a\left[1 + \dfrac{D_L(C_L+K_P)}{2A_a^2}\right]}}{S\,\dfrac{S^2}{\omega_n^2} + \dfrac{2\delta}{\omega_n}S + 1}$$

The hydraulic resonance ω_n and damping factor δ are defined in terms of significant parameters as:

$$\omega_n = \sqrt{\frac{2BA_a^2}{V_o M_L}\left[1 + D_L\frac{(C_L+K_P)}{2A_a^2}\right]}$$

$$\delta = \frac{\omega_n}{2}\left[\frac{\dfrac{D_L V_o}{2A_a^2 B} + \dfrac{M_L(C_L+K_P)}{2A_a^2}}{1 + \dfrac{D_L(C_L+K_P)}{2A_a^2}}\right]$$

For the system under consideration,

ω_n = 700 radians per second

δ = 0.092

The actuator hydraulic damping factor is small. It is based upon assumed values of damping and leakage coefficients. Actual damping and leakage values will probably be higher, resulting in better system damping. The hydraulic resonance is washed out by velocity feedback in the actuator so that it is not a significant factor in this application.

ANALOG COMPUTER SIMULATION

Simulation of the servovalve-actuator combination using preliminary design values was conducted on an Electronic Associates analog computer. Computer runs were made to determine whether the values of the design parameters selected provided sufficient phase margin to close the position loop at 100 radians per second. Results of analog simulation indicate no stability problem in closing the position loop at the desired frequency.

To facilitate computer scaling, the linearized system equations shown previously are nondimensionalized. The equations are nondimensionalized by presenting the output variables as percentages of maximum anticipated design values. The maximum assumed design values are designated by prime (') notation.

The nondimensionalized equations derived are listed below.

$$\Delta\left(\frac{E}{E'}\right) = \frac{L}{R} S \Delta\left(\frac{i}{I'}\right) + \Delta\left(\frac{i}{I'}\right) \tag{13'}$$

$$\Delta\left(\frac{T_M}{T'}\right) = K_M I' \Delta\left(\frac{i}{I'}\right) \tag{14'}$$

$$\Delta\left(\frac{T_M}{T'}\right) = J_F \theta' S^2 \Delta\left(\frac{\theta}{\theta'}\right) + D_J \theta S \Delta\left(\frac{\theta}{\theta'}\right) + (K_F + K_J) \theta \Delta\left(\frac{\theta}{\theta'}\right) \tag{15'}$$

$$V' \Delta\left(\frac{X}{V'}\right) = r_J \theta' \Delta\left(\frac{\theta}{\theta'}\right) \tag{16'}$$

$$\Delta\left(\frac{Z}{V'}\right) = \Delta\left(\frac{X}{V'}\right) - \Delta\left(\frac{V}{V'}\right) \tag{17'}$$

$$P_S \Delta\left(\frac{P_c}{P_S}\right) = K_x V' \Delta\left(\frac{Z}{V'}\right) - K_q Q'_J \Delta\left(\frac{Q_c}{Q_J}\right) \tag{18'}$$

$$Q'_J \Delta\left(\frac{Q_c}{Q'_J}\right) = A_c V' S \Delta\left(\frac{V}{V'}\right) + \frac{V_c P_S}{B} S \Delta\left(\frac{P_c}{P_S}\right) + C_c P_S \Delta\left(\frac{P_c}{P_S}\right) \tag{19'}$$

$$2A_c P_S \Delta\left(\frac{P_c}{P_S}\right) = M_V V' S^2 \Delta\left(\frac{V}{V'}\right) + D_V V' S \Delta\left(\frac{V}{V'}\right) \tag{20'}$$

$$Q'_V \Delta\left(\frac{\dot{V}}{\dot{V}'}\right) = K_v V' \Delta\left(\frac{V}{V'}\right) - K_p P_S \Delta\left(\frac{P_o}{P_S}\right) \tag{21'}$$

$$Q_V \Delta\left(\frac{Q_V}{Q_V'}\right) = A_a Y' S \Delta\left(\frac{Y}{Y'}\right) + \frac{V_a P_S}{B} S \Delta\left(\frac{P_o}{P_S}\right) + C_L P_S \Delta\left(\frac{P_o}{P_S}\right) \tag{22'}$$

$$2A_a P_s \Delta\left(\frac{P_o}{P_s}\right) = M_L Y' S^2 \Delta\left(\frac{Y}{\bar{Y}'}\right) + D_L Y' S \Delta\left(\frac{Y}{\bar{Y}'}\right) + K_L Y' \Delta\left(\frac{Y}{\bar{Y}'}\right) \tag{23'}$$

The block diagram representation of the above nondimensionalized system equations is shown in Figure C-5. The corresponding analog computer circuit diagram is shown in Figure C-6.

The computer was time-scaled so that one second real time was equal to 100 seconds computer time. Simulated response to step inputs were recorded to determine whether the preliminary actuator design was stable. Typical step response traces are shown on Figure C-7. The data presented show that the position response is well damped when the loop is closed at 100 radians per second.

Referring to the computer circuit diagram, Figure C-6, the potentiometer number and the parameter varied by its setting are listed as follows:

Potentiometer	Parameter
P1	K_A
P2	$K_A K_y$
P3	R/L
P4	R/L (Electrical time constant)
P5	D_{FJ}
P6	K_M
P7	K_{FJ}
P8	J_F
P9	$r K_x$
P10	K_x
P11	K_x
P12	K_z
P13	A_v
P14	C_L
P15	A_v
P16	
P17	
P18	$K_D + C_o$

Potentiometer	Parameter
P19	$K_v B/V_o$
P20	A_a
P21	K_L
P22	M_L
P23	D_L
P24	Scaling

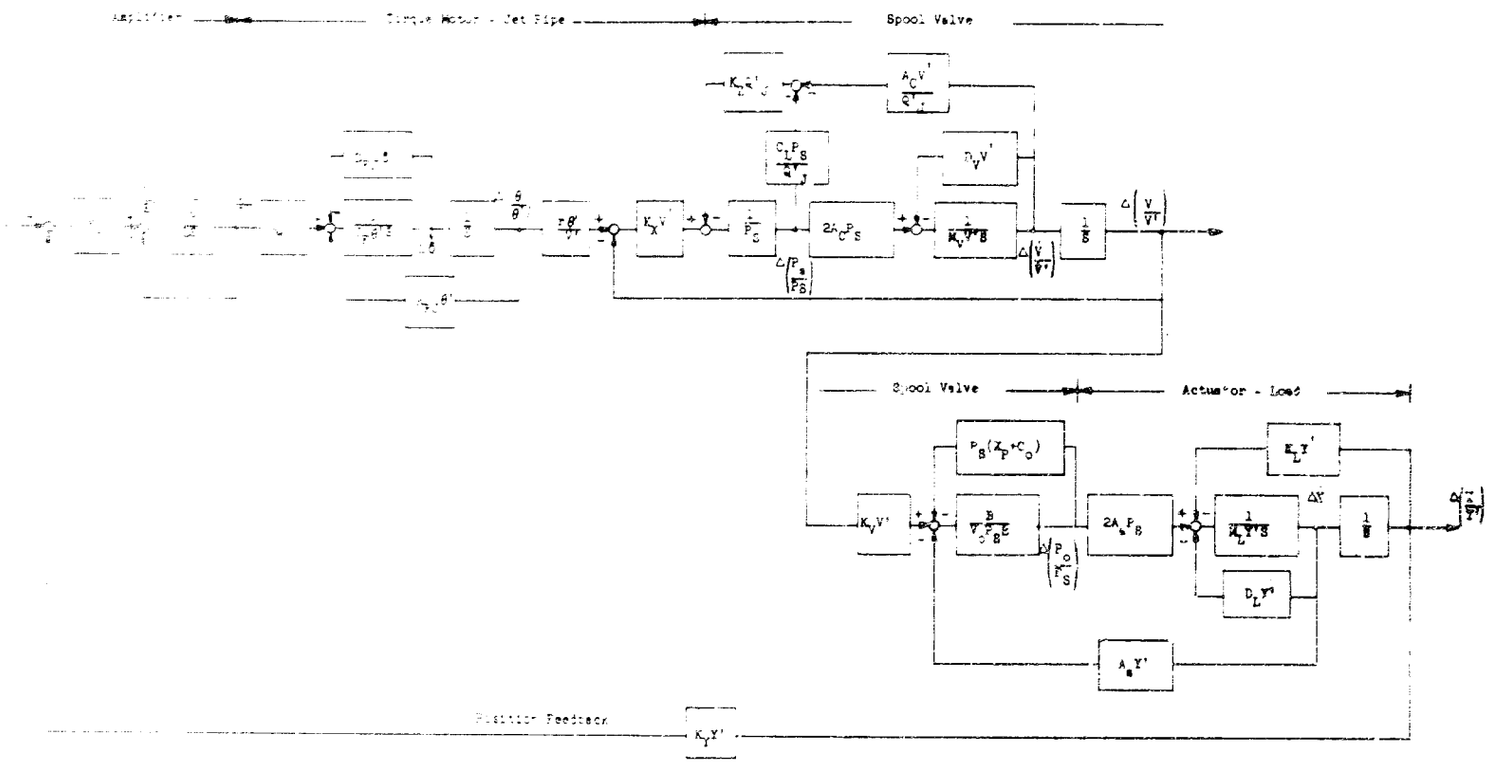

Figure C-5 - Liquid Metal Servoactuator Block Diagram

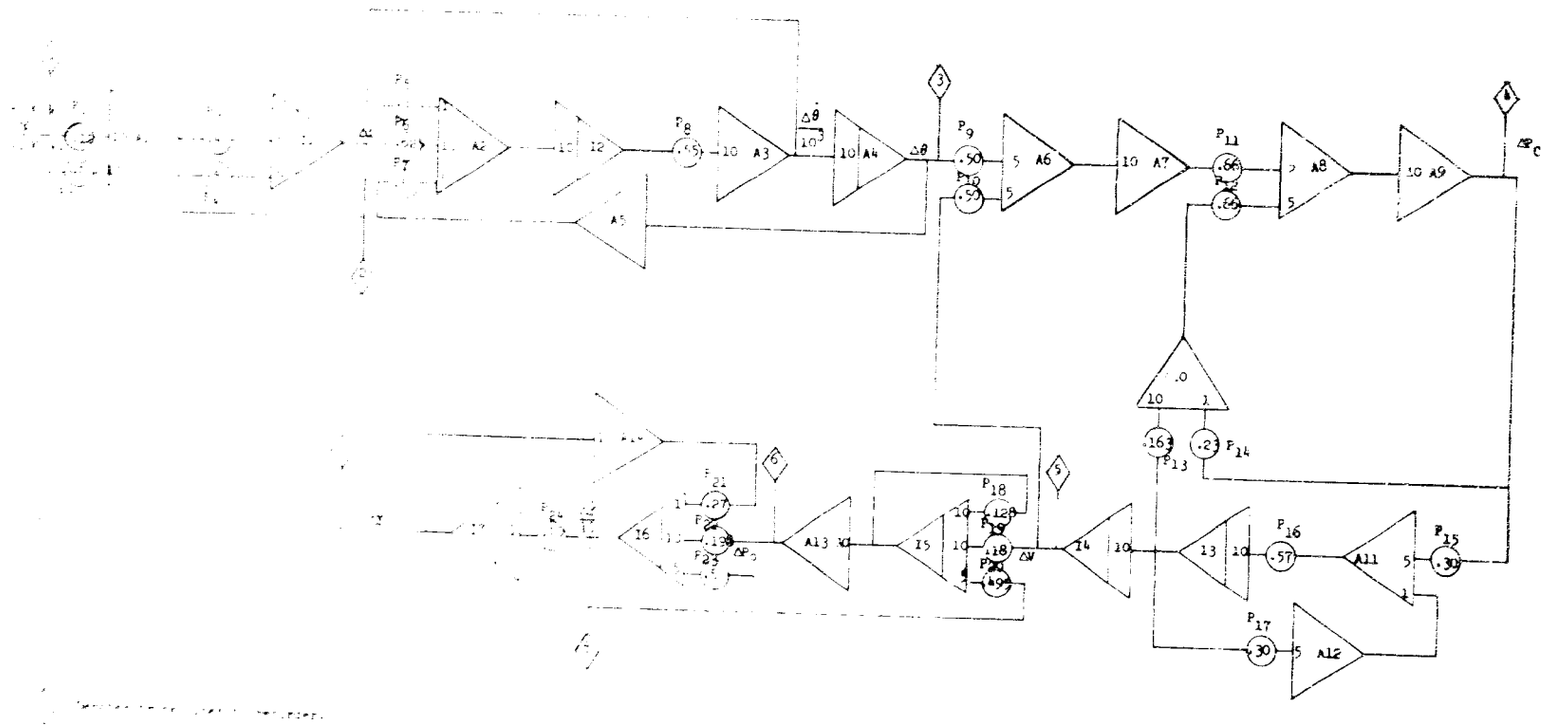

Figure C-6 - Liquid Metal Servoactuator Analog Computer Circuit Diagram

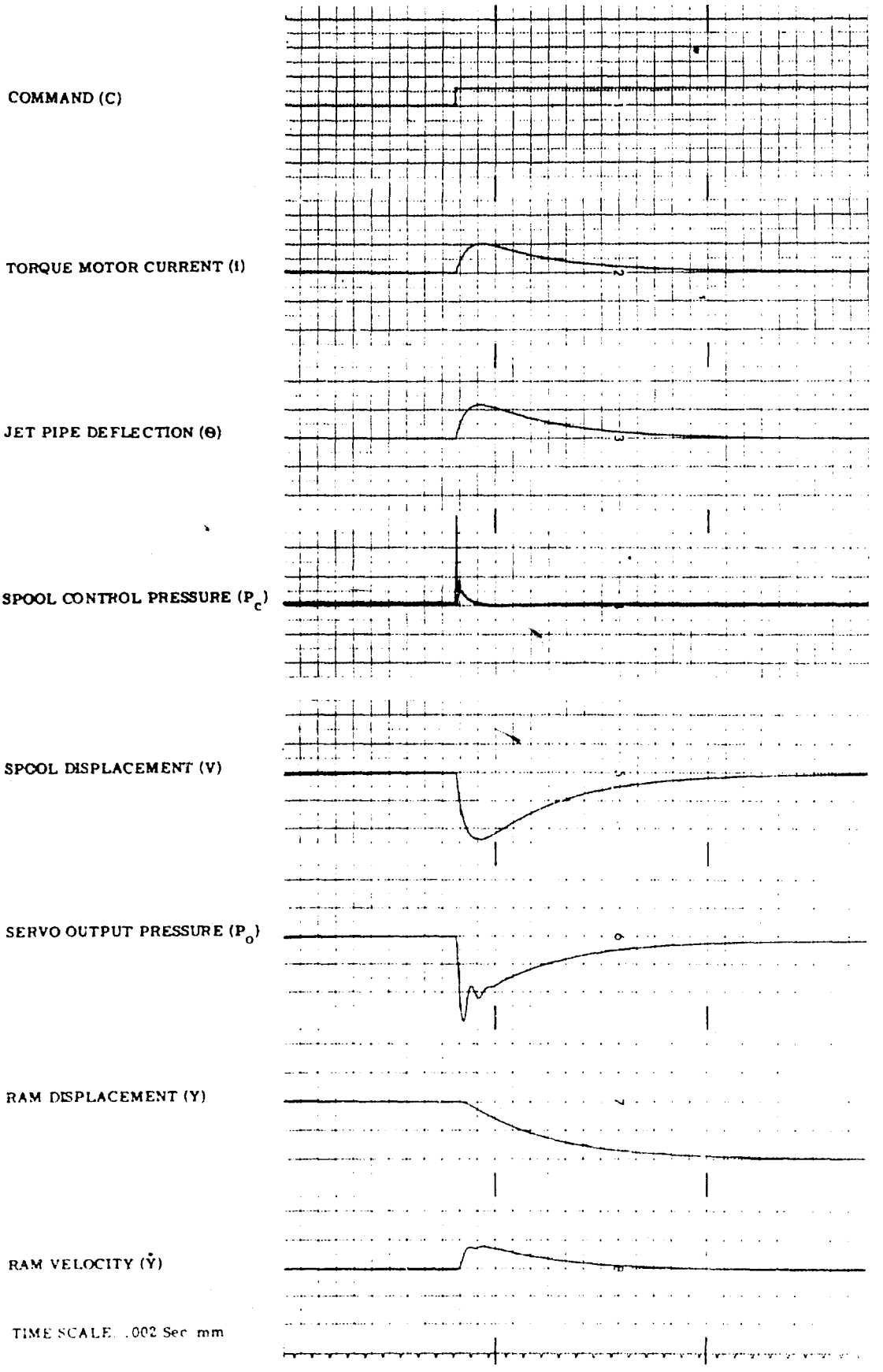

Figure C-7 Liquid Metal Servoactuator Simulated Transient Response

Appendix D

In the early phase of the servovalve program, consultations were held with Mr. J.V. Baum, Project Director, Aerospace Components Division of the Battelle Memorial Institute, Columbus, Ohio, to review the various valve concepts under consideration. The following correspondence from Battelle covers their observations and conclusions.

There are three types of first-stage and two types of second-stage servovalve sections under study. These types are as follows:

First-Stage

1. EM pump and bellows unit operating a jet pipe
2. High-temperature torque motor operating a jet pipe
3. Fluid logic element

Second-Stage

1. Mechanically connected dual poppet valve
2. Spool valve

These valve considerations are for control systems for advanced vehicles and for operating in environments beyond the capability of existing hydraulic systems. The hydraulic fluid being considered at the present time is NaK-77. The rated system pressure is expected to be of the order of 3000 psi and the operating temperature is expected to exceed 1000°F. These environmental aspects provide design conflicts that must be resolved in order to proceed with the development of a reliable, light-weight, servovalve. There are, however, some general considerations that may be helpful in selecting a promising valve design approach.

1. A considerable amount of experience exists and many publications have been presented on the design aspects of hydraulic servovalves for lower temperature applications.

2. Sufficient experience and published information exists on liquid metal applications to at least identify the critical problems to be expected when using this material as a hydraulic fluid.

The following discussion is intended as a guide in your selection of a design approach for the development of a servovalve using NaK-77 or a similar liquid-metal fluid for extreme environmental conditions including high temperature and radiation.

Summary and Suggested Approach

Many "new" design problems are anticipated for servovalves operating in a NaK-77 hydraulic system at temperatures of 1000°F or more. These in general include the problems of compatibility of materials with the hydraulic fluid and the response of selected materials and configurations to the high-temperature environment. The physical properties of the NaK-77 hydraulic fluid provide some potential advantages over fluids previously used for lower temperature applications. These include chemical and physical stability at temperatures over 1000°F, relatively high density, relatively high bulk modulus, and a reasonable range of viscosity over the desired operating temperature range. In addition, other properties such as the ability to conduct an electric current introduce the possibility of servovalve design innovations such as the EM pump first-stage unit that appear attractive for a long-range development effort.

In order to obtain an operating servovalve unit within a minimum development time, it is suggested that a conventional servovalve design approach be adapted for high-temperature operation. This suggested approach would include a high-temperature torque-motor first-stage unit operating either a flapper valve or a jet pipe arrangement with some type of mechanical feedback from a balanced-spool-type second-stage valve. It is also suggested that the diameters of all flow passages be maintained as large as possible with no orifices below 0.020 diameter to reduce the chances of plugging due to accumulation of contaminants. This approach is suggested primarily because:

1. A high-temperature torque motor is reported to have been developed and apparently is available for trial.

2. Considerable experience exists with the design, manufacture, and operation of balanced-spool-type second-stage valve units.

3. Although it is expected that wear problems will be troublesome for valves with mechanical feedback from the second stage to the first stage, it is expected that a lengthy development effort would be required for the hydraulic feedback approach to assure stability of operation.

It is further suggested that continued developmental work be carried out on a relatively long-range basis for the EM pump and the fluid-logic

first-stage servovalve design approaches. These concepts appear to be particularly attractive for possible applications at temperatures over 1200°F. The developmental effort required for these units appears to be more extensive and less specific than the developmental effort required for the suggested short-range approach.

EM Pump and Bellows Unit

The operational characteristics of EM pumps are generally readily calculable and many units have been built and operated(1). As indicated on your design sketch SK56110-294, you plan to use a "Lucalox" body with niobium tubes and electrical conductors fastened to it. As you know, the techniques for joining these materials are not, as yet, well developed. However, examples of successful joints have been reported and (2, 3, 4,) the techniques may be refined by the time your liquid metal control system is developed. The main problem is the differential expansion at the joints between the two materials when exposed to high temperature. Other aspects of your proposed pump design seem to be generally satisfactory. The materials are compatible with the fluid. The selected configurations provides an insulator in the flow path which should increase the pump efficiency.

The method of supplying fluid to the EM pump loop is not illustrated on the sketches and will probably be a problem, particularly as required to accommodate thermal expansion effects. If a fluid accumulator is used, it should be connected to the system at the average pressure point or approximately at the center of the pump section. Any further connections in this area would only add to the already precarious joining problem, although a small hole through the electrode might be used for this purpose. Such a fluid connection, unfortunately, would probably tend to reduce the response rate of the system.

---

(1) Liquid Metals Handbook, Atomic Energy Commission, Department of the Navy.

(2) LAMS-2917, "Ceramic-to-Metal Seals for High Temperature Operation, Los Alamos Scientific Laboratory, University of California.

(3) "High Temperature Alkali Metal Resistant Insulation", Westinghouse Electric Corporation, Aerospace Electrical Division, Lima, Ohio, USAF Contract AF33(615)-1360, Project No. 8128, Task No. 8128-06.

(4) "Ceramic to Metal Seals for High-Temperature Thermionic Convertors", TIR No. RTD-TDR-63-4109, Contract AF33(657)-10038.

There are some problems that may be anticipated with the bellows assemblies and the mechanical connections to the jet-pipe tube. Only very limited design data are available for bellows that are subjected to high-frequency fatigue loads. Also, if the bellows are made of conventional materials such as stainless steel or Inconel, the weldment of niobium tubing to the bellows material is expected to be a source of trouble. If the bellows assembly is made of niobium also, considerable attention must be given to the welding technique to prevent deterioration on exposure of the welded joint to the liquid metal.

In briefly reviewing the analysis material for the EM pump, it was noticed that the effect of the counter EMF developed in the liquid as it moves through the magnetic field was not included in the consideration of the pressure generated in the pump. While this simplification would have no effect on static pressure considerations, it would tend to provide an overoptimistic estimate of the response rate. Also, the length of the flow passage considered for the frictional flow loss was taken as 0.75 inch. The total passage length through the pump section is about 2 inches. Again, this dimensional simplification would not affect the static pressure but would affect the results obtained for dynamic conditions. Another difference between the dimensional representation used in the analysis and the valve configuration shown on the sketches is apparent in the calculations for the flow through the jet pipe. The flow through the jet pipe is calculated by standard nozzle equations. The jet pipe planned for use in your experimental unit is a tubular member of significant length. The flow through the relatively long tubular passage will be less than the flow calculated for a short nozzle. And correspondingly for a given pressure drop, the velocity of the jet will be less than calculated.

High-Temperature Torque Motor

The high-temperature torque motor as included in your plans is intended to operate a jet pipe. As you know, the most critical design requirement for the torque motor is the high temperature.

I suggest that priority be given to a demonstration of the proposed torque motors ability to operate in a high-temperature environment. If this capability can be demonstrated satisfactorily, the major developmental effort required would be concerned with the adaption of the torque motor to the second-stage parts of the valve. There are several problems that can be expected in the design of the interacting components. The connection between the torque-motor output shaft and the jet-pipe tube as illustrated on the sketch SK56110-296 is a close-fitting mechanical joint. This connection will be a source for lost motion and friction between the torque motor and the jet pipe.

The analysis indicates that a total spool displacement of approximately 0.010 is being considered. With this displacement and the approximate

configuration shown in the sketch, the air gap in the torque-motor armature must also be about 0.010. Although the operating characteristics of the torque motor have not been fully evaluated, it is expected that the torque-motor output may be nonlinear, particularly near the limits of its travel.

Fluid Logic Element

Fluid logic devices of the general type being considered for the first stage element in your servovalve are relatively new and a considerable amount of research effort will probably be required before the application can be attempted. As described in our discussion, it is anticipated that the fluid logic element would be a modulating type of control device using possibly an electrical control signal as a direct input for controlling fluid flow. The output of the device would be a high velocity jet of fluid that is proportioned between two alternative flow passages. The kinetic energy of the high velocity jets would be converted to pressure for control of the spool position.

Many opportunities for design variations appear to exist with this type of control element and because these possibilities have not yet been investigated, the development of a suitable fluid-logic first-stage element appears to require a considerable amount of research effort. Investigations should be made of possible methods for feedback of spool motion to the fluid logic element. The use of an electrical signal for fluid flow control should be investigated. The selection and experimental verification of the logic-element internal configuration will require significant effort. The effect of temperature on the fluid parameters that influence flow control will require investigation. Also, of course, the materials of construction must be selected that will allow electrical control of the fluid while satisfying other requirements such as corrosion resistance, fluid containment, strength at operating temperature, machinability, and availability.

Dual Poppet Valves

The use of dual poppet valves is being considered as second-stage elements in the NaK servo-control valves. As illustrated on your sketch SK-56110-277, the poppet valves would be arranged in pairs on guide stems that are interconnected. Each pair of poppets provides for static pressure balancing when the valves are closed.

The design problems anticipated for this valve concept are extensive. It is expected that a considerable amount of force unbalance will exist on the poppet valve stems when the valves are open due to the flow effects adjacent to the poppet faces. Extremely precise manufacturing operations would be required to obtain good seals at the four lines of contact between the poppets and the valve bodies. This problem would be accented by the high operating temperature required. The operating arm for the dual poppet unit is spring

loaded to allow for opening one set of poppets while the other set remains seated. This introduces a spring force that must be overcome by the first stage control section. The flow control characteristics of the poppets as influenced by the shape of the valve face, the skirt on the valve (if any) and the seat, will require a considerable amount of investigation. At high temperatures the tendency of the valve faces to be "cold welded" to the valve seats would probably be a significant problem that might be experienced as "pick-up" or "pitting" of the seal surfaces. Because valve shut-off depends upon precise location of the poppets with respect to the seats, and because the stems are relatively small, it is anticipated that minute deflections in the stems may cause unwanted control lags.

When it was decided to pursue the jet pipe-spool valve approach a preliminary design was prepared and submitted to Battelle for review. Their comments concerning this servovalve are as follows:

We are in general agreement that the design approach is promising particularly toward achieving an operable servovalve unit with a minimum of time spent on valve refinement and optimization. We are assuming that the torque motor is able to operate at the required temperature level as claimed by the manufacturer. The following list of comments includes most of the suggestions that I made during our discussions in Schenectady and is presented for your consideration and reference. There is no particular significance to the order of presentation of the comments.

1. In order to maximize the operating time for the torque motor, it is suggested that the unit be outgassed for a significant period of time in a high vacuum (say at least 48 hours at 10^{-7} mm HG) and then protected from contact with oxygen by submersion in an inert-gas atmosphere.

2. A rough calculation on leakage past the ends of the spool indicates a worst-case flow rate of the order of 2-1/2 pounds per minute based on assumed pressure levels. With this flow rate, the valve response time will be relatively high; however, this leakage rate could be reduced by reducing the spool-to-sleeve clearance.

3. A centering adjustment is provided for positioning the jet pipe with respect to the valve body. It is suggested that some means (maybe shims) be provided for positioning the sleeve in the valve body. Also, on the layout which shows part of the torque motor details, there is no indication of adjustments for magnetic and/or electrical null. This feature would be needed for production valves.

4. The torque motor and jet-pipe design arrangement does not seem to provide any possibilities for dynamic balancing. Although this will not be a problem for laboratory operation, any future valve designs should be arranged to accommodate vibrational loadings.

5. The springs that are shown for spool centering are likely to be a problem at elevated temperature conditions. Most common spring materials will undergo stress relaxation at the expected operating temperature for this valve. I suggest, as a minimum, that the springs be designed for very low stress levels and subjected to thermal cycles under load prior to assembly in the valve. It may be desirable to use a nonmetallic material such as quartz for the springs.

6. It is expected that the NaK that will be used in the valve will contain some contamination. The magnetic-gap area of the torque motor may be sensitive to the accumulation of oxides and other contaminants.

7. The jet receiver holes in the spool must be carefully aligned with the jet pipe to maximize the recovery pressure. The guide elements that align the spool, however, provide a potential drag force on the spool. I suggest that the clearance in the spool guide be as generous as possible (say 0.005) to minimize the possibility of build-up of contaminants with a resulting drag force on the spool.

8. In order to minimize the effect of thermal gradients on the spool-to-sleeve fit, I suggest that the sleeve be a loose fit in the valve body--on the order of 0.0005 clearance. Also, I suggest some kind of spring loading in the axial direction of the sleeve.

9. The manifold and valve body are made of different materials with thermal-expansion rates that will require some attention to the fastening problem. As long as the fasteners are the same material as the manifold, however, the thermal expansion problem will be minimized.

10. Some additional design effort should be applied to the fastener problem for the end caps and the torque-motor body. A rough calculation shows, for example, the minimum stress for direct tension and compression loads using a molybdenum sleeve and an A-286 bolt would be on the order of 120,000 psi for a temperature range of 1000°F. If the bolts and the covers cannot be made of the same material, I suggest that the design include some provision for deflection compensation. This could be a flange arrangement that acts like a cantilever beam or some other equivalent form of "spring" loading.

Unclassified

Security Classification

DOCUMENT CONTROL DATA - R&D

(Security classification of title, body of abstract and indexing annotation must be entered when the overall report is classified)

1. ORIGINATING ACTIVITY (Corporate author)
General Electric Company
Binghamton, New York

2a. REPORT SECURITY CLASSIFICATION
Unclassified

2b. GROUP
N/A

3. REPORT TITLE
STUDY OF LIQUID METAL NAK-77 FOR APPLICATION IN FLIGHT CONTROL SYSTEMS

4. DESCRIPTIVE NOTES (Type of report and inclusive dates)
Final Technical Report

5. AUTHOR(S) (Last name, first name, initial)
Kumpitsch, R. C.
Granan, J. R.

6. REPORT DATE	7a. TOTAL NO. OF PAGES	7b. NO. OF REFS
June 1968	177	16

8a. CONTRACT OR GRANT NO.	9a. ORIGINATOR'S REPORT NUMBER(S)
AF33(615)-2263	AFFDL-TR-66-227
b. PROJECT NO. 8225	
c. Task No. 822510	9b. OTHER REPORT NO(S) (Any other numbers that may be assigned this report) ACD 8176
d.	

10. AVAILABILITY/LIMITATION NOTICES
This document is subject to special export controls and each transmittal to foreign governments or foreign nationals may be made only with prior approval of the Air Force Flight Dynamics Laboratory, FDCL, Wright-Patterson Air Force Base, Ohio 45433.

11. SUPPLEMENTARY NOTES

12. SPONSORING MILITARY ACTIVITY
Air Force Flight Dynamics Laboratory
FDCL
Wright-Patterson AFB, Ohio 45433

13. ABSTRACT

A survey of potential aerospace applications and system performance requirements was made. A ten-stage centrifugal pump rated at 3000 psi, 16 gpm, and 1200 F was successfully tested at pressures above 2200 psi, temperatures exceeding 1000 F, and speed above 31,000 rpm. Flow exceeded the rated capacity of the unit.

A 1200 F, two-stage servovalve was designed and built. Static tests with oil and NaK-77 were conducted. A linear actuator rated at 15,000 pounds output at 1200 F was re-built and tested with NaK-77 for part of an experimental servoactuating subsystem.

A nuclear testing facility was located and a design layout of an experimental, air/nuclear servoactuating subsystem was completed. Design criteria and design layouts for a flight test system suitable for installation in the elevon section of the XB-70 was also completed.

DD FORM 1 JAN 64 1473

Unclassified

Security Classification

14. KEY WORDS	LINK A		LINK B		LINK C	
	ROLE	WT	ROLE	WT	ROLE	WT
Flight Control Servo Actuator Liquid Metal Actuator High Temperature Actuation						

INSTRUCTIONS

1. ORIGINATING ACTIVITY: Enter the name and address of the contractor, subcontractor, grantee, Department of Defense activity or other organization *(corporate author)* issuing the report.

2a. REPORT SECURITY CLASSIFICATION: Enter the overall security classification of the report. Indicate whether "Restricted Data" is included. Marking is to be in accordance with appropriate security regulations.

2b. GROUP: Automatic downgrading is specified in DoD Directive 5200.10 and Armed Forces Industrial Manual. Enter the group number. Also, when applicable, show that optional markings have been used for Group 3 and Group 4 as authorized.

3. REPORT TITLE: Enter the complete report title in all capital letters. Titles in all cases should be unclassified. If a meaningful title cannot be selected without classification, show title classification in all capitals in parenthesis immediately following the title.

4. DESCRIPTIVE NOTES: If appropriate, enter the type of report e.g., interim, progress, summary, annual, or final. Give the inclusive dates when a specific reporting period is covered.

5. AUTHOR(S): Enter the name(s) of author(s) as shown on or in the report. Enter last name, first name, middle initial. If military, show rank and branch of service. The name of the principal author is an absolute minimum requirement.

6. REPORT DATE: Enter the date of the report as day, month, year, or month, year. If more than one date appears on the report, use date of publication.

7a. TOTAL NUMBER OF PAGES: The total page count should follow normal pagination procedures, i.e., enter the number of pages containing information.

7b. NUMBER OF REFERENCES: Enter the total number of references cited in the report.

8a. CONTRACT OR GRANT NUMBER: If appropriate, enter the applicable number of the contract or grant under which the report was written.

8b, 8c, & 8d. PROJECT NUMBER: Enter the appropriate military department identification, such as project number, subproject number, system numbers, task number, etc.

9a. ORIGINATOR'S REPORT NUMBER(S): Enter the official report number by which the document will be identified and controlled by the originating activity. This number must be unique to this report.

9b. OTHER REPORT NUMBER(S): If the report has been assigned any other report numbers *(either by the originator or by the sponsor)*, also enter this number(s).

10. AVAILABILITY/LIMITATION NOTICES: Enter any limitations on further dissemination of the report, other than those imposed by security classification, using standard statements such as:

(1) "Qualified requesters may obtain copies of this report from DDC."

(2) "Foreign announcement and dissemination of this report by DDC is not authorized."

(3) "U. S. Government agencies may obtain copies of this report directly from DDC. Other qualified DDC users shall request through AFFDL (FDCL) ."

(4) "U. S. military agencies may obtain copies of this report directly from DDC. Other qualified users shall request through _____."

(5) "All distribution of this report is controlled. Qualified DDC users shall request through _____."

If the report has been furnished to the Office of Technical Services, Department of Commerce, for sale to the public, indicate this fact and enter the price, if known.

11. SUPPLEMENTARY NOTES: Use for additional explanatory notes.

12. SPONSORING MILITARY ACTIVITY: Enter the name of the departmental project office or laboratory sponsoring *(paying for)* the research and development. Include address.

13. ABSTRACT: Enter an abstract giving a brief and factual summary of the document indicative of the report, even though it may also appear elsewhere in the body of the technical report. If additional space is required, a continuation sheet shall be attached.

It is highly desirable that the abstract of classified reports be unclassified. Each paragraph of the abstract shall end with an indication of the military security classification of the information in the paragraph, represented as *(TS), (S), (C), or (U)*.

There is no limitation on the length of the abstract. However, the suggested length is from 150 to 225 words.

14. KEY WORDS: Key words are technically meaningful terms or short phrases that characterize a report and may be used as index entries for cataloging the report. Key words must be selected so that no security classification is required. Identifiers, such as equipment model designation, trade name, military project code name, geographic location, may be used as key words but will be followed by an indication of technical context. The assignment of links, rules, and weights is optional.